RECLAMATION
Managing Water in the West

ESTIMATING CLIMATIC CHANGE IMPACTS ON WATER RESOURCES IN ARID ENVIRONMENTS: THE ROLE OF DOWNSCALING METHODOLOGY

Research and Development Office
Science and Technology Program
(Final Report) ST-2019-9039-01

U.S. Department of the Interior
Bureau of Reclamation
Research and Development Office

July 2019

.

Mission Statements

The Department of the Interior (DOI) conserves and manages the Nation's natural resources and cultural heritage for the benefit and enjoyment of the American people, provides scientific and other information about natural resources and natural hazards to address societal challenges and create opportunities for the American people, and honors the Nation's trust responsibilities or special commitments to American Indians, Alaska Natives, and affiliated island communities to help them prosper.

The mission of the Bureau of Reclamation is to manage, develop, and protect water and related resources in an environmentally and economically sound manner in the interest of the American public.

Disclaimer:
This document has been reviewed under the Research and Development Office Discretionary peer review process https://www.usbr.gov/research/peer_review.pdf consistent with Reclamation's Peer Review Policy CMP P14. It does not represent and should not be construed to represent Reclamation's determination, concurrence, or policy.

<table>
<tr><td colspan="4">REPORT DOCUMENTATION PAGE</td><td colspan="2">Form Approved
OMB No. 0704-0188</td></tr>
<tr><td colspan="2">T1. REPORT DATE:
JULY, 2019</td><td colspan="2">T2. REPORT TYPE:
RESEARCH</td><td colspan="2">T3. DATES COVERED
October 1, 2015 – July 9, 2019</td></tr>
<tr><td colspan="4" rowspan="3">T4. TITLE AND SUBTITLE
Estimating Climatic Change Impacts on Water Resources in Arid Environments: The Role of Downscaling Methodology</td><td colspan="2">5a. CONTRACT NUMBER
16XR0680A1
RY.1541CC20.1629039</td></tr>
<tr><td colspan="2">5b. GRANT NUMBER
R16AC00024</td></tr>
<tr><td colspan="2">5c. PROGRAM ELEMENT NUMBER
1541 (S&T)</td></tr>
<tr><td colspan="4" rowspan="3">6. AUTHOR(S)
Eylon Shamir
Eve Halper</td><td colspan="2">5d. PROJECT NUMBER
ST-2019-9039-01</td></tr>
<tr><td colspan="2">5e. TASK NUMBER</td></tr>
<tr><td colspan="2">5f. WORK UNIT NUMBER
PXAO-7000</td></tr>
<tr><td colspan="4">7. PERFORMING ORGANIZATION NAME(S) AND ADDRESS(ES)
Hydrologic Research Center, 11440 W Bernardo Ct #375, San Diego, CA 92127
Reclamation Phoenix Area Office, 6150 West Thunderbird Rd, Glendale, AZ 85306</td><td colspan="2">8. PERFORMING ORGANIZATION REPORT NUMBER</td></tr>
<tr><td colspan="4" rowspan="2">9. SPONSORING / MONITORING AGENCY NAME(S) AND ADDRESS(ES)
Research and Development Office
U.S. Department of the Interior, Bureau of Reclamation,
PO Box 25007, Denver CO 80225-0007</td><td colspan="2">10. SPONSOR/MONITOR’S ACRONYM(S)
R&D: Research and Development Office
BOR/USBR: Bureau of Reclamation
DOI: Department of the Interior</td></tr>
<tr><td colspan="2">11. SPONSOR/MONITOR’S REPORT NUMBER(S)
ST-2019-9039-01</td></tr>
<tr><td colspan="6">12. DISTRIBUTION / AVAILABILITY STATEMENT
Final report can be downloaded from Reclamation’s website: https://www.usbr.gov/research/</td></tr>
<tr><td colspan="6">13. SUPPLEMENTARY NOTES: Data sets available from Phoenix Area Office. Contact Russ Bryant at: 623-773-6410</td></tr>
<tr><td colspan="6">14. ABSTRACT: This study evaluated the impact of “downscaling” methods on two types of water resources assessments in arid environments under projected climate change.</td></tr>
<tr><td colspan="6">15. SUBJECT TERMS: Climate, Statisical Downscaling, Dynamical Downscaling, Water, Arid, Weather Generator</td></tr>
<tr><td colspan="3">16. SECURITY CLASSIFICATION OF:</td><td rowspan="2">17. LIMITATION OF ABSTRACT
U</td><td rowspan="2">18. NUMBER OF PAGES</td><td>19a. NAME OF RESPONSIBLE PERSON Eve Halper</td></tr>
<tr><td>a. REPORT
U</td><td>b. ABSTRACT
U</td><td>c. THIS PAGE
U</td><td>19b. TELEPHONE NUMBER
623-773-6279</td></tr>
</table>

ESTIMATING CLIMATIC CHANGE IMPACTS ON WATER RESOURCES IN ARID ENVIRONMENTS: THE ROLE OF DOWNSCALING METHODOLOGY

Eylon Shamir, Hydrologic Research Center, San Diego

Eve Halper, Bureau of Reclamation, Phoenix Area Office

Project Final Report: March 2019

A study funded by the Bureau of Reclamation Science and Technology Grant Program under a Cooperative Agreement between the Hydrologic Research Center and Reclamation, Lower Colorado Region (Agreement # R16AC00024).

EVE HALPER Digitally signed by EVE HALPER Date: 2019.03.21 18:24:27 -07'00'

Prepared by: Eve Halper
Planner (Water Resources)
Program Development Division
Lower Colorado Region
Phoenix Area Office

3/21/19
Date

3/29/19

Peer Review: Noe Santos, P.E.
Civil Engineer, River Operations Group
Lower Colorado Regional Office

Date

Acknowledgements

Funding for this project was provided by the Bureau of Reclamation (Reclamation), Science and Technology Grant Program under a Cooperative Agreement between the Hydrologic Research Center and Reclamation’s Lower Colorado Region (Agreement # R16AC00024). The authors of this study thank Christopher Castro, Hsin-I Chang, Timothy Lahmers and Sujan Pal from the University of Arizona, Department of Hydrology and Atmospheric Sciences, for providing the dynamically downscaled climate projections and guiding our use of them.

We thank Paul Miller and Craig Peterson from the Colorado River Forecast Center (CBRFC), National Weather Service for their assistance in providing the CBRFC data and hydrologic model setup and Ben Livneh for his assistance with the observed gridded dataset. Jason Lee and Jon Sweeten from the US Army Corps of Engineers, Los Angeles District supplied the Alamo Lake historic water level data. Noe Santos from the Bureau of Reclamation-Lower Colorado Region’s Boulder Canyon Operations Office in Boulder City, Nevada and Subhrendu Gangopadhyay and Lindsay Bearup from Reclamation’s Water Resources Planning and Operations Support Group, Denver provided advice and technical support. Noe Santos also provided final peer review for this report.

We greatly appreciate the efforts of Olga Hart and Keith Nelson from Arizona Department of Water Resources, whose numerous discussions on modeling issues in the Santa Cruz River have influenced and guided many of the derived concepts presented.

We thank Konstantine Georgakakos, Theresa Modrick, Robert Jubach and Nicholas Graham from the Hydrologic Research Center for their support and advice throughout the project’s development. The opinions expressed in this report are those of the authors and do not reflect those of the funding agency or the individuals acknowledged.

This page intentionally left blank

Table of Contents

List of Tables

List of Figures

I. Executive Summary

This study evaluated the impact of "downscaling" methods on two types of water resources assessments in arid environments under projected climate change. Downscaling is the process of translating Global Climate Model (GCM) projections with scales of one to two degrees latitude and longitude to a spatial resolution suitable for basin-scale hydrologic modeling. The approach compares an empirical method based on historical observations (statistical downscaling) to a physics-based method using GCM output as the input to a high-resolution Regional Climate Model (RCM) (dynamical downscaling).

The focus is the projected impact of changes in mid-21st century precipitation patterns on water resources management in two Arizona basins: The Upper Santa Cruz River (USCR) Basin, a binational (U.S. – Mexico) watershed where intermittent flows recharge the groundwater reservoirs serving the city of Nogales, Arizona and the Bill Williams River Basin upstream of Alamo Dam, in western Arizona. Alamo Dam regulates high flow events into Lake Havasu, where the Central Arizona Project (CAP) diverts Colorado River water for delivery to central and southern Arizona. Reclamation staff at the Boulder Canyon Operations Office expressed interest in evaluating potential changes in flood size and frequency for effects on downstream water quality, CAP diversions, and Lake Havasu reservoir regulation.

Both watersheds feature ephemeral streams and precipitation that is highly variable in space and time, which trigger highly variable streamflow events. In these areas, even small, nuanced changes in precipitation patterns may substantially impact water resources management and planning.

Precipitation simulations from three Global Climate Models (GCMs) were statistically and dynamically downscaled: 1) HadGEM2-ES (Global Environmental Model, Version 2 from the United Kingdom Meteorological Office, the Hadley Centre), 2) MPI-ESM-LR (Earth System Model) running on low resolution (LR) grid from the Max Planck Institute for Meteorology, and 3) GFDL-ESM2M (NOAA Geophysical Fluid Dynamic Laboratory – Earth System Model). The GCMs are derived from the Coupled Model Intercomparison Project Phase 5 (CMIP5) simulated with Representative Concentration Pathway 8.5 (RCP 8.5). The RCP 8.5 scenario assumes global greenhouse gas emissions will continue to increase through the 21st century. These GCMs were selected for their plausible representation of the historic climatology and prevailing precipitation-bearing synoptic conditions in the southwest United States.

The study incorporated statistically downscaled (SD) precipitation simulations from the Localized Constructed Analogs (LOCA) dataset produced by researchers at Scripps Institution of Oceanography at the University of California San Diego. The dynamically downscaled (DD) precipitation simulations are available from the North America Coordinated Regional Climate Downscaling Experiment (NA-CORDEX) program. These simulations, contributed to NA-CORDEX by the University of Arizona, used the Advanced Research version of the

Weather Research and Forecasting (WRF) model (Version 3.1) as the Regional Climate Model.

An analysis of statistically and dynamically downscaled simulations for these three GCMs projected an increase in the frequency of dry winters and a weaker signal for a decrease in the frequency of wet winters during the mid-21st century (2020-2059). For summer precipitation, the GCMs were inconclusive and yielded contradicting projections. The most notable contradiction was between the dynamically downscaled HadGEM2 and MPI models. While the dynamically downscaled HadGEM2 projection (DD-HAD) projected wetter summers (decreasing frequency of dry summer and increasing frequency of wet summer), the DD-MPI projected drier summers (increasing frequency of dry summer and decreasing frequency of wet summers).

To evaluate the impact of the projected changes in precipitation on water resources, we developed a modeling framework for each watershed that included the following components: 1) a weather generator (WG) that produces an ensemble of likely-to-occur hourly precipitation events; 2) a hydrologic model that simulates streamflow and 3) a water resources model simulating the operations of each facility. Appropriately representing regional rainfall characteristics, including the natural variability and uncertainty associated with the observed record, requires that a WG produce a sufficiently large number of realizations. For these basins, an hourly time scale is necessary to accurately simulate input to the hydrologic models.

For the USCR Basin, we used a groundwater reservoir model to estimate recharge and water storage in conjunction with prescribed groundwater withdrawal management. For the Bill Williams River (BWR) Basin, we used a lake model based on the Army Corps of Engineers recommended operational rules to simulate the water levels and outflow from Alamo Lake.

The WGs were initially created to represent the variability of the observed historical precipitation record. They were modified to simulate ensembles of likely-to-occur realizations of projected mid-21st century precipitation as inferred from the downscaled simulations. These modifications are based on analyses comparing the climate model simulations of the historic period (1950-2005) with the projected mid-21st century models (2020-2059) for key inter- and intra-seasonal characteristics. Seven ensembles were created, one representing the historic period and six representing the projected mid-21st century changes in precipitation, as inferred from the analysis of inter- and intra-seasonal characteristics. These hourly precipitation ensembles were used as input to the modeling framework described above.

For the USCR watershed, we analyzed the 40-year cumulative deficit of groundwater withdrawal. This is the volume of water required from an alternative source to fully satisfy the water demand for the city of Nogales under specified groundwater withdrawal conditions over 40 years. This index provides critical information for Reclamation's on-going Nogales Area Water Storage Study, which is evaluating future water needs and developing alternatives for improving water supply and storage. For the BWR Basin, we estimated the cumulative time that projected water levels at Alamo Lake will drop below the target operational and the recreation threshold level. We also examined the projected impact of climate change on large precipitation events and the chance for a spill over the dam's crest or large releases.

In both basins, the dynamically downscaled MPI and HAD simulations yielded contradictory results. While the DD-HAD projected a wetter future, the DD-MPI projected a drier future. The statistically downscaled HAD projection also predicted a slightly wetter future in the BWR Basin. For both watersheds, the changes projected by the dynamically downscaled projections are larger than the statistically downscaled projections, for both wetter and drier futures.

The results provide critical information for Reclamation planners concerned with estimating future water supply and demand. To evaluate the full range of future risks, it may be prudent to include dynamically downscaled simulations in a water resources analysis. In addition, the study shows that changes in rainfall patterns can be magnified as the precipitation is converted to streamflow and then to stored water. Even a relatively small change in projected precipitation may be of concern if the hydrologic system of interest resembles those described in this study.

This page intentionally left blank.

II. Background

Under the Council for Environmental Quality's Principles and Requirements for Federal Investments for in Water Resources (March 2013), federal investments in water resources require an evaluation of risk and uncertainty using the best available science. Spatial downscaling of global climate model outputs to basin-relevant scales is one area of scientific uncertainty noted in Reclamation's 2016 SECURE Water Act Report to Congress. Reclamation's "Technical Guidance for Incorporating Climate Change Information into Water Resources Planning Studies" document also discusses the importance of selecting the appropriate set of climate projections for water management planning studies. This guidance document requires staff to understand the strengths and weaknesses of available climate projections and to assess which set is appropriate for a given study.

At present, little is known about the impact of the choice of spatial downscaling method on the outcome of the water resources assessments performed for Reclamation's planning studies. This analysis compares the results of the two fundamental downscaling approaches, statistical downscaling and dynamical downscaling, for areas where regional and local scale precipitation phenomena are understood to be important. The authors also evaluated the use of a stochastic rainfall generator, or weather generator, forced by either Global Climate Models (GCMs) or Regional Climate Models (RCMs) for this study.

This investigation targets primary aspects of Reclamation's mission - river operations and drought resilience - in areas where the selection of a downscaling method may have a significant impact on the results of a water resources assessment. To investigate the range of impacts associated with the choice of a downscaling method, we compare the results of hydrologic models for both flooding and water supply evaluations. Flooding assessments are concerned with short-term, high precipitation events and stream flow levels, water supply studies consider long-term hydrologic patterns. In considering the effects of drought on water supplies, the continuous duration of low precipitation and low stream flow levels are of particular concern. Through this study, we investigate the impact of spatial downscaling on both types of studies and their hydrologic variables of interest

This page intentionally left blank

III. Introduction

This study explores the range of uncertainty attributable to the method of spatial downscaling for a flood control and water supply application. Both assessments address relatively small, semi-arid Arizona basins with highly variable precipitation patterns and a strong monsoon signal. In these basins, streamflow levels are tightly coupled with the nuances of rainfall events (e.g. hourly precipitation patterns). For an accurate assessment, it is necessary to reproduce not just the mean rainfall, but also the statistical variability and the number of rainfall events.

We explicitly compare the effect of two fundamental approaches to spatial downscaling: statistical downscaling (SD) and dynamical downscaling (DD), with the use of raw Global Climate Model (GCM) output. SD procedures derive empirical relationships between the atmospheric forcing data of the GCM and the surface variable of interest at a finer resolution and apply those relationships to GCMs' projections. SD assumes that the statistical relationships between the predictors (GCM) and predictand (surface variables) do not change over time and are therefore stationary (e.g., Carpenter and Georgakakos, 2001).

The main advantage to the SD procedures is no requirement for special technical expertise or special computational resources. Therefore, they can be used to produce high-resolution simulations and can be applied to many GCMs and emissions scenarios. For this study, we used SD projections from the Localized Constructed Analogs (LOCA) dataset produced by researchers at Scripps Institution of Oceanography at the University of California San Diego (Pierce et al., 2014).

Dynamically downscaled (DD) projections use Regional Climate Models nested within the GCM to simulate local climate features. They respond in physically consistent ways to resolve regional atmospheric processes and simulate mesoscale variables of interest, such as convective storms, extreme events, and snowfall versus rainfall. They simulate internally consistent multivariate quantities within an atmospheric column. DD projections require a high level of expertise to produce as well as intensive computational resources. Consequently, DD simulations are only available for a limited number of GCMs and emissions scenarios. The requirement for intensive computational resources also puts a practical limit on the spatial resolution of DD simulations.

The pros and cons of selecting a downscaling approach have been the subject of multiple manuscripts (e.g. Fowler et al. 2007; Maraun et al. 2010; Kotamarthi et al. 2016). Basin-scale hydrologic assessments often face the dilemma of having to choose between SD and DD approaches. SD simulations are easier to obtain and there are several readily available datasets that include simulations for many GCM runs. DD simulations, however, are available for only a few GCMs and emissions scenarios, and their spatial resolution may be relatively coarse.

This study is geared to evaluate the impact of these downscaling approaches on two assessments of semi-arid basins with event-based hydrology, where the monsoon rains play a key role in the hydrologic cycle (Figure 1). The Upper Santa Cruz River (USCR) Basin is the site of Reclamation's Nogales Area Water Storage Study, an appraisal-level study which focuses on enhancing water supplies for the city of Nogales, Arizona, on the U.S.-Mexico border. This region has experienced several years of drought and projections for water storage needs developed a decade ago may no longer reflect the current hydrology of the basin.

We also examined potential changes in the flood control capacity of Alamo Lake in western Arizona. Alamo Dam serves to regulate the Bill Williams River (BWR) and is located directly upstream of the Central Arizona Project (CAP) intake on Lake Havasu. The CAP provides about 1.5 million acre-feet of renewable water resources to cities, farms and tribes in Arizona.

Reclamation staff expressed concern that changing precipitation patterns in the BWR Basin might interfere with downstream water quality, CAP diversions, and Lake Havasu reservoir regulation and therefore supported an investigation of the impacts of downscaling methods on projections of flood control capacity.

Rainfall in both the Upper Santa Cruz River and BWR Basins is highly variable over seasonal and diurnal scales. This situation is conducive to the use of a weather generator to simulate a distribution of model outcomes, rather than the mean only. A weather generator is a probabilistic model that can develop a large number (ensemble) of plausible "weather realizations" for a particular set of atmospheric conditions.

Each realization is run through a surface hydrology model, producing a probability distribution of, for instance, runoff volumes. The use of a weather generator produces a description of the range of future runoff volumes rather than a single projection of mean runoff. This study refined an existing weather generator for the USCR Basin and developed a custom weather generator for the BWR Basin.

Following the description and evaluation of the selected Global Climate Models and the statistical and dynamical downscaled simulations in Sections IV.A and IV.B, we present the impacts on the water resources assessments for the Upper Santa Cruz River and the Bill Williams River watershed, respectively. Summary and conclusions are provided in Section VII.

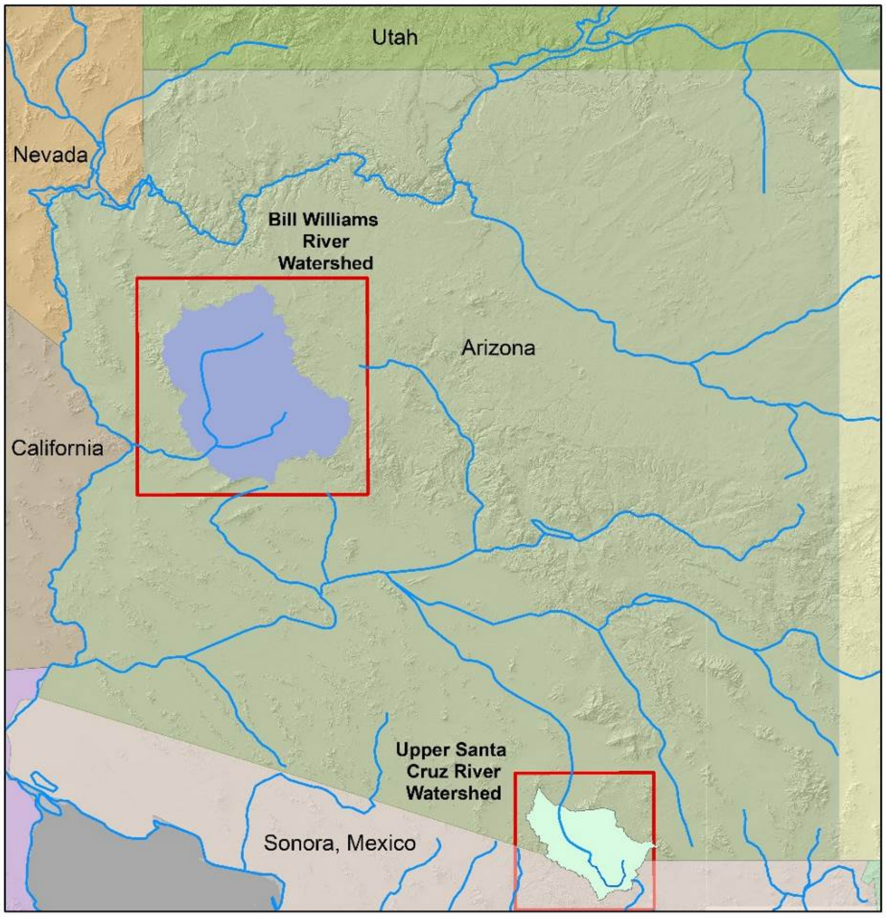

Figure 1: A map of the study areas.

The two watersheds are indicated as shaded polygons and the red squares outline the domains that were used for the climate analyses.

This page intentionally left blank.

IV. Climate Models

A. Selected Global Climate Models (GCM)

Three GCMs from the Coupled Model Intercomparison Project Phase 5 (CMIP5), simulated with Representative Concentration Pathways 8.5 (RCP 8.5), were selected for this study. The selected GCMs are: 1) HadGEM2-ES (Global Environmental Model, Version 2 from the United Kingdom Meteorological Office, the Hadley Centre), 2) MPI-ESM-LR (Earth System Model) running on low resolution (LR) grid from the Max Planck Institute for Meteorology, and 3) GFDL-ESM2M (NOAA Geophysical Fluid Dynamic Laboratory – Earth System Model). These GCMs were selected for dynamical downscaling due to the high quality of their performance over North America and because they represent the range of sensitivities provided by all CMIP5 GCMs over North America (Sheffield et al. 2013 a, b).

DD precipitation simulations of the three GCMs are available for the historic period (1950-2005) and future projections (2006-2100) at ~25 km (~15.5 miles) horizontal grid resolution from the National Center for Atmospheric Research (NCAR) and the University of Arizona, Department of Hydrology and Atmospheric Sciences. The simulations followed the specifications of the North America Coordinated Regional Climate Downscaling Experiment (NA-CORDEX) program (https://na-cordex.org/), an initiative sponsored by the World Climate Research Program to provide dynamically downscaled climate simulations for studies of regional climate change impacts.

The three GCMs were downscaled for the domain of the NA-CORDEX program using the Advanced Research version of the Weather Research and Forecasting (WRF) model (Version 3.1) as the Regional Climate Model. The configuration of the WRF model is described in Castro et al. (2017). The simulations are available at 3-hour intervals for the WRF-HadGEM2-ES, and six-hour intervals for the WRF-MPI-ESM-LR and WRF-GFDL-ESM2M. An equivalent WRF reanalysis six-hour precipitation dataset (1979-2015) nested within ERA-Interim global reanalysis (Dee et al. 2011) is also available at a similar spatial resolution and model configuration as the GCM DD simulations.

SD daily precipitation for 1950-2005 and 2006-2099 at 1/16° (~6km, 3.7 miles) horizontal grid spacing for the three CMIP5 RCP 8.5 GCMs is available for the western U.S from the state-of-the-art Localized Constructed Analogs (LOCA) methodology (Pierce et al., 2014). LOCA's leading downscaling assumption is that the projected period will evolve in the same way as the best matching historical event. An observed gridded precipitation dataset with similar spatiotemporal resolution for 1950-2015 is available from Livneh et al. (2013). This dataset, which was used as the reference for the derivation of the LOCA dataset, was developed for the conterminous Mexico, and U.S. and regions in Canada south of 53° N latitude.

GCMs used for water resources impact assessments in the Southwest U.S. should represent the region's distinctive winter and summer precipitation characteristics. The prevailing winter storms from November to March primarily originate from large-scale low-pressure frontal systems approaching from the west and southwest. These storms may last for a few days, drop persistent rain over large areas and often produce snowfall at higher elevations. In our study areas the snow commonly melts within a few days and is not a major contributor to runoff into the USCR or Alamo Lake.

The prevailing summer rainfall from June to September is driven by the North American Monsoon (NAM) climate system. This system triggers isolated convective cells, often producing intense short-lived rainfall events. Winter rainfall events generate gradually rising streamflow events, with low flows that persist following a rain event. Summer rainfall events trigger quick and sudden rising flows followed by short-lived low flows.

A comprehensive evaluation of GCMs for winter precipitation is available from the California Department of Water Resources (2015) which used a 3-step model screening process to evaluate the historical performance of 31 CMIP 5 GCMs at three spatial scales: global, Southwestern U.S, and California. Most winter storms in Arizona originate in the mid-latitude Pacific Ocean and cross over California, so this evaluation is also useful for Arizona. In this analysis, the HadGEM2-ES was one of the ten top performing GCMs while the MPI-ESM-LR and GFDL-ESM2M were among the 15 top performing models.

The ten GCMs selected for their realistic representation of California’s hydrology and water management metrics and their institutions are listed in Table 1. The evaluation metrics used for this analysis are presented in Table 2.

Table 1: List of ten GCMs identified by the California Department of Water Resources that provide realistic historical simulations of global, Southwestern U.S. and California climate measures.

Ref: (California Department of Water Resources, Perspective and Guidance for Climate Change Analysis, August 2015, Climate Change Technical Advisory Group, p.32)

Model Name	Institution
ACCESS-1.0	CSIRO (Commonwealth Scientific and Industrial Research Organization, Australia), and BOM (Bureau of Meteorology, Australia)
CCSM4	National Center for Atmospheric Research
CESM1-BGC	National Science Foundation, Department of Energy, National Center for Atmospheric Research
CMCC-CMS	Centro Euro-Mediterraneo per I Cambiamenti Climatici
CNRM-CM5	Centre National de Recherches Meteorologiques / Centre Europeen de Recherche et Formation Avancees en Calcul Scientifique
CanESM2	Canadian Centre for Climate Modeling and Analysis
GFDL-CM3	Geophysical Fluid Dynamics Laboratory

HadGEM2-CC	Met Office Hadley Centre
HadGEM2-ES	Met Office Hadley Centre (additional HadGEM2-ES realizations contributed by Instituto Nacional de Pesquisas Espaciais)
MIROC5	Atmosphere and Ocean Research Institute (The University of Tokyo), National Institute for Environmental Studies, and Japan Agency for Marine-Earth Science and Technology

Table 2: Evaluation Metrics for Selection of Global Climate Models by California Department of Water Resources

Ref: (California Department of Water Resources, Perspective and Guidance for Climate Change Analysis, August 2015, Climate Change Technical Advisory Group, p.26).

Scale of Analysis	Metric
Global	Longwave (LW) or Shortwave (SW) Cloud Radiative Effects
	Top of the Atmosphere Reflected Shortwave & Longwave Radiation
	Total Precipitation
	Surface Air Temperature
	Geopotential Height
	Meridional (VA, North-South) and Zonal (UA, West-East) wind speeds at two different levels in the atmosphere 200hPa and 850hPa
	Temperature at two different levels in the atmosphere 200hPa & 850hPa
Western U.S.	Mean Annual Temperature (T) and Precipitation (P), 1960-1999 DTR-MMM
	Mean diurnal temperature range, 1950-1999
	Mean amplitude of seasonal cycle (temperature and precipitation)
	Correlation of simulated with observed the mean spatial pattern of temperature and precipitation, 1960–1999
	Standard deviation of the mean spatial pattern of temperature and precipitation, 1960-1999
	Variance of temperature calculated at frequencies (time periods of aggregation) ranging for N=1 and 8 years, 1901–1999
	Coefficient of variation (CV) of precipitation calculated at frequencies (time periods of aggregation) ranging for N=1 & 8 water years, 1902–1999
	Linear trend of annual temperature and precipitation, 1901–1999

	Correlation of winter temperature and precipitation with Niño 3.4 index, 1901-1999
	Hurst exponent using monthly difference anomalies (T) or fractional anomalies (P), 1901-1999
California	Standard deviation of 10-year totals of the number of dry years
	Maximum 3-day total precipitation, as a ratio of average water year precipitation 1961-1990 (%)
	Spatial structure of correlation of precipitation to the Niño 3.4 ENSO index derived from a GCM, gauged by pattern correlation to that from historical observations
	Niño 3.4, temporal variation, a measure of the El Niño Southern Oscillation

Representing the NAM in the relatively spatially coarse GCM is a challenge, since it is dominated by regional (mesoscale) processes, e.g. Castro et al. 2012 and 2017; Bukovsky et al. 2013 and; 2015, Geil et al. 2013). Evaluation of large-scale features of the NAM system by GCMs is an active research topic (Arritt et al. 2000; Liang et al., 2008; Lin et al., 2008; Geil et al. 2013; Pascale et al., 2016). The selected GCMs for this study were selected to represent the NAM's large-scale features well (Geil et al., 2013).

B. Evaluation of the Historic Period Simulations of the Selected Global Climate Models

The evaluation of the GCMs' performance was conducted for the domains of the two watersheds as indicated in Figure 1. In Figures 2 and 3, we compare the average monthly total precipitation (upper panels) and the average monthly number of daily rainfall events (lower panels) for the SD, DD, raw GCM, WRF ERA-Interim reanalysis, and gridded observations for the historical period, 1950-2005. The one exception to this date range is the WRF ERA-Interim Reanalysis, which is shown for 1979-2015. These variables are shown for the Had-GEM2-ES (left), MPI-ESM-LR (center), and GFDL-ESM2M (right). Figure 2 displays the values for the USCR Basin, Figure 3 is for BWR Basin. These figures compare the spatial averages over the watersheds domain as shown in Figure 1.

The SD simulations closely follow the observed gridded dataset. This is expected because the LOCA SD procedure was designed to conform to the observed record of Livneh et al. (2013). The WRF ERA-Interim reanalysis follows the seasonal patterns fairly well, except for overestimating the August and September rainfall in USCR Basin. Since this overestimation is not apparent in the frequency of occurrence (lower panels), it is attributed to the WRF simulations of rainfall depth. In the BWR Basin, the only apparent deficiency of the WRF simulation is the underestimation of the number of rainfall events in July (Figure 3, lower panels). This relatively good performance is indicative of the skill of WRF for producing monthly climatological averages when it is nested within optimal boundary conditions.

The WRF was used as the regional climate model to dynamically downscale the three GCMs. The influence of WRF is seen by comparing the raw GCMs to the DD simulations. In the USCR, marked differences are seen for the summer, where raw GCMs underestimate the precipitation. However, the DD HAD simulation overestimates the monthly mean precipitation. The MPI raw GCM captures the seasonal climatology fairly well and the use of WRF does not add value in this analysis. In the BWR Basin, the WRF creates a monsoonal signal that was missing from the raw GCM but yields an overestimate of the summer rainfall. For the MPI, the WRF improves the GCM performance during the winter months. The GFDL GCM lacks the summer rain signal and the WRF creates summer rain that is lagged by about two months for both the USCR and BWR Basins.

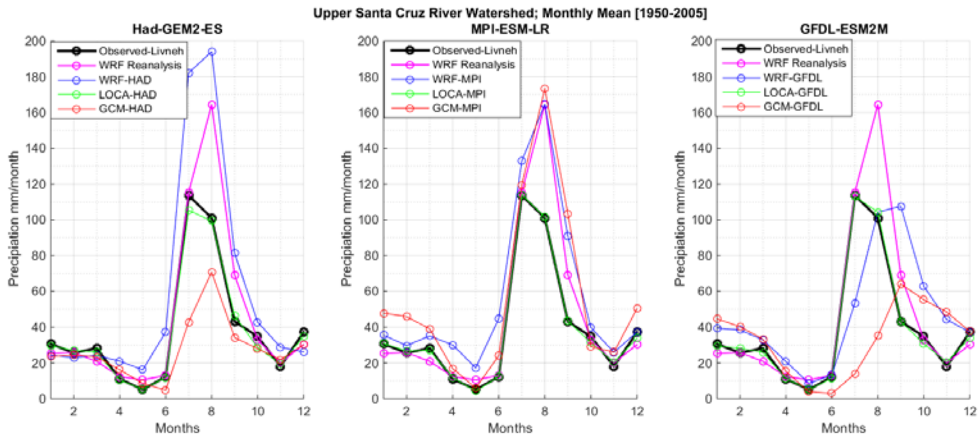

Correlation Coefficient, Monthly Mean Precipitation	HAD	MPI	GFDL
DD	0.96	0.92	0.64
SD	>0.99	>0.99	>0.99
GCM	0.87	0.91	0.07

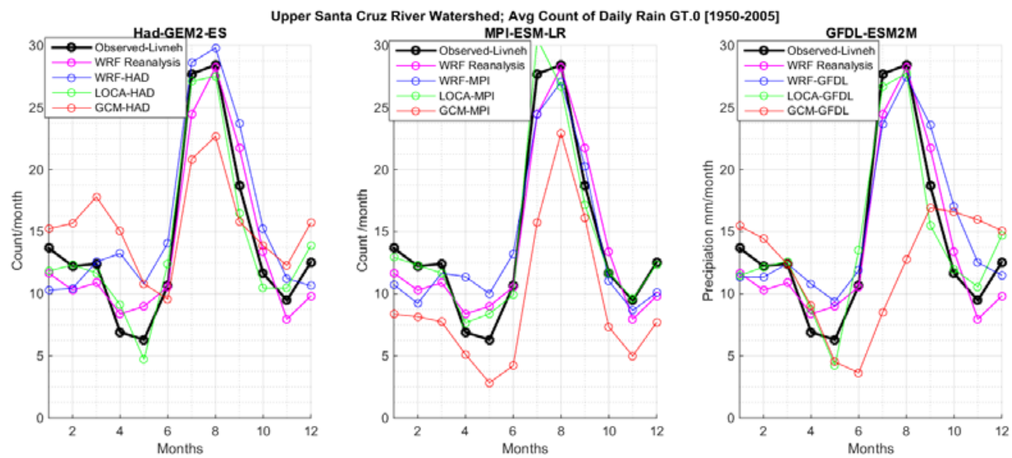

Correlation Coefficient, Average Count Daily Rain Events	HAD	MPI	GFDL
DD	0.91	0.93	0.91
SD	0.97	0.98	0.97
GCM	0.84	0.94	0.14

Figure 2: Upper Santa Cruz River Basin mean areal average monthly precipitation totals (upper panels) and average number of daily rainfall events (lower panels)

From observations, WRF reanalysis, DD, SD, and raw GCMs for the HAD, MPI, and GFDL from left to right, respectively. The analysis is shown for 1950-2005 except from the WRF ERA reanalysis that is available for 1979-2015.

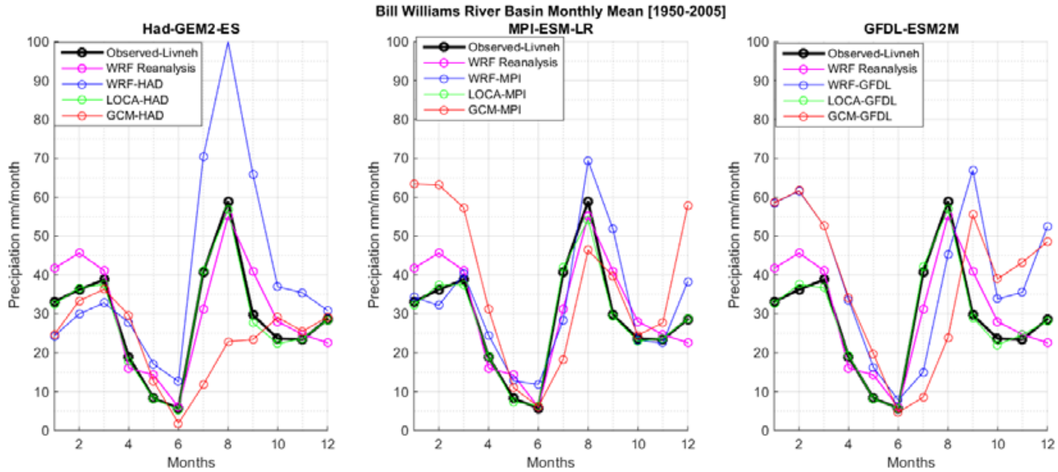

Correlation Coefficient, Monthly Mean Precipitation	HAD	MPI	GFDL
DD	0.8	0.85	0.51
SD	>0.99	>0.99	>0.99
GCM	0.42	0.61	0.26

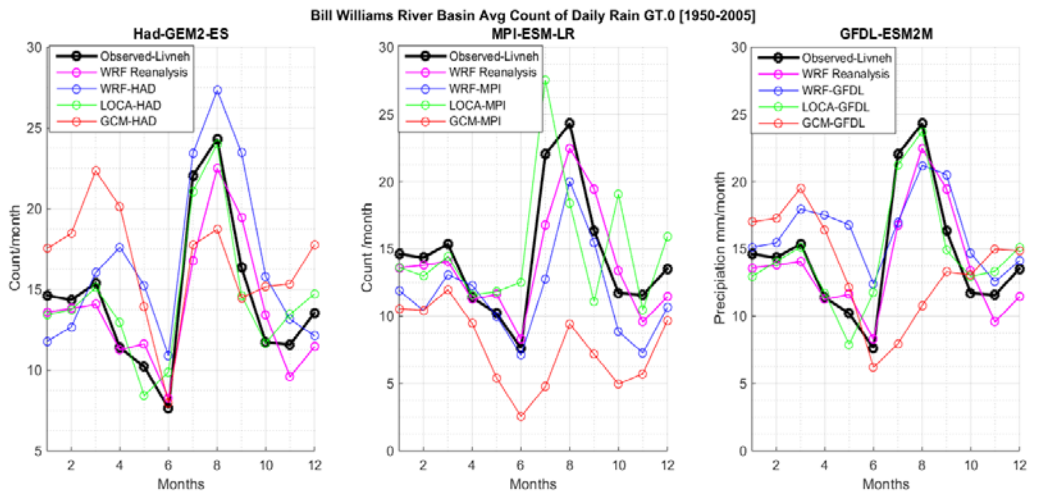

Correlation Coefficient, Average Count Daily Rain Events	HAD	MPI	GFDL
DD	0.81	0.84	0.69
SD	0.96	0.64	0.92
GCM	0.5	0.31	-0.1

Figure 3. Same data reflected for the Bill Williams River.

This page intentionally left blank.

V. Case Study I: Climate Change Impact Assessment in the Upper Santa Cruz River Watershed

A. Study Area: Upper Santa Cruz River Watershed (USCR)

The Santa Cruz River is an ephemeral tributary in southern Arizona that drains into the Gila River, a branch of the Colorado River (Figure 4). The drainage area at the USGS Nogales streamflow gauge (USGS # 09480500), about 10 km (6.2 miles) east of the city of Nogales, Arizona, is 1,400 km^2 (540.5 square miles), of which approximately 1,150 km^2 (444 square miles) are in Mexico. From its headwaters in the San Rafael Valley in southern Arizona, the river flows southward into Mexico and bends northwards towards Arizona to re-cross the international border. The river length in Mexico is about 60 km (37 miles) and includes short sections with perennial flow. The drainage area is sparsely populated, and its landscape is comprised of heavily grazed desert scrub with deciduous broad leaf forest in the higher elevations. Downstream of the USGS Nogales gauge near the border crossing, there is a series of four relatively small, shallow alluvial aquifers (microbasins) bounded by the low permeability Nogales Formation. The microbasins are separated from each other by outcrops of the less permeable Nogales formation and/or shallow bedrock that limit the hydraulic connection between them (Page et al., 2016; Halpenny and Halpenny, 1988).

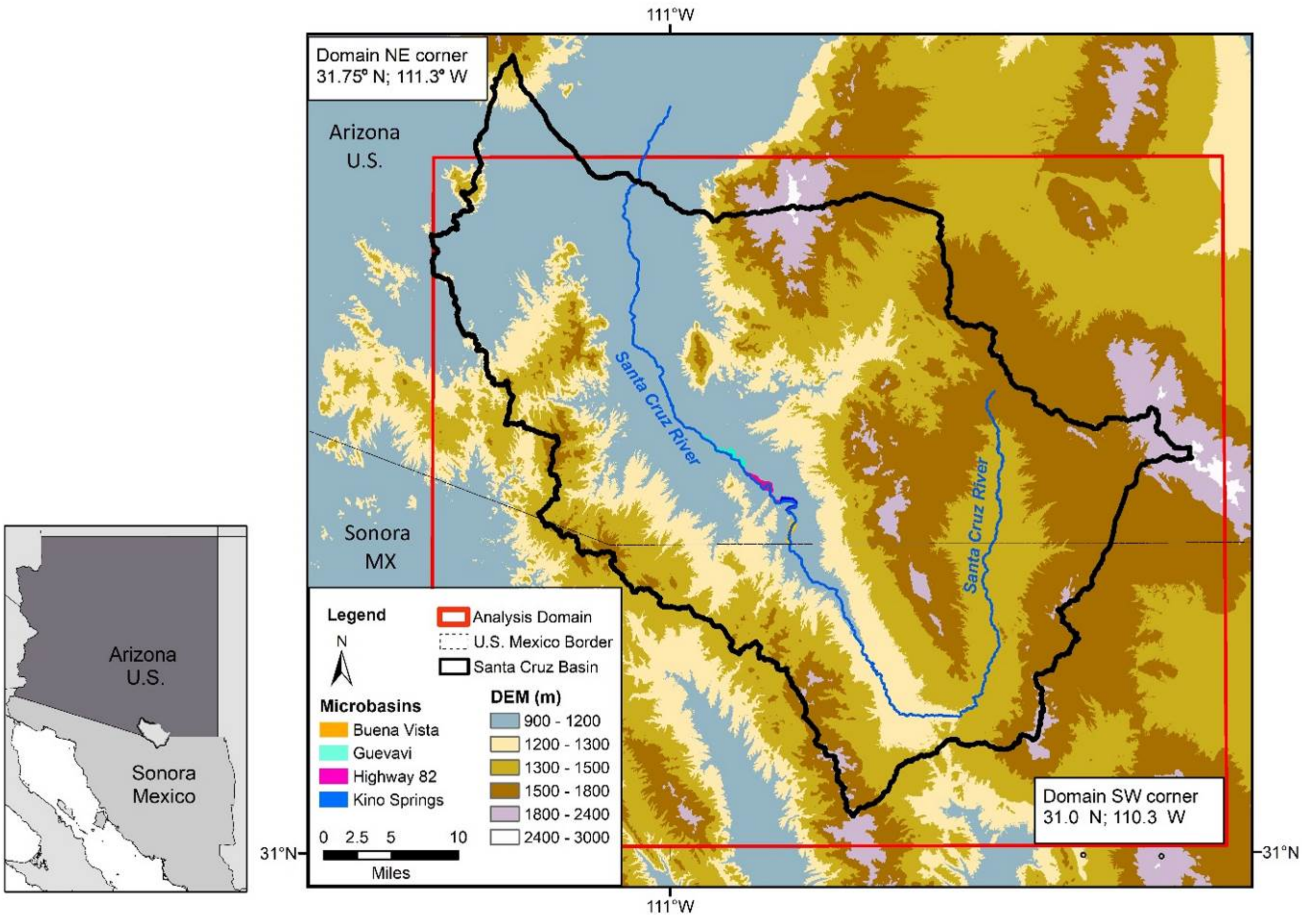

Figure 4a: Map of the Upper Santa Cruz River.

The red outline indicates the domain of the climate analysis.

The younger alluvium in the four microbasins is a highly productive geologic formation with transmissivity values ranging from 400 to 2,800 m^2 d^{-1} (4,305 to 30,100 ft^2 d^{-1}) (Erwin, 2007). The thickness of the younger alluvium in the microbasins ranges from 10 to 40 meters (~33 to 131 feet) (Erwin, 2007).

Recent and yet unpublished modeling results, geophysical studies, and exploration borings indicate the existence of a deep underflow zone out of the microbasins. For instance, during long periods without streamflow recharge, water levels in the microbasins drop considerably. This underflow from the microbasins is estimated at about 4,000-6,000 ac-ft yr^{-1} (~5 - 7.5 Mm^3 [million cubic meters] yr^{-1}). Recently, it was estimated that about 4,000 ac-ft yr^{-1} (~5 Mm^3 yr^{-1}) of groundwater flows north from the Guevavi microbasin (the northernmost microbasin) to the downstream aquifer. This is likely a larger amount than the receiving underflow that crosses from Mexico to the Buena Vista microbasin (the southernmost microbasin) (Figure 4b). The net water loss from the microbasins compounds the impact of drought on water resources in this region.

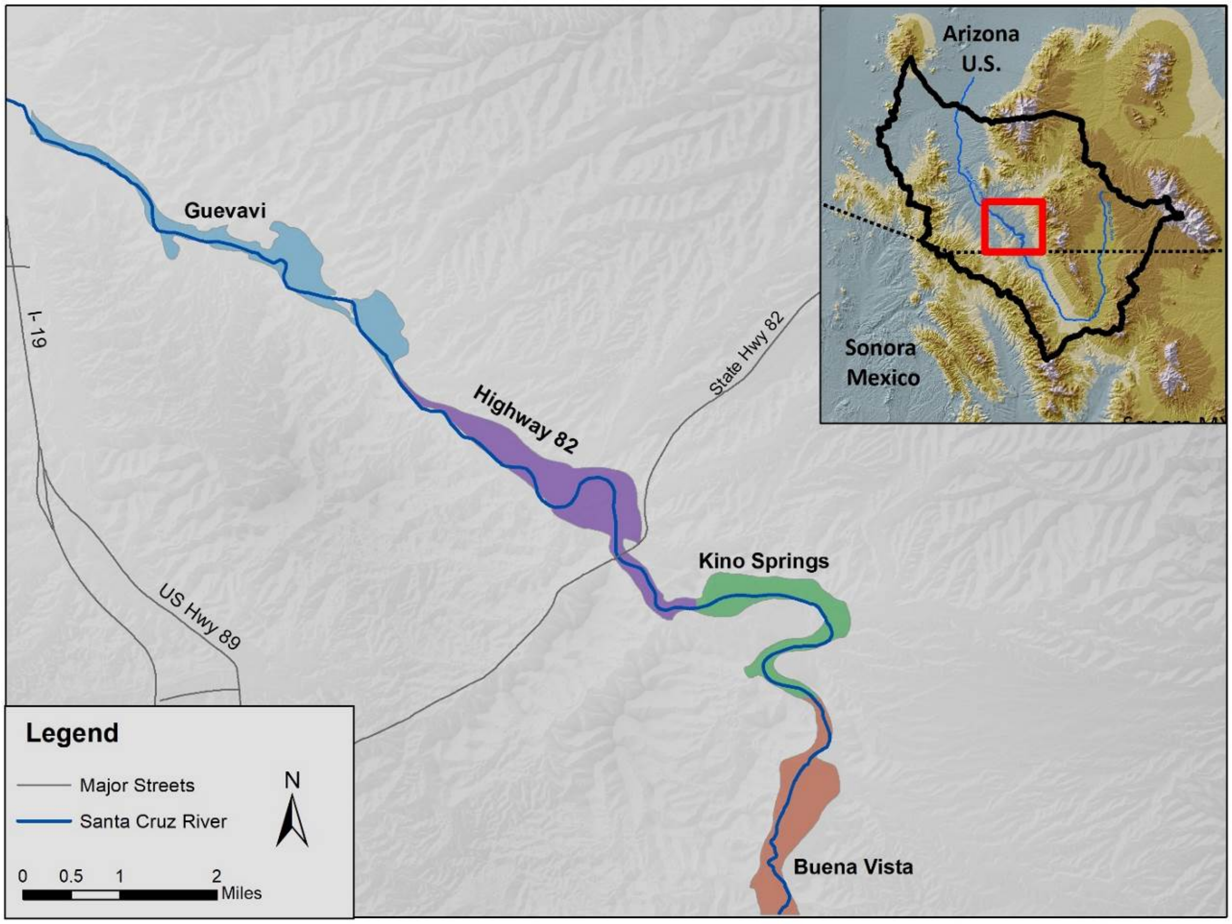

Figure 4b: Close-up map of the microbasins.

The seasonal hydrologic response and inter-annual variability in the USCR Basin are briefly discussed below. In Figure 5, the gauge-observed total annual streamflow and precipitation are shown for the summer (black) and winter (red) in the upper and lower panels, respectively. The straight lines in these figures are the arithmetic seasonal averages. Although the winter and summer average streamflow are almost equal, the average summer rainfall is more than twice of the average winter rainfall (220 mm versus 100 mm; 9 versus 4 inches). These differences between the summer and winter rainfall and streamflow exemplify the distinctively seasonal spatial and temporal variability of rainfall and its impact in streamflow generation (Shamir et al., 2007a).

While the average streamflow for both winter and summer is about 10 million m^3 yr^{-1} (8,100 acre-feet per year), the large inter-annual variability means that arithmetic averages have little value for projecting flow or for water resources management planning. The inter-annual variability can be demonstrated by the fact that 23% [33%] of the winters were above average for streamflow [rainfall] and 36% [43%] of the summers were above average for streamflow [rainfall]. This positively skewed characteristic implies that most years are relatively dry, and the infrequent wet seasons contribute to the relatively high average values.

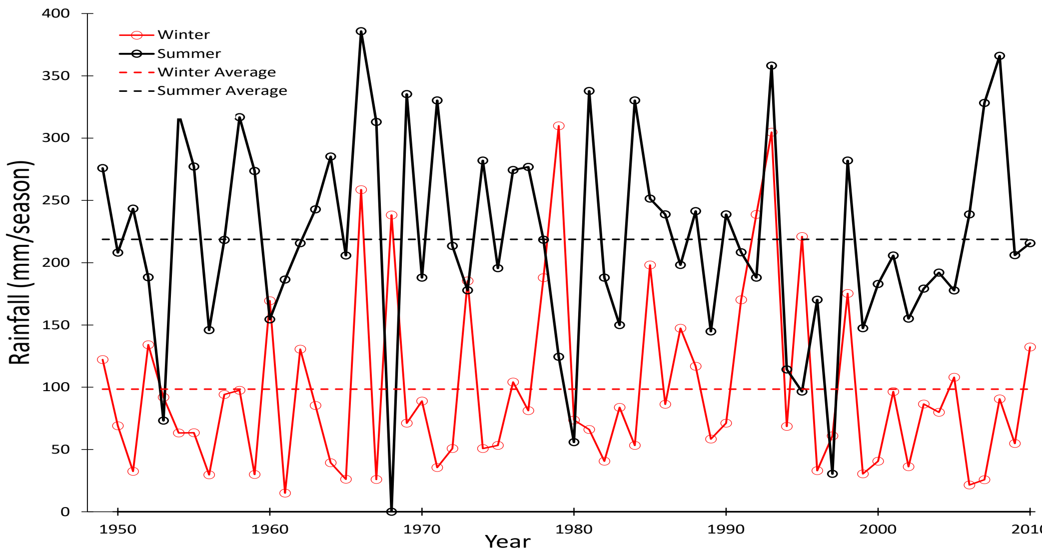

Figure 5: Summer (black) and winter (red) seasonal streamflow volume (upper panel) and total seasonal rainfall (lower panel) time series in the Nogales area.

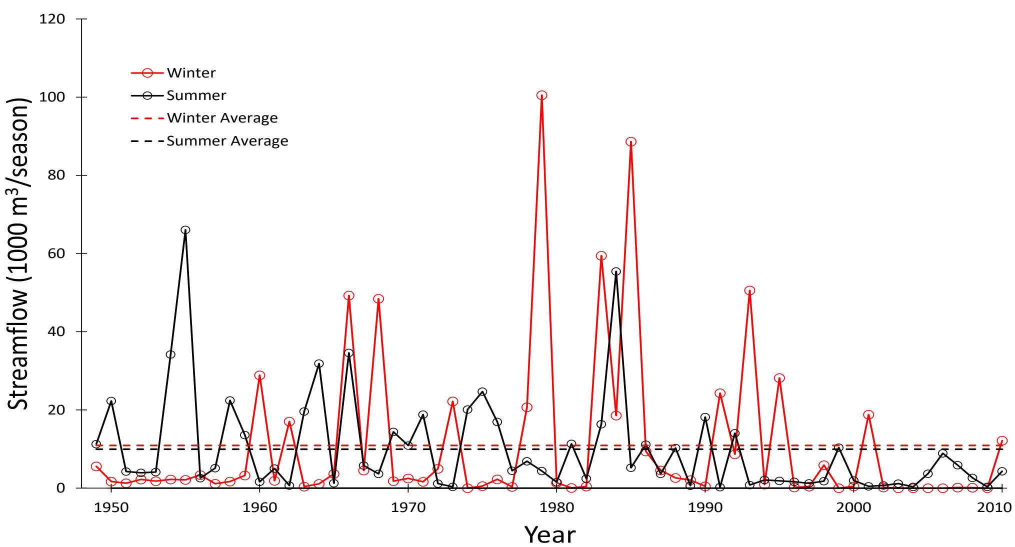

Straight lines indicate the arithmetic inter-annual averages.

B. Analysis of the projected future changes in precipitation

The projected changes in total seasonal precipitation by the three GCMs and their respective SD and DD simulations are examined for the winter and summer seasons in Figures 6 and 7. The red dashed lines in these figures mark the 33.3 and 66.7 quantiles for the historic period (1950-2005) and two future projected horizons (2020-2059 and 2060-2099). The red tercile lines indicate the interpretation of changes in the frequency of occurrence of three wetness categories (i.e. wet, medium, dry). For example, in Figure 6 - the WRF-MPI (DD-MPI), the upper tercile of the 2020-2059 projected horizon is visibly lower than the upper tercile of the historic period. This implies that the DD-MPI projects a decrease in the frequency of occurrence of wet winters. In addition, the lower tercile of the 2020-2059 projected horizon is lower than the historic lowest tercile. This indicates that the frequency of dry winters is projected to increase.

Notable results for the projected mid-21st – century (2020-2059) indicated that for the raw GCMs, only the GFDL has a clear signal of a projected increase in occurrences of dry winters. All the SD and DD simulations project increased frequency of dry winters and decreased frequency of wet winters. The outlier is the downscaled simulation in DD-HAD which projects an increase in the frequency of wet winters and dry winters meaning the DD-HAD projects less frequent medium winters.

Similarly, in Figure 7, we examine the climate model projections for the summer season. A clear signal of dryer summers is projected in the SD, DD and raw MPI models. These three models clearly indicate an increase in the frequency of dry summers and a decrease in frequency of wet summers. A similar trend appears for the raw HAD, but the DD-HAD displays a contradictory trend of more wet summers in the 2020-2059 period and decreased frequency of both wet and dry summers in the 2060-2099 period. The SD-HAD does not show significant changes in the projected mid-21st century. The GFDL does not show a substantial trend, except for a clear signal of wetter summers in the raw GCM and both downscaled simulations.

The projected frequencies of the wetness categories in the mid-21st century, as defined by the tercile of the historic period, are listed in Table 3. Probabilities that are significantly different than the historical period are indicated with asterisks. The significance test was determined by conducting a Monte Carlo experiment with 100,000 iterations in which the terciles were identified from 40 values randomly sampled from a uniform distribution.

In this experiment, we found that 5% of the terciles were below 0.22 and above 0.46 and 1% of the terciles were below 0.18 and above 0.51. It can be deduced that a projected wetness category with a frequency that is either below 0.18 or above 0.51 has chance of less than 1% of being selected from a uniform distribution. If this is the case, we assume that the frequency of the projected wetness category is significantly different than 33%

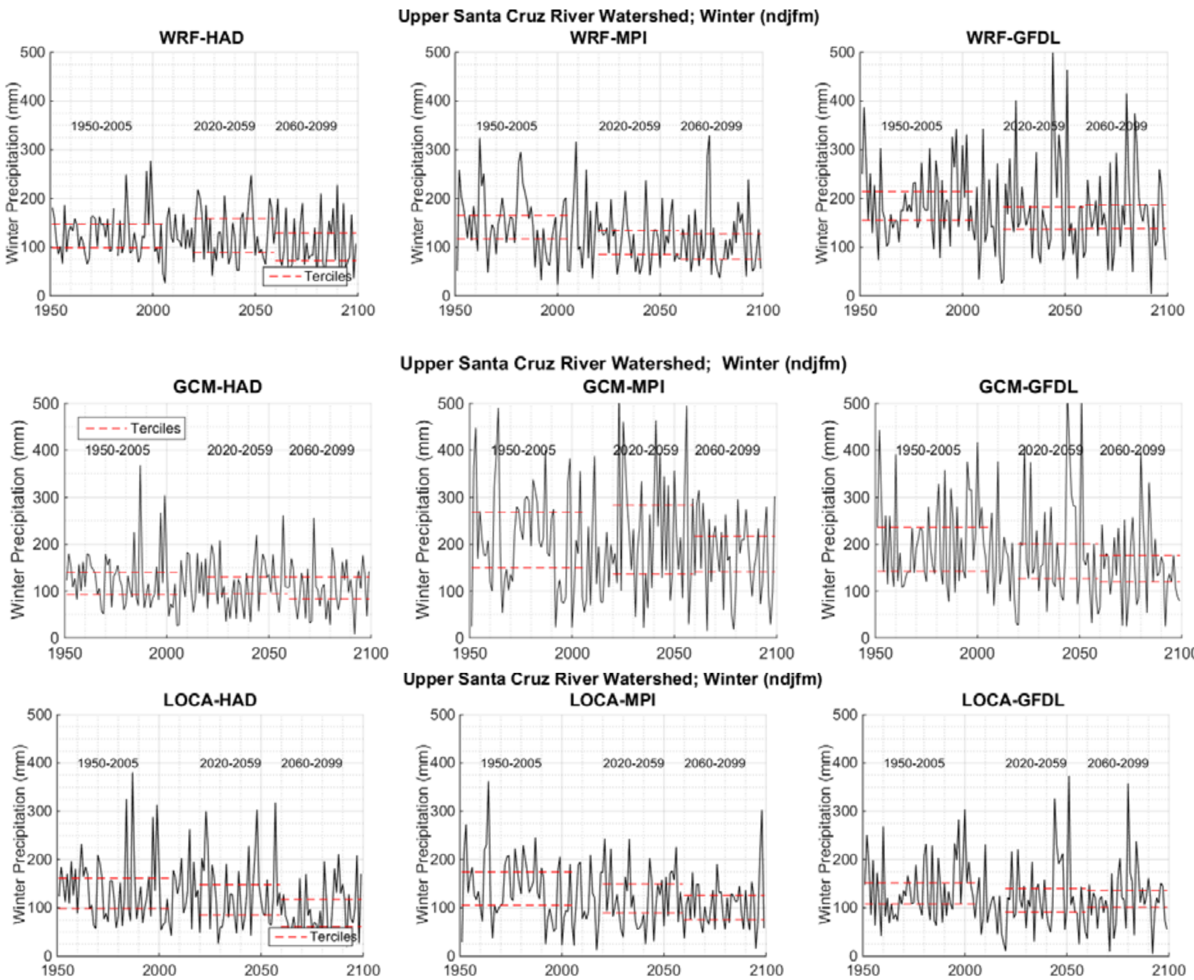

Figure 6: Total winter (November–March) mean areal precipitation over the study domain during 1950-2099 for the DD (upper row), SD (middle row), and raw GCMs (lower row).

The dashed red lines mark the 33.3 and 67.7 quantiles during 1950-2005, 2020-2059, and 2060-2099.

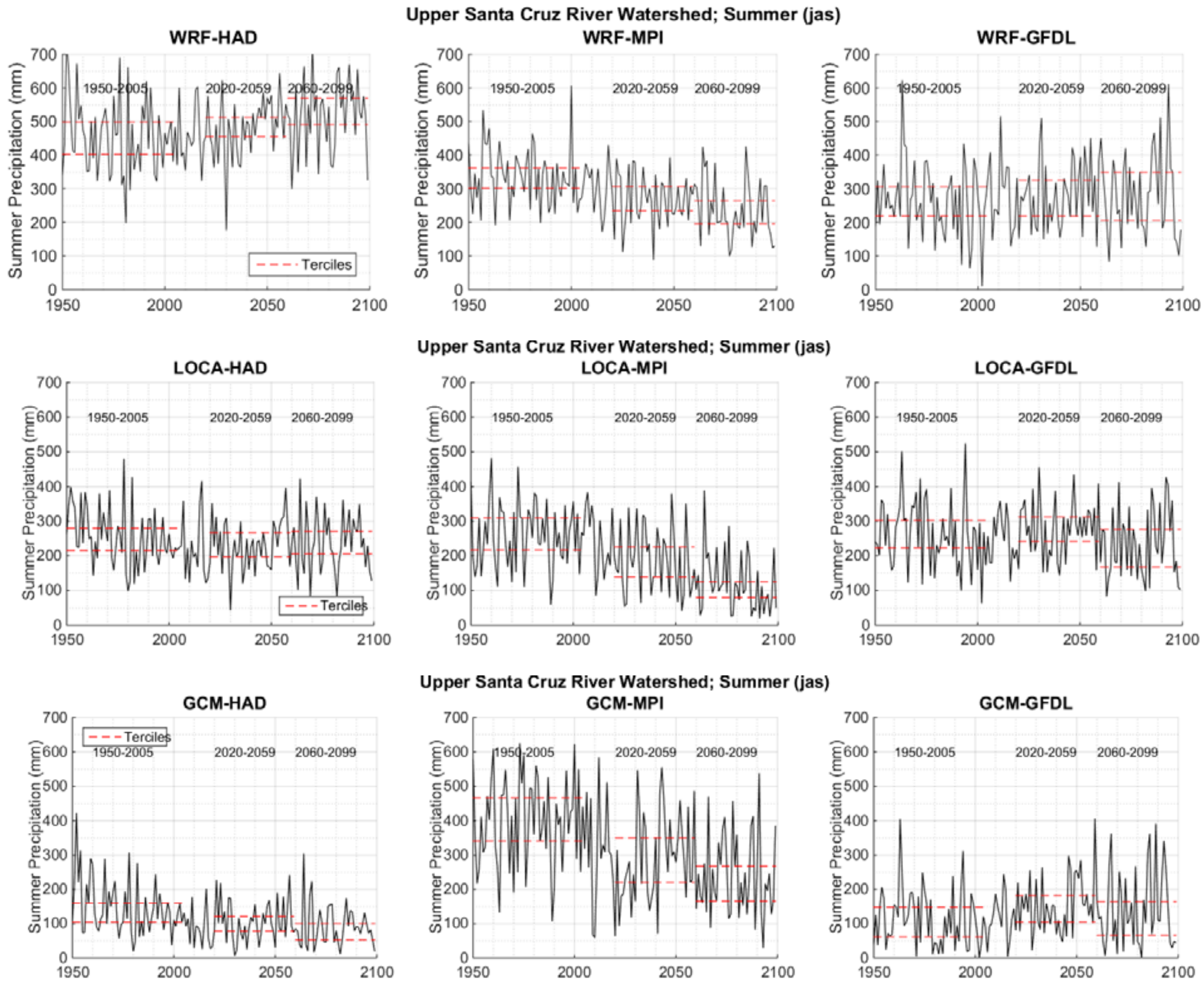

Figure 7: As Figure 6 but for the summer (July-September).

The projected chance of the historic wetness categories occurring in the 2020-2059 period for the different climate models and downscaling procedures are shown in Table 3. These probabilities were derived by identifying the percentiles in the future projections using the terciles' values in the simulation of the historic period (1950-2005). Simply stated, we identified the probability of the projected simulations present in a given wetness category, as defined by the simulation of the historic record.

Table 3. Projected 2020-2059 probabilities of occurrence for the wetness categories.

WINTER									
	DD			SD			GCM		
	Dry	Normal	Wet	Dry	Normal	Wet	Dry	Normal	Wet
HAD	0.4	0.2*	0.4	0.4	0.3	0.3	0.325	0.425	0.25
MPI	0.525**	0.35	0.125**	0. 5*	0.15**	0.35	0.425	0.225	0.35
GFDL	0.5*	0.25	0.25	0.525**	0.225	0.25	0.4	0.35	0.25
SUMMER									
	DD			SD			GCM		
	Dry	Normal	Wet	Dry	Normal	Wet	Dry	Normal	Wet
HAD	0.15**	0.35	0.5*	0.4	0.35	0.25	0.6**	0.2*	0.2*
MPI	0.65**	0.225	0.125**	0.65**	0.15**	0.2*	0.625**	0.275	0.1**
GFDL	0.325	0.275	0.4	0.4	0.35	0.25	0.075**	0.425	0.5*

*** less than 5% chance if sampled from a random distribution**
**** less than 1% chance if sampled from a random distribution**

C. Hydrologic Modeling Framework

The hydrologic modeling framework used for the region's water resources management assessment was initially developed in Shamir et al. (2005, 2007a, b) and later used in Nelson (2010); Liu et al. (2012); Shamir et al., (2015); Eden et al. (2016); Shamir, (2017a). The modeling framework consists of a stochastic Weather Generator (WG) module that produces sequences of likely-to-occur hourly rainfall events. These rainfall sequences are used as input to a hydrologic model that simulates hourly streamflow discharge in the Santa Cruz River at the U.S.-Mexico border. The streamflow is then routed along the river channel and the surface water recharge into each of the microbasin (MB) aquifers is calculated. In addition, the storage volume and water levels at the four MBs are updated dynamically. A simplified schematic of the components of the modeling framework is shown in Figure 8.

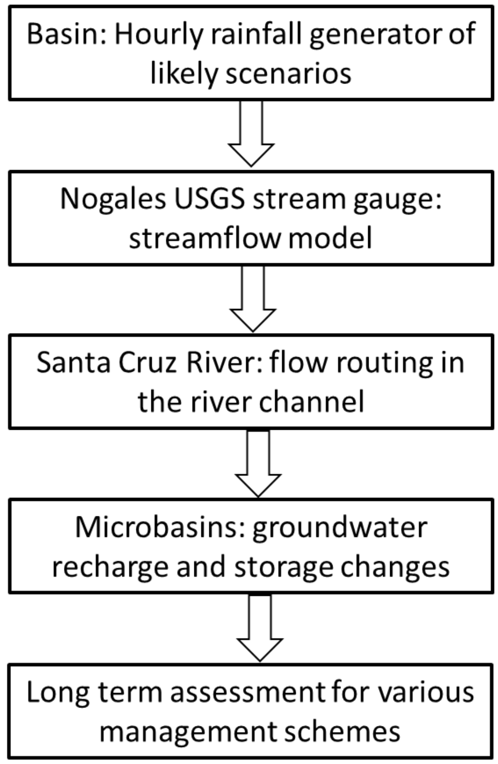

Figure 8: Schematic of the sequencing and links of the hydrologic modeling framework components

The WG is a computer script that produces likely hourly precipitation time series for a point in space. It produces a sufficiently large ensemble of synthetic precipitation time series to represent the regional rainfall characteristics, natural variability and uncertainty that are associated with the observed record (Wilks and Wilby, 1999). The ability of the WG to produce time series that are representative of the region in a probabilistic manner makes it an appealing tool for water resources planning and management studies. In conjunction with hydrologic models that simulate the natural water system, it can be used to assess the impact of changes in atmospheric input, water demand, and construction of infrastructure. In addition, WG simulations can be used to identify best management practices that accommodate competing objectives.

A concise description of the modeling framework is provided below. The most recent formulation and evaluation of the USCR Basin WG is in Shamir, (2017b) and the hydrologic model is described in Shamir (2014). The point process WG was developed to simulate likely-to-occur hourly precipitation scenarios for four seasonal periods: fall (October), winter (November-March), spring (April-May) and summer (June-September). Winter and summer precipitation values are represented as three wetness categories; wet, medium and dry; to accommodate the large inter-annual variability for each season. The division of the wetness categories is based on total seasonal precipitation terciles. The selection of a season’s wetness category is sampled from a uniform distribution, that is a distribution that has constant probability, and it is independent from the selected wetness category of the previous seasons.

For each winter and summer wetness category, the WG produces likely scenarios in an ordered sequence. The first step defines the duration of the rainy season by selecting the seasonal onset and offset. The first storm event of the season is sampled following the seasonal onset and the following steps are repeated until the end of the season, which is determined by the selected offset. These steps consist of sampling for the duration of the storm; the chance of precipitation occurring in each hour; the magnitude of hourly precipitation and the duration of the dry period until the next storm arrives. For the commonly dry spring and fall seasons, the WG only samples for the chance of hourly precipitation occurring and the hourly precipitation magnitude.

In a previous analysis, a mesoscale model (i.e. PSU/NCAR MM5) was used to investigate the spatial distribution of rainfall over the Santa Cruz River headwaters and identified a fairly uniform rainfall distribution over the drainage area (Shamir et al., 2007a). The statistical characteristics of the observed rainfall time series near Nogales is therefore assumed to represent the rainfall characteristics of the entire basin drainage area. The sequences of hourly rainfall realizations were used as forcing for a conceptual hydrologic model that simulates hourly streamflow at the Nogales stream gauge. The model was constructed to represent the distinct variability and characteristics of the hydrologic responses for the winter and summer (Shamir, 2014).

The hourly streamflow simulated at the International Border is routed along the Santa Cruz River channel, while transmission losses to the alluvial channel recharge the MB aquifers. The rate of groundwater recharge to a given MB is dependent on the infiltration rate coefficient and the groundwater in storage at the MB. The area over which recharge occurs is estimated as a function of the wetted width and length of the channel that overlays the MB. A groundwater model is implemented to represent the MBs as a series of four spatially lumped and disconnected reservoirs. The parameters for the groundwater model were estimated from the aquifer characteristics reported in Erwin (2007). This simplified groundwater model simulates an effective depth-to-water estimate for the MBs and does not represent the spatial variability of the groundwater level.

This modeling framework was used to experiment with various water management scenarios for a given MB, including prescribed monthly withdrawal rates and a depth to groundwater threshold below which pumping is ceased (Shamir, 2017a; Shamir et al., 2015). The management scenario used in this study consists of a varying level of monthly withdrawal totaling 5,000-acre feet per year as shown in Figure 9. To sustain healthy riparian vegetation along the river corridor, withdrawal is ceased when the depth-to-water in an MB drops below 3 meters. In the cases where withdrawal is ceased, it is assumed that the City’s water demand is satisfied from an alternative source.

The management strategy described above is not consistently being followed for the MBs. Water resources management in the region has not been formalized and decisions regarding pumping from the microbasins are driven by the needs of the

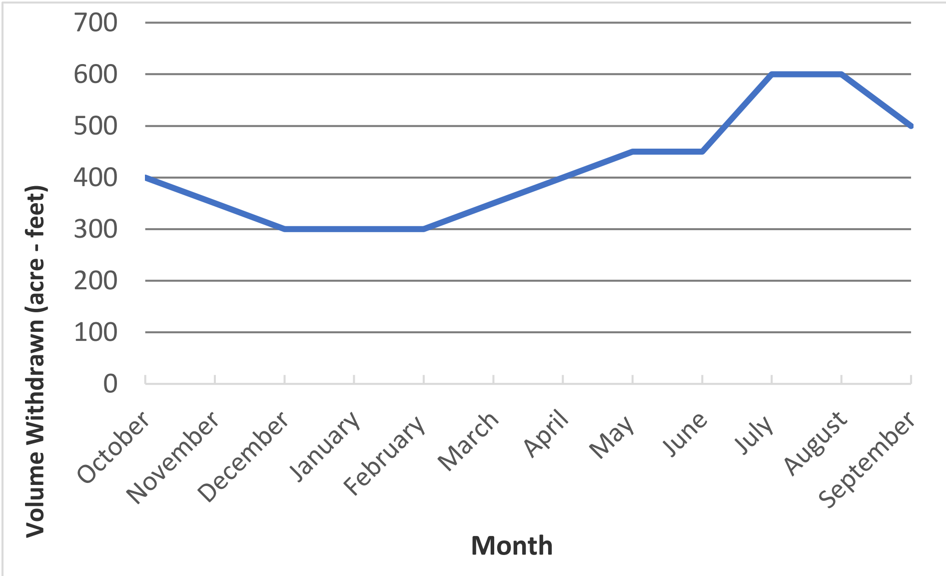

Figure 9: Water management scenario used for Upper Santa Cruz River Basin example.

D. Likely Scenarios of The Projected Future Precipitation

Projected rainfall scenarios were developed by modifying the WG to reflect the changes between the simulations of historic and future periods for each of the downscaled climate models. In this study, the WG was modified to generate six ensembles of hourly precipitation realizations. These realizations represent the projected future climate in the 2020-2059 period for each combination of the three GCMs and two downscaling procedures. Each ensemble is comprised of 100 realizations of hourly precipitation for 40 years, the future period of study. To create these ensembles, we modified the probability of realizing a wetness category for winter and summer (Table 3). An additional seventh ensemble was generated to represent the historical period. The modification assumes that the characteristics of future seasonal precipitation remain similar to the seasonal precipitation described in the WG, and that changes are reflected in the frequency of the seasonal wetness categories.

The decision to modify the WG using the frequency of seasonal wetness category is based on a comprehensive analysis. This analysis compared the historic and future projections for all the features of the WG, such as seasonal onset/offset, event duration, precipitation magnitude and the event inter-arrival time. The authors conclude that the main differences between the historic and future projections for a given model can be described by the frequency of seasonal wetness category.

The cumulative distributions of the 40-year annual average precipitation for the seven ensembles are shown in Figure 10. Except for the HAD-DD, all projections indicate a dryer mid-21st century. The DD simulations of the HAD and MPI, which have contradictory trends, display the most extreme changes. We note that the 40-year annual average is provided here only as one index. The inter-annual average is rarely the expected annual value because of the large inter-annual variability.

Figure 10 and many of the following results present an opportunity to distinguish between projected variability and uncertainty, terms that are sometimes misunderstood. *Variability* is defined as the spread of possible outcomes, while *uncertainty* refers to the measure of unexplained variation. This unexplained variation can be caused by measurement errors or by lack of understanding about cause and effect (e.g. Desser et al. 2012).

In Figure 10, variability can be described as the spread of each distribution, which in this case is the coefficient of variation that ranges from 0.055-0.072. The uncertainty is shown as the difference among the climate projections. One way to quantify the uncertainty is to look at the range of the cumulative distributions' medians. In this case, the median of the cumulative distribution is 315 mm/year for the DD-MPI and 400 mm/year for the DD-HAD. Compared with the median of the historic simulation, this yields an uncertainty range of +7.5% to -15% for the projected median annual rainfall.

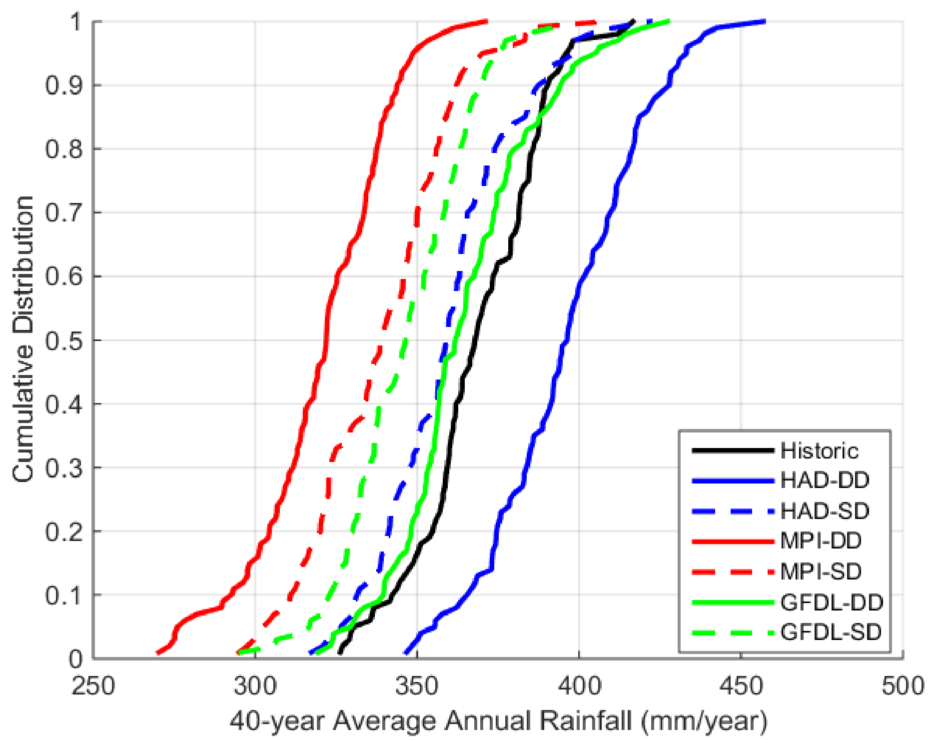

Figure 10: Cumulative distribution of the 40-year precipitation averages (mm/year) calculated from the WG ensembles

From the historic period and the mid-21st century projections of the three climate models and two downscaling methodologies.

Figure 11 shows the seven ensembles of streamflow at the Nogales border crossing, developed by using the seven precipitation ensembles as input into the hydrologic modeling framework. This figure is representative of the cumulative distribution of the 40-year average annual streamflow in units of acre-feet per year. Again, this streamflow value should not be expected in any given year, since the distribution of flow is highly skewed. Similarly, to the projected precipitation in Figure 10, the DD-HAD and DD-MPI exhibit large projected changes with contradicting trends. The projected change in the median of the cumulative distribution is a 13% increase for the DD-HAD and a 22% decrease for the DD-MPI.

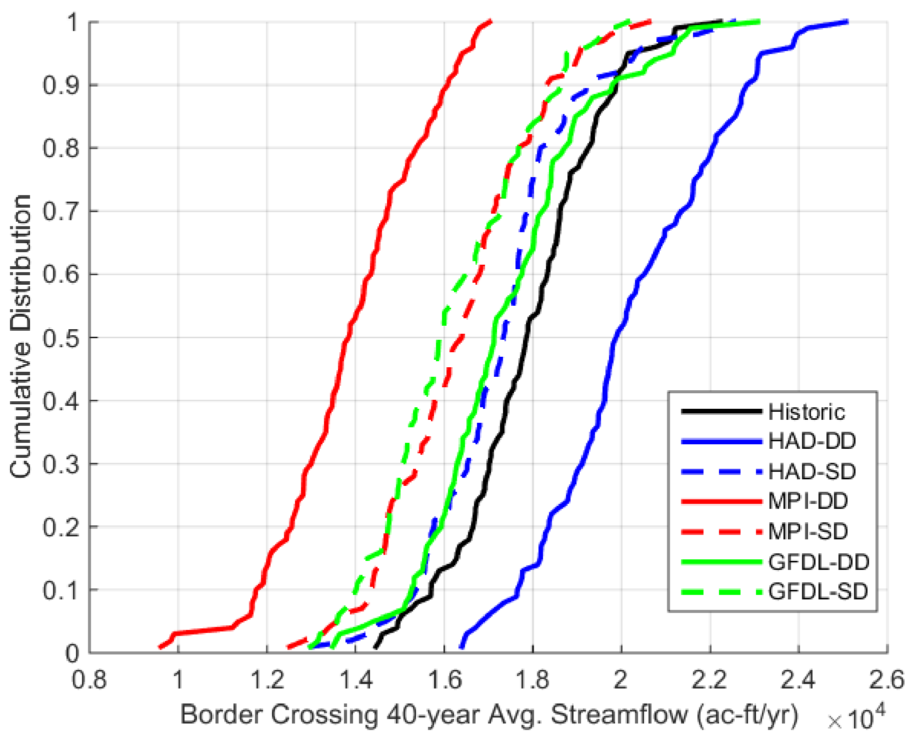

Figure 11: Cumulative distribution of the 40-year annual averages of streamflow (ac-ft /year) on the USCR at the international border crossing.

The streamflow was calculated from the WG ensembles of the historic period and the mid-21st century projections of the three climate models and two downscaling methodologies.

The City of Nogales' annual demand is 5,000acre-feet per year. Using the modeling framework simulating the flow along the SCR channel and interactions with the MBs aquifer, it is feasible to calculate the withdrawal (pumping) deficit under a prescribed management strategy. The monthly pattern of pumping under this strategy is shown in Figure 9. In this simulation, pumping from the MBs is ceased when the simulated depth-to-water in a given MB drops below three meters. The "pumping deficit" is calculated as the water demand not met by pumping from the MBs. The City of Nogales maintains another wellfield but prefers to pump from the microbasins because of the need to treat the alternative supplies for arsenic.

The distributions of the 40-year cumulative pumping deficits from the MBs is shown in Figure 12. Again, the DD-MPI and DD-HAD present the largest differences and have opposing trends. The DD-HAD projects a 7.3% decrease in unmet demand, while the DD-MPI projects a 15% increase. This index of the cumulative pumping deficit can be used to determine the amount of water needed to augment supplies from the microbasins to sustain the current demand under this particular set of operational rules. The model does not account for growth in demand over time.

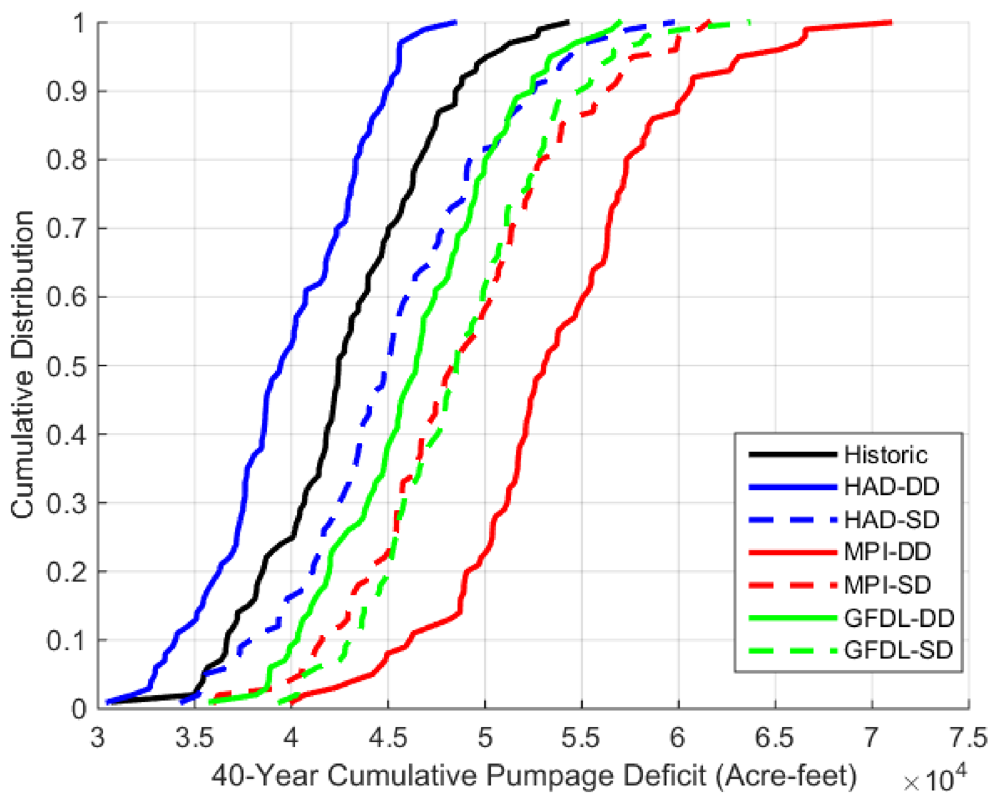

Figure 12: Cumulative distributions of the 40-year cumulative pumping deficit from the microbasins for the 7 WG ensembles.

VI. Case Study II: Climate Change Impact Assessment in the Alamo Lake and the Bill Williams River Basin

A. Study Area: Bill Williams River Watershed and Alamo Lake

The Bill Williams River (BWR) in west-central Arizona, is a tributary of the Colorado River that drains into Lake Havasu just upstream of Parker Dam. Alamo Dam, 58 km (36 miles) upstream of the confluence with the Colorado River, was built in 1968 to form Alamo Lake. Alamo Lake is a multi-purpose facility, but its primary objective is to control flooding downstream of the dam on the lower BWR. Secondary objectives of the lake include water supply and conservation, recreation, and fish and wildlife enhancement. The lake's contributing drainage area is about 12,354 km^2 (4770 $mile^2$) from three mainly ephemeral tributaries with a few perennial sections. These are the Big Sandy River, the Santa Maria River, and Burro Creek. No significant flood control structures exist in the drainage area of these tributaries. A map of the 13,968 km^2 (5,393 $mile^{2)}$) BWR watershed with eleven sub-basins (based on elevations bands) developed for the hydrologic model is shown in Figure 13.

The diverse physiography of the BWR watershed (BWRW) ranges from high elevation forested mountains to rugged desert terrain in the lower elevations. A detailed hydrologic and geomorphic description of the watershed is provided in House et al. (1999).

Alamo Dam is operated by the U.S Army Corps of Engineers (USACE). Its releases have a direct impact on the operation of the Lower Colorado River by the Bureau of Reclamation's Boulder Canyon Operations Office. Downstream of Alamo Lake, the lower BWR flows through a series of alternating narrow canyons and wider alluvial valley reaches. The peak discharge in the U.S Geological Survey (USGS) gauge just below Alamo Dam (USGS09426000) during the pre-dam era was estimated at 200,000 $ft^3\,s^{-1}$ (5,660 $m^3\,s^{-1}$) in February 1891 (Patterson and Somers, 1966). Post-dam maximum discharge as of September 2018 has not exceeded 7,000 $ft^3\,s^{-1}$ (~200 $m^3\,s^{-1}$), the maximum possible release rate from the dam.

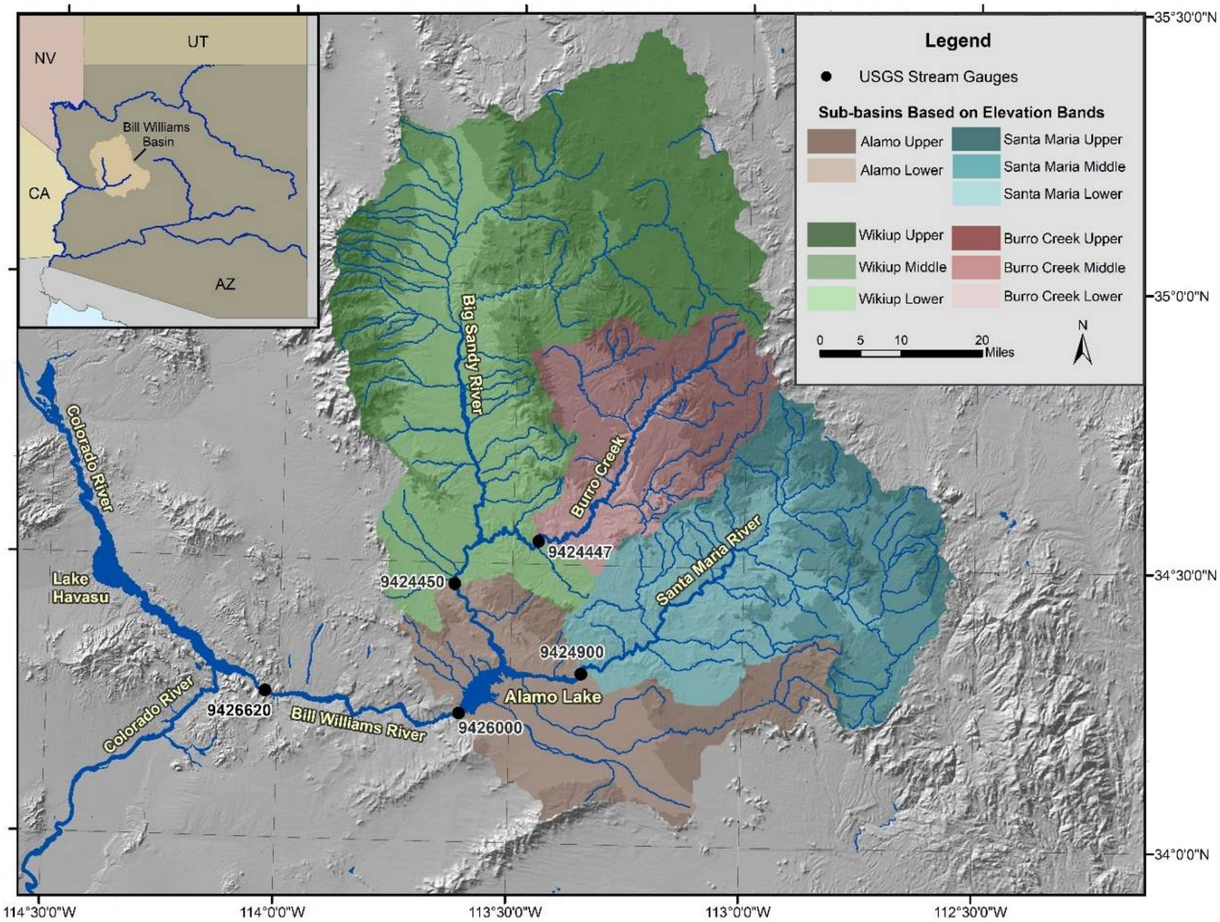

Figure 13: A map of the Bill Williams River Watershed.

A description of the eleven sub-basins is in Table 4.

B. Observation Datasets

Hourly mean areal precipitation (MAP) data from the Colorado Basin River Forecast Center (CBRFC), National Weather Service (NWS) (www.cbrfc.noaa.gov) presented in Table 4 are available for eleven sub-basins in the BWR watershed for the period of October 1st, 1980 - September 30th, 2010 . These historical MAP time series were purposely derived by CBRFC to calibrate their hydrologic models. Each of the three tributaries that drain into Alamo Lake (Figure 13) was divided into three sub-basins: upper, middle, and lower by using elevation thresholds. Two additional downstream sub-basins, an upper and lower, just upstream of the lake were also configured by CBRFC.

The MAP derivation procedure consists of quality control of the rain gauge records and spatial interpolation with the Mountain Mapper technique used by the NWS River Forecast System (Schaake et al., 2004).

The inflow into Alamo Lake was calculated from a mass balance equation, using Alamo Lake's water level from the USACE (1980-2010), outflow from the lake as observed at the gauge just below the dam, and estimated monthly lake evaporation from CBRFC. We used the historic monthly evaporation values for the analyses of precipitation projections. It is likely that the future climate changes will impact lake evaporation. However, lake evaporation is a complex process and the projection of future evaporation requires an analysis of the lake energy balance in addition to the energy and hydrodynamic atmospheric conditions over the lake (e.g. Shilo et al. 2015). Such an effort is outside the scope of this investigation.

Table 4. CBRFC Sub-basins

	Sub basins		CBRFC Codes	Area (mile^2/km^2)	Elevation (m) centroid and (range)	*Summer / Winter Average MAP (mm/season)
1	Alamo	Upper	alma3luh	287 / 743	992 (758 - 1908)	143 / 194
2		Lower	alma3llh	451 / 1168	588 (363 - 758)	95 / 148
3	Santa	Upper	smba3huh	196 / 508	1654 (1515 - 2092)	213 / 240
4	Maria	Middle	smba3hmh	413 / 1070	1369 (1212 - 1515)	179 /215
5		Lower	smba3hlh	516 / 1336	938 (470 - 1212)	126 / 182
6	Wikiup	Upper	wkpa3luh	823 / 2132	1692 (1515 - 2405)	163 / 202
7		Middle	wkpa3lmh	445 / 1153	1371 (1212 - 1515)	135 / 175
8		Lower	wkpa3llh	850 / 2201	911 (434 - 1212)	93 / 143
9	Burro	Upper	bcba3huh	231 / 598	1654 (1515 - 2092)	220 / 267
10	Creek	Middle	bcba3hmh	224 / 580	1369 (1212 - 1515)	197 / 250
11		Lower	bcba3hlh	151 / 388	938 (620 - 1212)	146 / 202

***Average summer (April-September) and winter (October –March) were calculated for 1980-2010 from CBRFC MAP for the eleven sub-basins.**

C. Hydrologic Analysis

Figure 14a indicates the difference between winter and summer MAP over the entire BWR watershed. Long-term average winter and summer precipitation, as indicated by the dashed lines, are 180 and 130 mm/season, respectively. Although the winter season is occasionally very wet, with a maximum of 430 mm, it is more often drier than the average, which implies a skewed distribution. The skewness coefficients are 0.95 and 0.52 for winter and summer, respectively. The higher variability of winter precipitation can also be shown by comparing the coefficient of variations: 0.6 and 0.4 for winter and summer, respectively.

Summer streamflow events are triggered by the relatively short-lived and local convective storms. The hydrographs of these events have a short duration with fast rising limbs and limited baseflow. On the other hand, the large-scale winter storms generate longer streamflow events with larger volumes and higher daily maxima, but the duration between the streamflow events is shorter. The shorter duration between winter streamflow events may be attributed to longer events with long lasting baseflow (Shamir et al. 2017).

In Figure 14b total winter and summer seasonal inflows into Alamo Lake are compared with total seasonal outflows. Notice that although average summer precipitation is ~75% of the average winter precipitation, the average summer inflow into Alamo Lake is only ~10% of the average winter inflow. Summer outflows are also much lower than winter releases, although the dam data show a few higher than normal winter releases due to its flood control mission. It is also noted that many winters had very low inflows. The large seasonal differences between the precipitation and streamflow ratios emphasizes the need to consider the properties of precipitation events and the interactions with land surface processes that control the generation of streamflow.

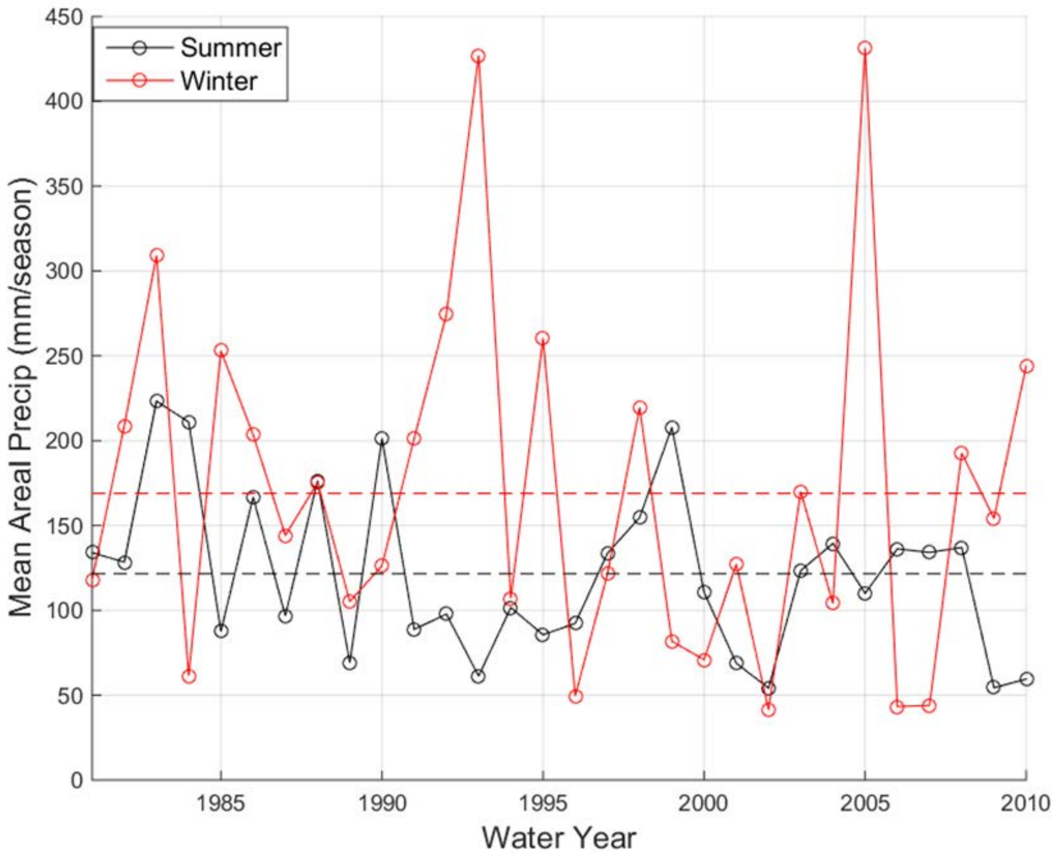

Figure 14a: Summer and winter mean areal precipitation (mm/season) over the entire BWR watershed.

Dashed horizontal lines are the inter-annual averages.

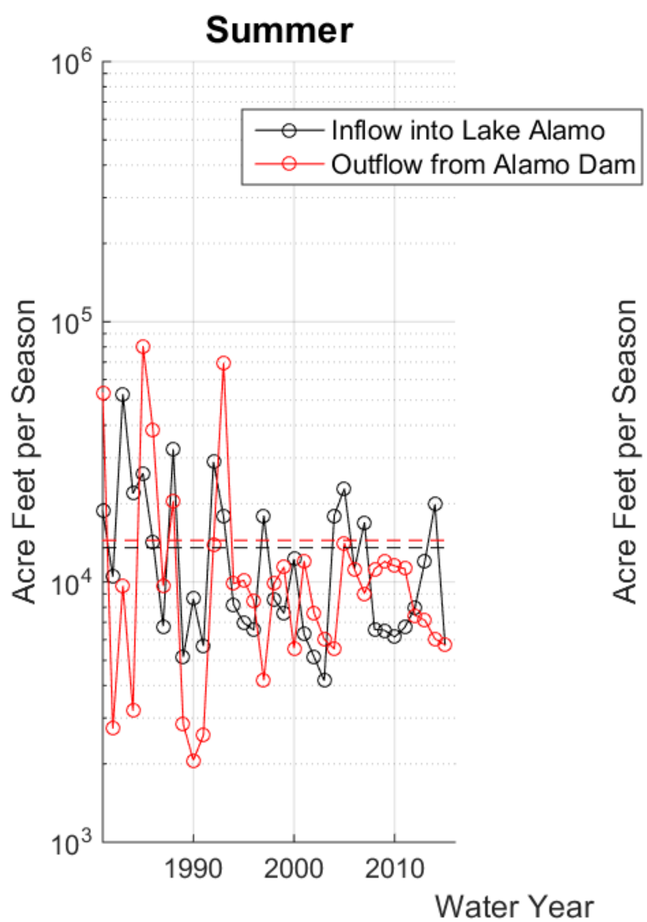

Figure 14b: Summer (left) and winter (right), total estimated inflow (black) and outflow (red), into and from Alamo Lake.

D. Hydrologic Modeling Framework

To assess the impact of the projected climate on the BWR hydrologic system, a hydrologic modeling framework was configured using a precipitation Weather Generator (WG), hydrologic model and lake model. To assess future impacts, the WG was modified to reflect the projected changes inferred from the DD and SD simulations. This study only considers projected changes in precipitation. The detailed development and evaluation of the hydrologic framework is described in Shamir et al. (2017). In this section, we provide a description of the modeling framework components.

E. Precipitation Weather Generator

The analysis of precipitation and lake inflow in the BWR watershed points to the importance of representing the temporal and spatial characteristics of rainfall events. The purpose of the precipitation WG is to produce numerous equally likely, realistic scenarios of hourly precipitation sequences. An ensemble that includes a sufficient number of realizations of these scenarios should represent the spatiotemporal statistical characteristics of the observed record, including the natural variability of events, and their likelihood of occurring.

A WG was developed to simulate likely hourly MAPs for the 11 sub-basins of the BWR watersheds. It was based on analysis of the sub-basins MAP from CBRFC (1980-2010). Since the WG is based on the MAPs used for the development of the hydrologic model, the WG realizations can be directly input to the hydrologic model.

By modifying the WG to reflect the changes between historic and projected climate model simulations, it is possible to assess the impact of projected precipitation changes on the lake inflow and lake level. The precipitation WG concept that is presented herein follows previous work by Shamir et al., (2007a&b, 2015), Shamir (2017), and Wang et al., (2007). A detailed description and evaluation of the WG for the BWR watershed is provided in Shamir et al. (2017). A brief description is provided below.

The WG is comprised of two successive modules: a point process module to derive hourly MAP that represents the entire BWR watershed (Figure 15, left) and a spatial disaggregation module to estimate hourly MAPs in the eleven sub basins (Figure 15 right).

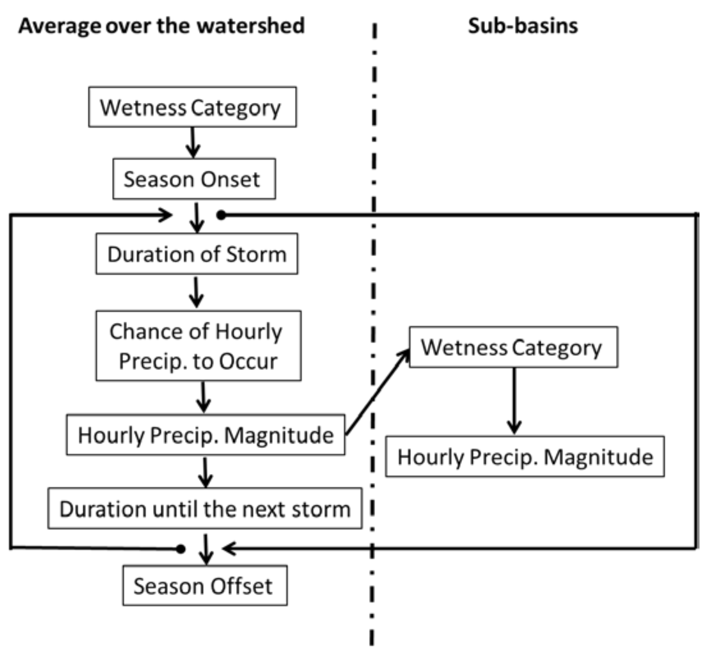

Figure 15: A schematic outline of the WG components in the winter or summer.

The left column describes the point process sequential sampling to derive the basin average hourly time series. The right column is the sequential sampling to disaggregate the synthetic time series to the sub-basins. The looping arrow indicates a repetitive sampling sequence that continues until the precipitation simulation is completed for the duration between the onset and offset of the winter or summer.

F. Point Process Module

The point process module is developed for the three wetness categories of wet, medium and dry for both winter and summer. The highly skewed precipitation distribution and the very large inter-annual variability in the arid Southwest U.S. calls for a WG with wetness categories that can be developed independently (Shamir et al. 2007a, b). The wetness categories represent the tercile statistics of the total observed summer and winter seasonal precipitation from 1980-2010. The selection of a wetness category in a given season is sampled from a uniform distribution and is independent of the previously selected wetness category.

Following the sampling of a wetness category, the duration of winter or summer is determined by sampling the season's precipitation onset and offset. The onset and offset of the rainy season are selected from a normal distribution with a mean and standard deviation calculated from the historical record for the winter and summer and for the different wetness categories.

Next a precipitation time series is created for the winter or summer season by sequentially sampling from the following distributions: inter-arrival time of storms, duration of storms, probability for an hourly precipitation event to occur, and the magnitude of the hourly event. This sequential sampling repeats until a time series is generated for the duration of the season's onset to its offset, as seen in looping arrow in Figure 15. Each distribution is developed independently for the three wetness categories (i.e. wet, medium, and dry).

The point process module assumes that precipitation storm events tend to arrive in clusters, as a response to a transient synoptic scale atmospheric disturbance. Each synoptic event may produce multiple hourly precipitation pulses with a possibility of intermittent dry hours. The definition of a storm is a key component required to derive a sample of observed storms, which is used for the estimation of the WG parameters. In this study, the storm definition procedure assumes that the distribution of the storms' inter-arrival time constitutes a Poisson stochastic process and therefore the distribution of storms' inter-arrival times conforms to an exponential distribution (Restrepo-Posada and Eagleson, 1982).

Thus, it is possible to select a minimum inter-arrival time between storms. The inter-arrival between storms is the number of dry hours beyond which the occurrence of rainfall marks the beginning of a new event. This is used to develop a statistical sample of storms with an inter-arrival distribution with a coefficient of variation of one, as in an exponential distribution. In this study the minimum inter-arrival times were prescribed as 84 and 36 hours for the winter and summer, respectively. A storm event is defined as one that follows the previous storm by a period longer than the minimum inter-arrival time and starts and ends with hourly precipitation events.

G. Precipitation WG Spatial distribution

The BWR basin-wide hourly MAP realizations derived by the point process module are further disaggregated into MAP for the 11 sub-basins. The disaggregation consists of two steps. First, for each wet hour, a wetness category is independently assigned for each sub-basin. The wetness categories, which can include an assignment of a no-rain event, were sampled for winter and summer from a uniform random distribution with probability coefficients calculated from the observed MAP records. The probability coefficients indicate the chance of a precipitation event in a sub-basin being in a tercile, independently of the other sub-basins, as a function of the wetness category of the average master time series.

Second, the magnitude of the hourly precipitation in the sub-basins, if in the upper tercile, is assigned from a Generalized Pareto distribution with a threshold of the observed 67th percentile. Otherwise, the precipitation magnitude is selected from a log normal distribution. The parameters of these distributions were derived independently for each sub-basin. To simulate large extreme events, probability was added, for one day per season, of sampling a precipitation event from Generalized Pareto distributions parameterized to represent the annual maxima series of the observed records for each sub-basin.

In Shamir et al., (2017) the performance of the WG was comprehensively assessed for the winter and the summer with respect to the frequency of hourly events, the distribution of seasonal totals and the occurrence of extreme hourly events. These are understood to be the precipitation features that control runoff generation in ephemeral streams. Figure 16 displays the WG performance in simulating total winter precipitation as an example. The cumulative distributions of 100 WG realizations, each 30 years of hourly MAP for the 11 sub-basins are shown in gray. The WG realizations are compared with the cumulative distribution of the observed MAPs from CBRFC shown in red. The WG simulations encompass the observed distribution, indicating that these distributions are simulated well. The total seasonal precipitation was not accounted for in the derivation of the WG and therefore may be considered an independent evaluation measure.

It is interesting to note that, to the authors' knowledge, there is no formal methodology for evaluating the performance of a WG ensemble. The spread of the ensemble realizations should represent the uncertainty associated with the observed record. The width of the ensemble spread should neither be too wide or too narrow: a narrow spread does not describe the uncertainty and variability in the data, while a spread that is too wide, may fail to capture the unique characteristics of the data.

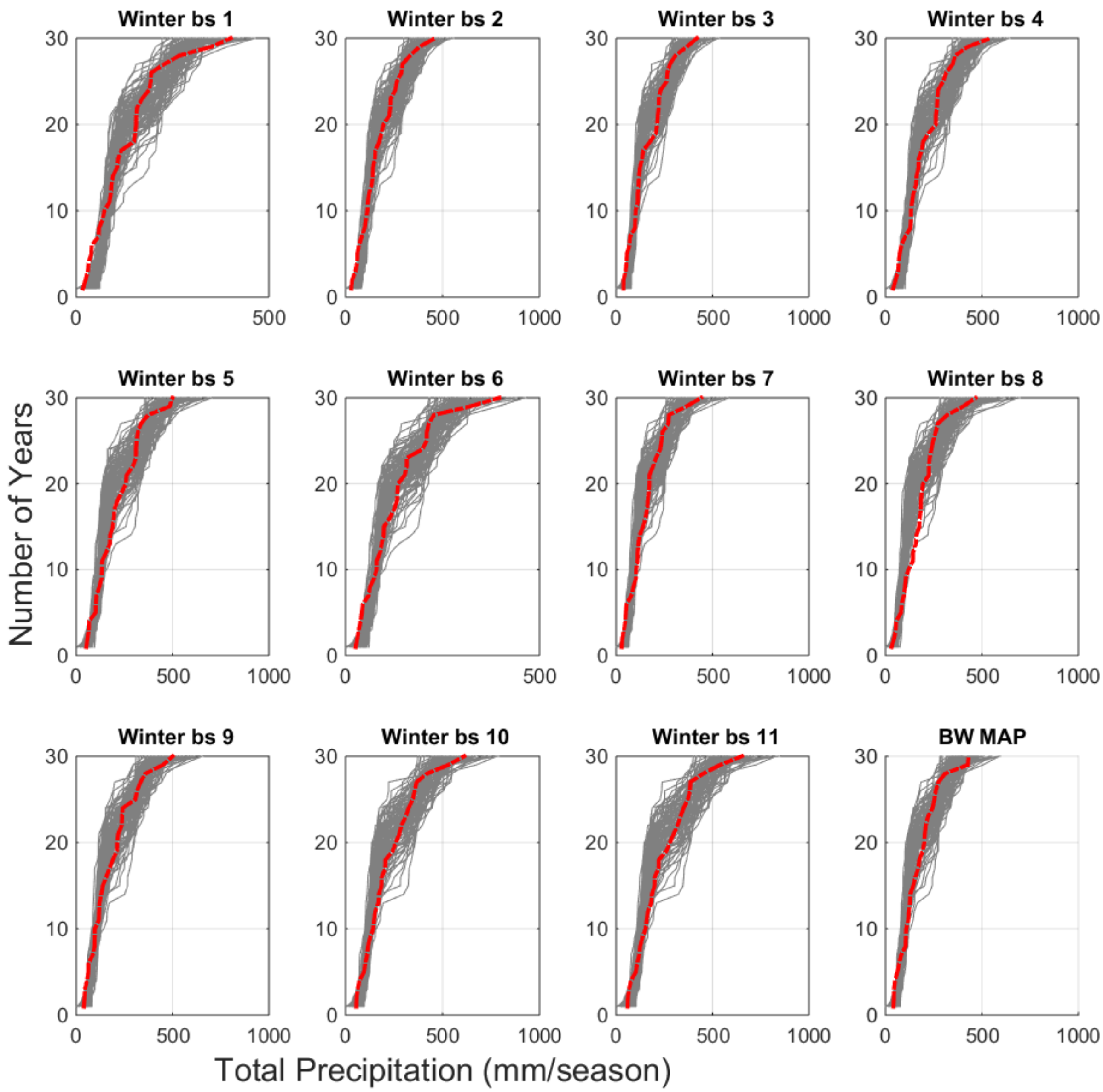

Figure 16: The cumulative inter annual distributions of the winter total precipitation in the sub-basins and the watershed average.

The WG simulated ensemble (gray) and the observed (1980-2010) MAPs from CBRFC (red).

H. Hydrologic Model: Sacramento Soil Moisture Accounting

We implemented the CBRFC hydrologic model configuration and parameters for the BWR watershed in the hydrologic framework. The CBRFC uses the NWS River Forecast System including the Sacramento Soil Moisture Accounting model (SAC-SMA), a hydrologic model that continuously updates the soil moisture conditions and simulates runoff and streamflow in the channels (Burnash et al., 1973); the Snow17 model which keeps track of snow accumulation and ablation in the basins (Anderson, 1976) and a unit hydrograph to route the channels' streamflow into the sub-basins outlet. The CBRFC operational model is mainly used to simulate high flow events, and the SAC-SMA parameters were further refined to accommodate water resources assessments.

Parameter refinement was conducted by comparing the daily streamflow simulations to the observed daily flows at the Big Sandy River (USGS 09424450), Burro Creek (USGS 09424447) and Santa Maria River (USGS 09424900) (Figure 12). The calibration assumed that the MAP model input was quality-controlled and the WG was developed to reflect the temporal and spatial statistical characteristics of the historic MAP.

Figure 17 displays the simulated winter and summer cumulative distributions of daily inflow into the lake compared to the calculated inflow. For the winter, the calculated and simulated cumulative distributions are well aligned. Conversely, the summer simulation overestimates the calculated record. The weak model performance during the summer period was also noticeable in the hydrographs. Calibrating the model to match the summer events more accurately requires a compromise with the winter model performance. The poor model performance is attributed to the inability to capture the short and locally intense characteristics of summer rainfall. The use of MAP over relatively large basins likely has a smoothing effect in the data that misrepresents the convective characteristics of summer rainfall events. Thus, a good simulation of summer events would require a higher resolution model configuration with input data to represent convective summer storm characteristics.

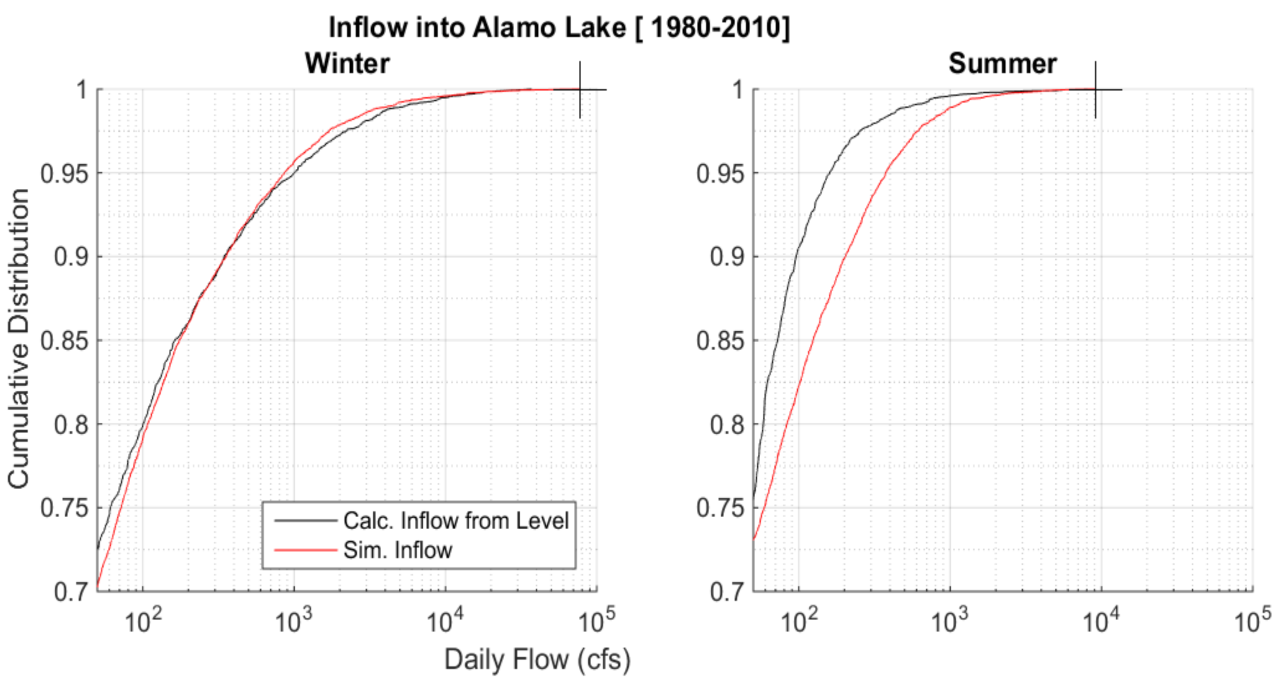

Figure 17: Winter and summer cumulative distributions of the simulated inflow into the lake compared to the calculated inflow from lake level and observed outflow

I. Alamo Lake Model

An hourly mass balance model that simulates lake level, storage, and releases from Alamo Dam as a function of inflow into the lake is described below. The lake operation rules are based on a “rain on the ground” strategy, which implies that the operational rules react to the observed inflow into the lake. The physical dimensions of the lake and the relationships between water level, storage and surface area are from Kirby and Burnham (1998) and the U.S. Army Corps of Engineers (USACE) website (http://resreg.spl.usace.army.mil/pages/alamo.php). The rules that specify dam releases as a function of lake level and season, the specification of the dam’s dimensions, and the monthly lake evaporation values are from the USACE Operational Manual (2003).

The operation of the lake is intended to maintain the lake water level at, or near, 342.9 m (1125 feet), for as long as possible. This level is considered optimal to satisfy all the objectives of the authorizing legislation and optimize downstream benefits. The actual operation of the dam, however, often deviates from the recommended rules. During storm events that impact large areas of the Colorado River basin, releases from Alamo Dam are coordinated to control the flow on the Colorado River. Other cases of deviation from the rules are due to operational considerations such as dam maintenance and specific downstream demands.

The simulations and observations of the lake’s water level and outflow are shown in Figure 18. Although the lake’s actual operation occasionally deviated from the rules, the simulated water level and outflow overall represent the observed record well. The correlation coefficients between the observed and simulated lake level and outflow are 0.75 and 0.64, respectively.

The flood control storage compartment of the lake holds about 740 x 10^6 m^3 (600,000 acre-feet), and at this water level the maximum release rate is ~200 $m^3 s^{-1}$ (7,000 $ft^3 s^{-1}$). This is a relatively large volume that has been used to store water during flood events in the Colorado River Basin. Notably, at the maximum release rate, it takes more than 40 days to drain the entire volume of the flood control storage, which may be too slow for emergency situations.

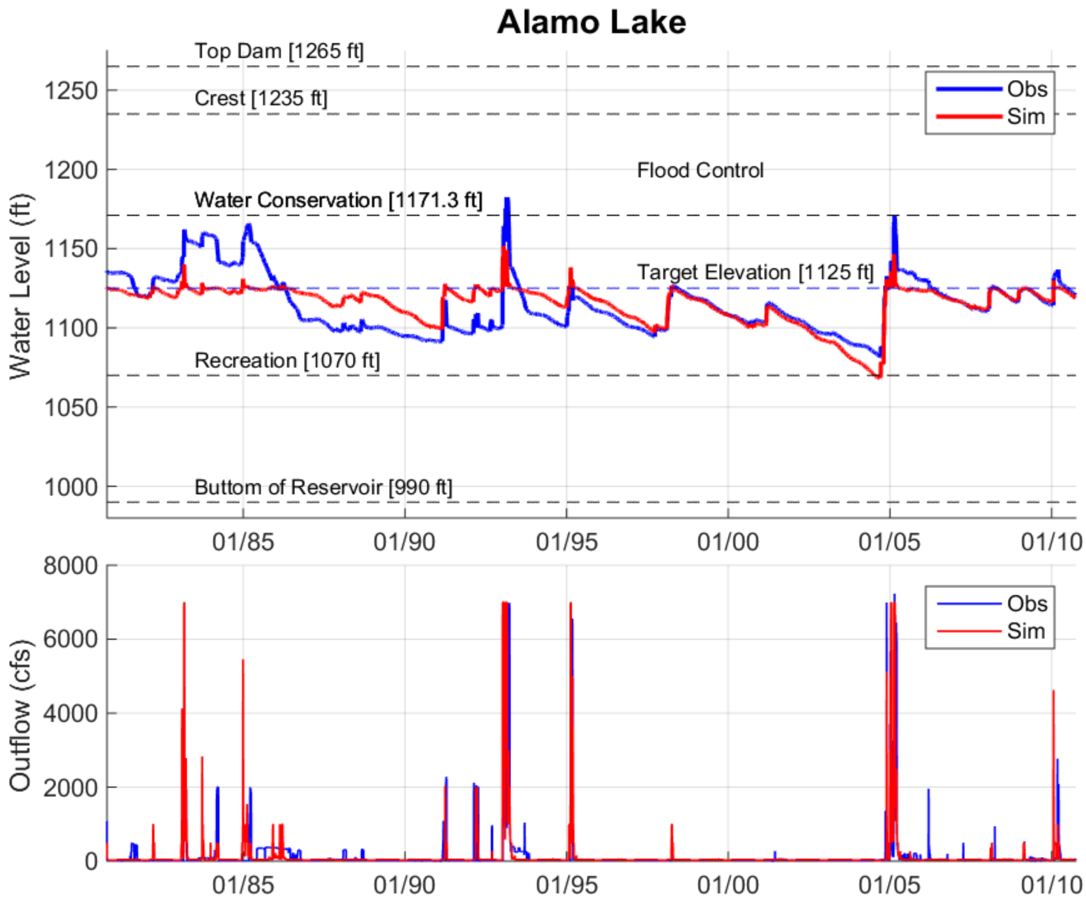

Figure 18: Observed and simulated lake water level and outflow in the upper and lower panels, respectively for 1980 -2010.

The correlation coefficients for the lake level and outflow are 0.75 and 0.64 respectively.

J. Results

1. *DD vs. SD for the historical period*

Figure 19 compares the cumulative distributions of the historical daily inter-annual precipitation characteristics of mean, standard deviation, and number of rainy days, from top to bottom, respectively, for the DD, SD, reanalysis and observed MAP. The WRF reanalysis simulation matches the observed MAP distribution well, which implies that at least at the analyzed scale, the reanalysis simulation captures the precipitation features important for hydrologic assessment. The SD simulations of the three models are, as expected, very similar to each other, since they were created to conform to the Livneh dataset. However, compared with the observed MAP, the SD simulations and therefore also the Livneh dataset, underestimate the mean and standard deviation and overestimate the number of daily events. This underestimation suggests that although the LOCA simulations represent the Livneh dataset well, they do not represent the CBRFC MAP for the study area well.

The DD simulations exhibit larger differences among the GCMs. The three DD simulations overestimate the mean and standard deviation, and the frequency of the daily precipitation is underestimated by the MPI and overestimated by both HAD and GFDL.

These differences indicated in Figure 19 between the downscaled simulations (DD and SD) and the observed MAP emphasize the need to prepare hydrologic model rainfall input that has consistent characteristics to the input used for the configuration of the hydrologic model. Bias correction of the SD and DD simulations, a practice commonly used, may show a good fit in the upper panel of Figure 19 but will likely not resolve the differences that are seen in the middle and lower panels, which are important precipitation features in arid environment.

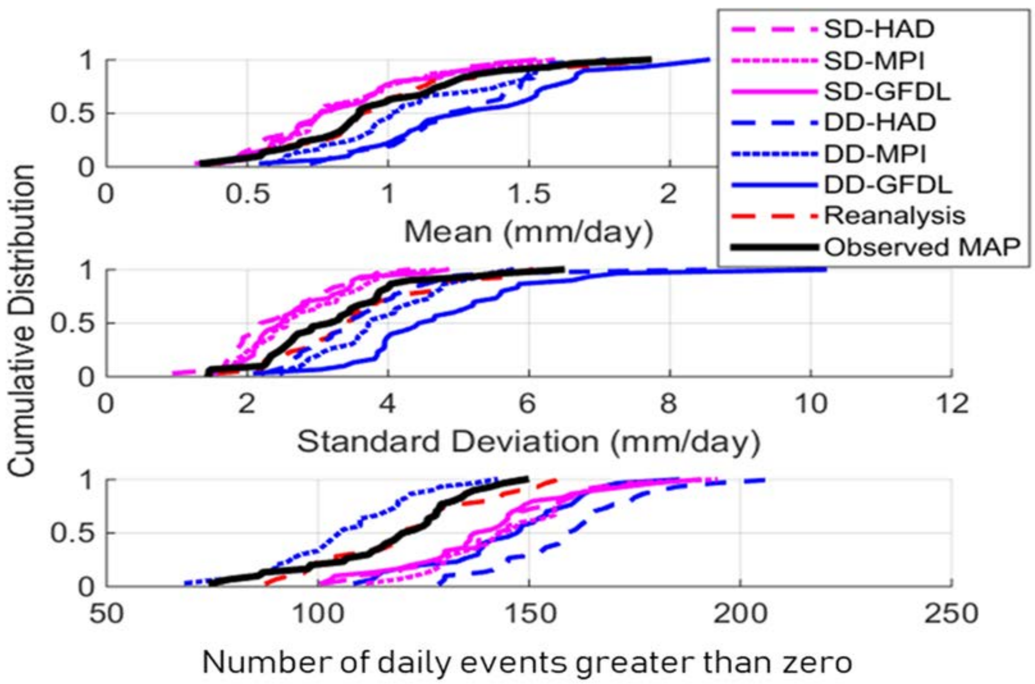

Figure 19. Cumulative distributions of the inter-annual mean (upper panel), standard deviation (middle panel), and number of daily precipitation events (lower panel)

For the three GCMs, historic SD and DD simulations, reanalysis, and the observed MAP for the historic period.

2. *SD vs. DD Future Change*

Tercile Analysis

An analysis of projected mid-21st century (2020-2059) precipitation changes, focusing on the rainfall characteristics used for the development of the WG, is presented in this section. Changes in projected total precipitation by the DD, SD and the raw GCMs are examined in Figures 20 and 21, for the winter and summer respectively. The red dashed horizontal lines show the 33.3 and 66.7 quantiles for the historic period (1950-2005) and the two future projected horizons (2020-2059 and 2060-2099).

Focusing on the projected changes for the mid-21st century (2020-2059), in Figure 20, there is no clear consensual signal of a projected trend. While the DD-HAD showed no clear projected change, the SD-HAD projects decreases in the occurrence of both dry and wet winters, which implies a higher frequency of medium winters. The DD-MPI, SD-MPI, DD-GFDL and SD-GFDL project dryer winters in the mid-21st century, which is expressed as a higher frequency of dry winters and a lower frequency of wet winters.

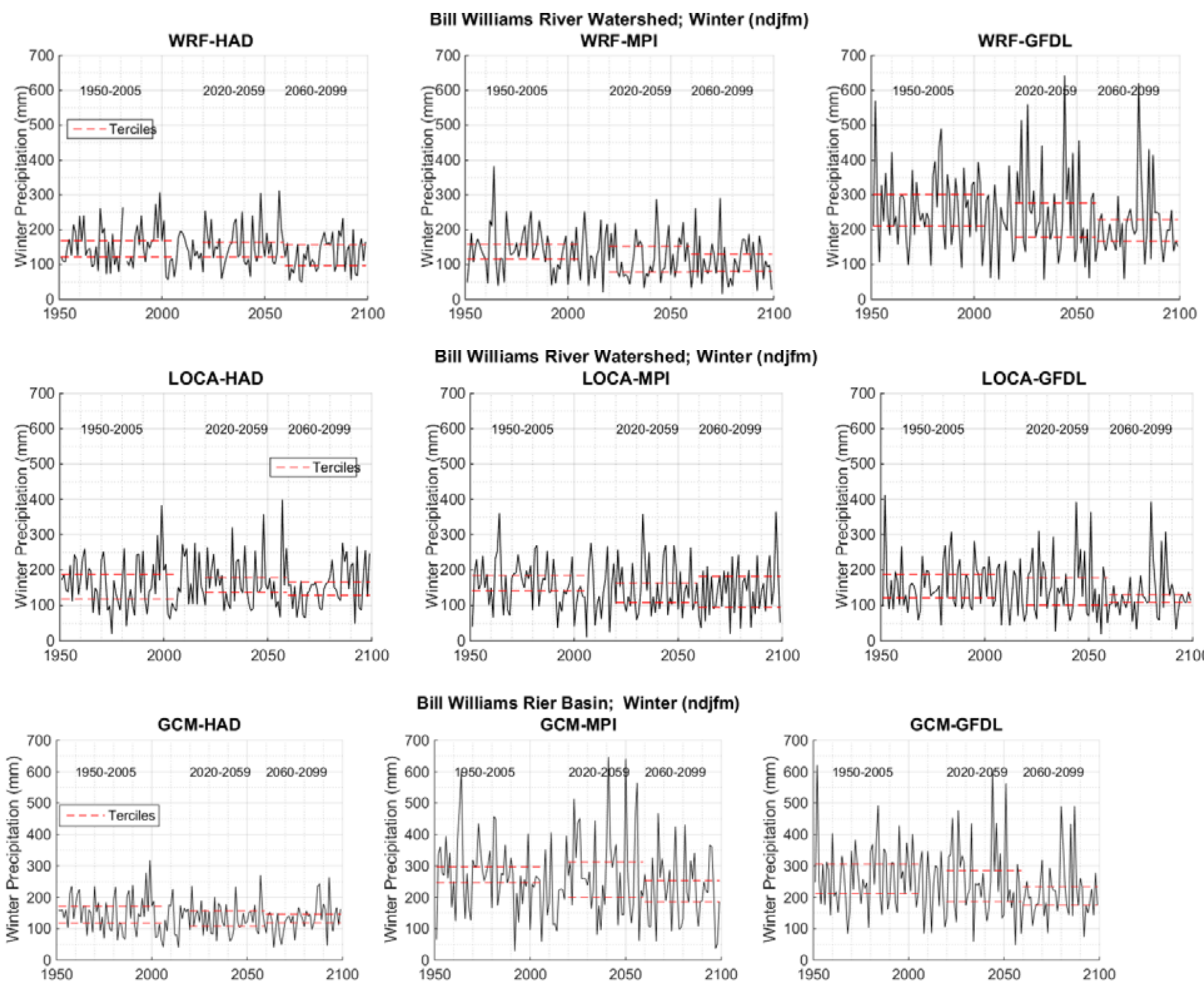

Figure 20: Total winter (November –March) mean areal precipitation over the study domain during 1950-2099 for the DD (upper row), SD (middle row), and raw GCMs (lower row).

The dashed red lines mark the 33.3 and 67.7 quantiles during 1950-2005, 2020-2059, and 2060-2099.

Similarly, the summer projections for the mid-21st century in Figure 21 do not show a clear trend. The DD-HAD and DD-GFDL projected wetter summers, while the DD-MPI projects dryer summers. Interestingly, the DD-HAD has the opposite trend from the raw HAD. The only notable signal seen for the SD is for the MPI, which projects an increase in the frequency in dry summers. The raw HAD and MPI project drying summers, while the raw GFDL projects wetter summers.

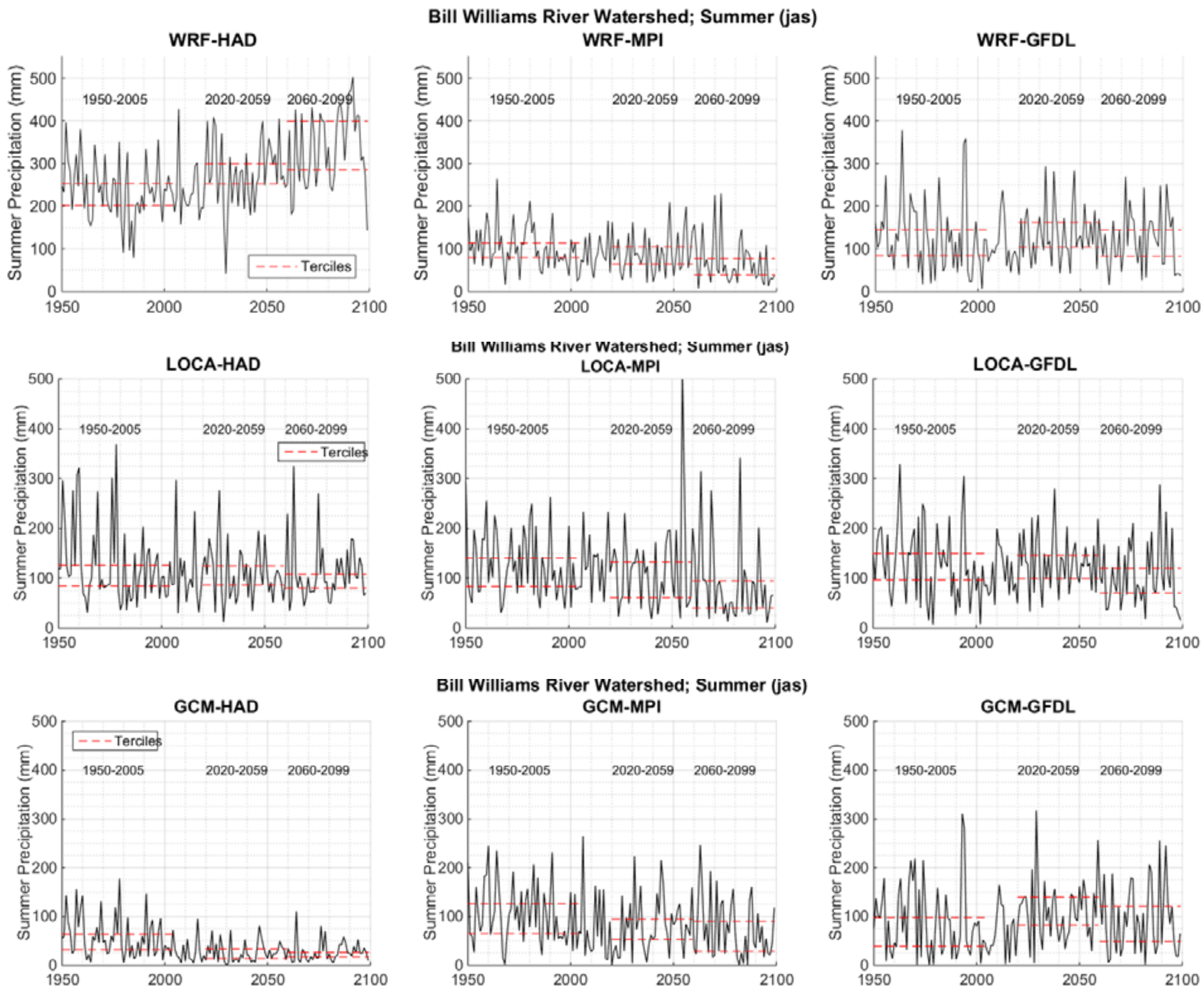

Figure 21: As Figure 20 but for the summer season

The projected frequencies of the seasonal wetness categories in mid-21st century, as defined by the terciles of the historic period, are listed in Table 5. In this table, probabilities significantly different than the historical period are indicated with asterisks.

The significance test is based on a Monte Carlo experiment in which an ensemble of 100,000 members was randomly drawn from a continuous uniform distribution that takes values from 0 to 1. Each ensemble member consists of 40 values representing the 40-year projection duration of interest. The authors found that 5% of the ensemble member terciles were below 0.22 and above 0.46, and 1% of the ensemble terciles were below 0.18 and above 0.51. Therefore, a given projected wetness category with frequency either below 0.18 or above 0.51 has a less than 1% chance of being selected from a uniform distribution, and therefore we assume that it is significantly different than 33%.

For winter season, the MPI DD and SD simulations project a significantly higher frequency of dry winters. The DD-MPI indicates a decreased frequency of wet winters and both the DD- and SD-MPI indicate decreased medium winters. The DD-GFDL, similarly to the DD-MPI, shows an increased frequency of dry winters and decreased frequency of medium winters. No significant changes in winter projections are seen for the HAD-GCM. The projection for a higher frequency of dry winters is congruent with the Assessment of Climate Change in the Southwest U.S report (Garfin et al., 2013) that projects a decreasing trend in winter precipitation.

For the summer season, the DD-HAD projects a lower frequency of dry and medium summers and a higher frequency of wet summers in mid-21st century. The only other significant result is shown in the DD-GFDL, which projects a decrease in frequency of dry summers. An analysis of the GCMs in the IPCC Fifth Assessment Report indicates a delay in the onset of the monsoon season and increased rainfall in the late summer (Cook and Seager, 2013).

Table 5. Projected 2020-2059 chances of occurrence for the wetness categories.

WINTER (November-March)						
	Dynamically Downscaled (DD)			Statistically Downscaled (SD)		
	Dry	Medium	Wet	Dry	Medium	Wet
HAD	0.35	0.3	0.35	0.3	0.4	0.3
MPI	0.55**	0.2*	0.25	0.55**	0.15**	0.3
GFDL	0.525**	0.2*	0.275	0.375	0.325	0.3
SUMMER (April – September)						
	Dynamically Downscaled (DD)			Statistically Downscaled (SD)		
	Dry	Medium	Wet	Dry	Medium	Wet
HAD	0.175**	0.175**	0.65**	0.325	0.35	0.325
MPI	0.425	0.275	0.3	0.425	0.275	0.3
GFDL	0.2*	0.45	0.35	0.275	0.425	0.3

*** less than 5% chance if sampled from a random distribution**
**** less than 1% chance if sampled from a random distribution**

K. Hydrologic impact results

To assess projected hydrologic impacts, the authors modified the WG by applying the frequencies of winter and summer wetness categories, as indicated in Table 5, to generate six additional ensembles (SD and DD for three GCMs) of MAPs for the 11 sub-basins for the mid-21st century period. Each ensemble consists of 100 realizations of hourly precipitation, and each realization is 30-years long, the same duration as the observed record that was used for the development of the WG. These ensembles were used as input to the hydrologic model and the lake model to generate ensembles of lake inflow, outflow and water level.

Figure 22 shows the cumulative distribution of 100 realizations of the 30-year mean annual precipitation over the entire BWR watershed. The right panel of this figure shows the ratio between the quantiles of the cumulative distributions for the historic and projected simulations. The average changes in the ratios of the quantiles are indicated in the upper right. While the DD-MPI has a clear signal of drying, the DD-HAD and SD-HAD shown a wetting trend. The smallest changes are found for the DD and SD GFDL.

For both the MPI and HAD, the largest changes are seen for the DD simulations. This behavior is likely the result of the changes in the forcing of the regional climate model as shown in Table 5.

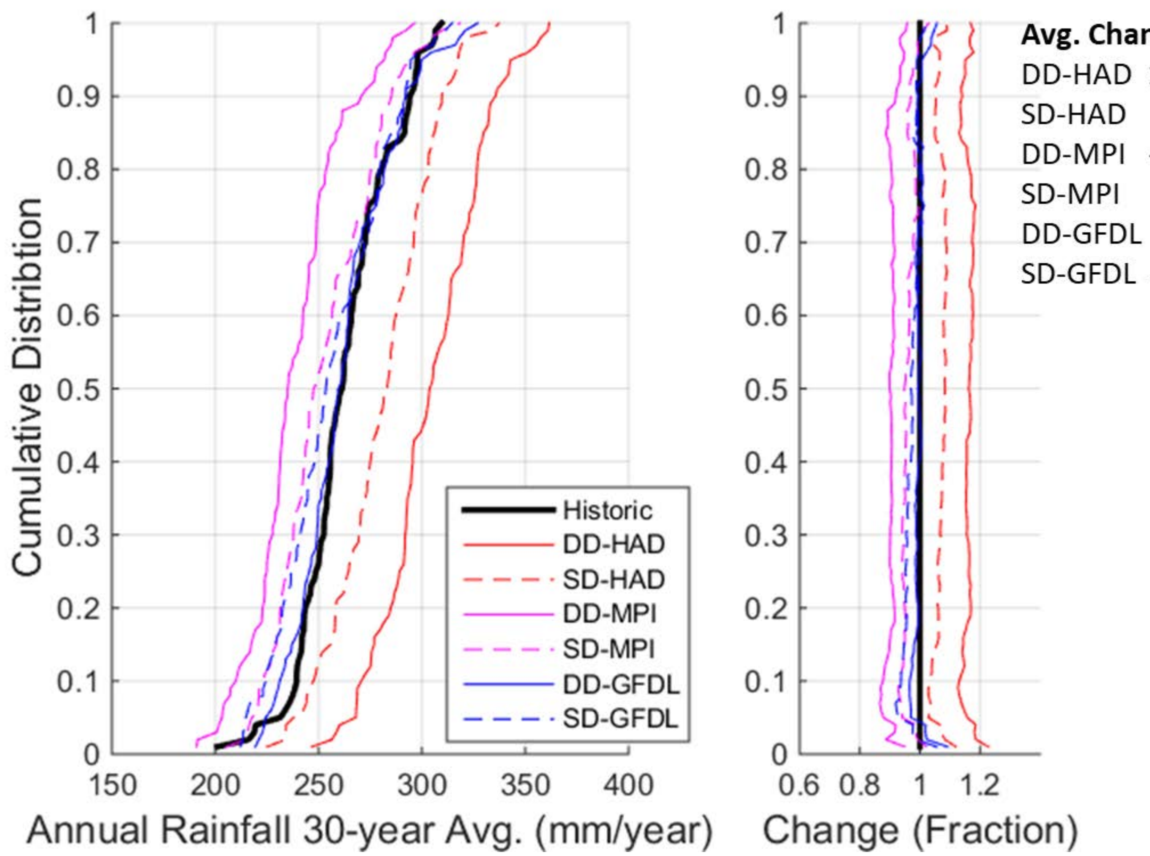

Figure 22. Cumulative distribution of 30-year mean annual precipitation over the BWR watershed from the 100 realizations of the 7 ensembles.

The right panel shows the quantiles ratio between the historical and projected ensembles. The average changes are indicated in the upper right.

In Figure 23, we plot the 30-year mean annual inflow into the lake. As expected, the directions of the trends for the different projections are similar to the trends shown in Figure 11 for precipitation in the Upper Santa Cruz Basin. However, the magnitude of the projected change is much larger for the lake inflow than for precipitation in the BWR watershed. The two extreme examples are the DD-HAD, with an average projected increase in precipitation by 16% and lake inflow by 42%, and the DD-MPI with average projected decrease in precipitation by 9% and lake inflow by 23%. This underscores the high sensitivity of the BWR watershed to small changes in precipitation, which is attributed to the complex hydrologic response in ephemeral streams.

The results for the projected changes in the outflow from the lake (not shown) are very similar to the changes projected for the inflow with projected average changes within 2% of the changes indicated in Figure 23.

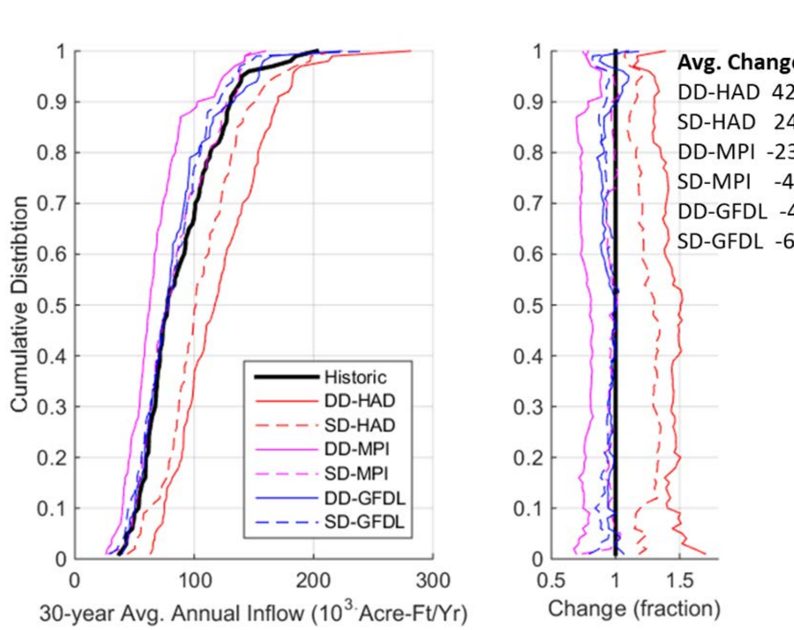

Figure 23. Cumulative distribution of 30-year mean annual inflow into Alamo Lake from the 100 realizations of the 7 ensembles.

The right panel shows the quantiles ratio between the historical and projected ensembles. The average changes are indicated in the upper right.

The projected climatic impact on Alamo Lake is shown in Figure 24. This figure shows the cumulative distribution of the percent of the time, in the 30-year duration, that the water level is projected to drop below 1070 feet which is the optimal lake level for operations shown in Figure 18. While the HAD shows fewer events with lake levels below this marker, the MPI shows a substantial increase in frequency of lake levels below 1070 feet. The MPI and HAD DD simulations produce the extremes for wet and dry events, respectively.

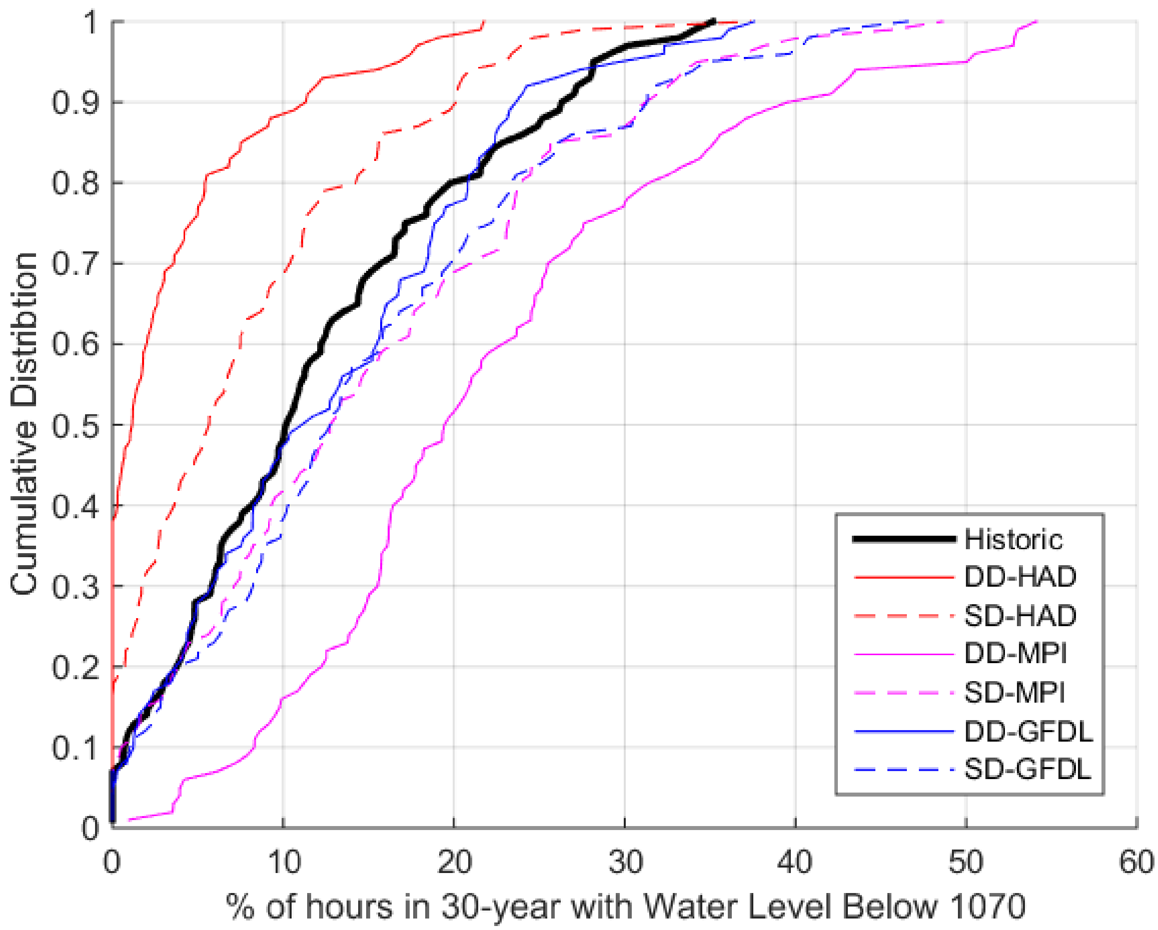

Figure 24: Cumulative distribution of the percent total hours in a 30-year duration that the lake level is below the recreation threshold of 1070 feet.

The projected extreme high levels of the lake are explored in Figure 25 for the flood control threshold of 1171.3 feet and the dam's crest of 1235 feet. The authors note that the projected encroachment into the flood control reservoir is not substantially different from the historic period, and the probabilities for this exceedance are minimal. Moreover, with the current lake operational rules and the historic simulation, the likelihood of reaching the crest level in any year is less than 3% because the large volume of flood control storage provides a buffer and would require multiple days of very high flow to fill.

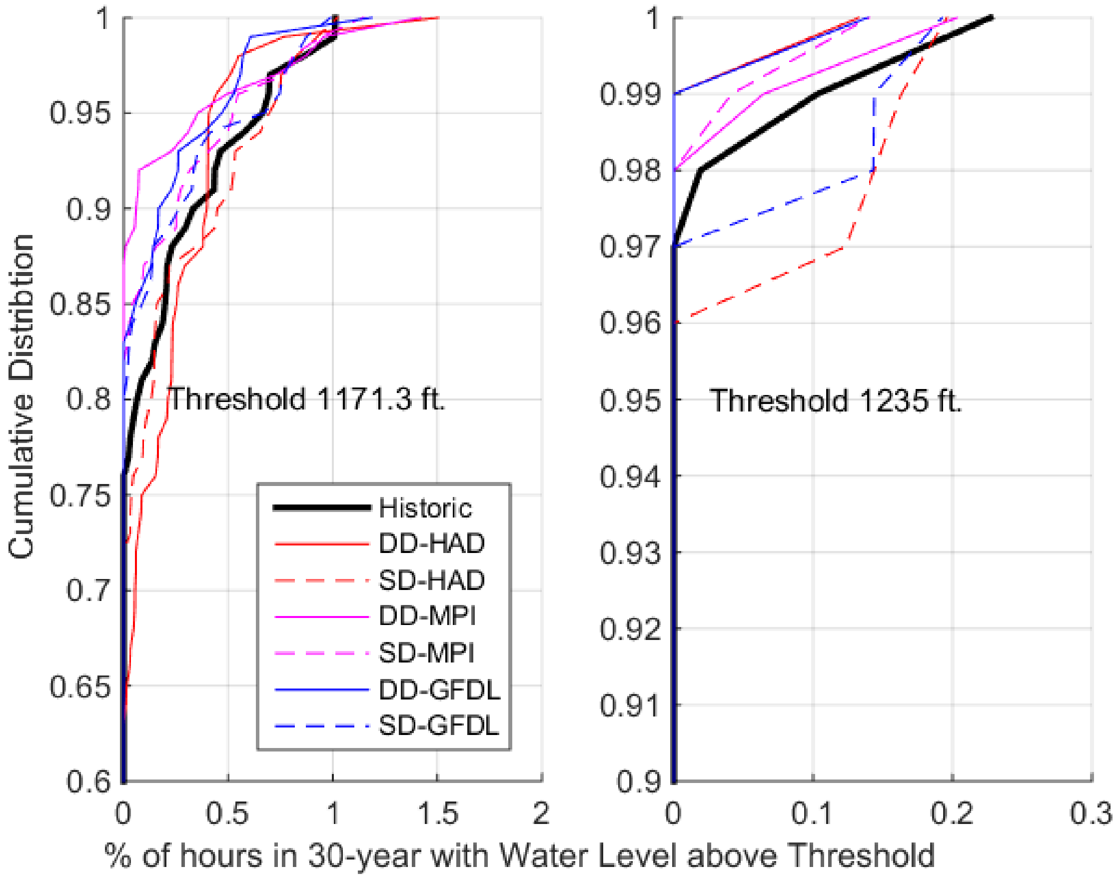

Figure 25: Cumulative distribution of the percent total hours in a 30-year duration that exceed the flood control threshold at 1171 ft (left) and the dam crest at 1235 ft (right).

This page intentionally left blank.

VII. Summary and Conclusions

This study assesses the influence of statistical versus dynamic GCM downscaling methodology on hydrologic impacts projected for the mid-21st century in two arid watersheds. The authors focused on two Arizona basins with different hydrological characteristics and water resources needs. The Upper Santa Cruz River (USCR) Basin is a shallow groundwater-based system that relies on intermittent flow events on the Santa Cruz River for recharge. The second is the Bill Williams River Watershed (BWRW) upstream of Lake Alamo, which is used to regulate flow events into Lake Havasu, in coordination with the Colorado River flow management.

Mid-21st century (2020-2059) precipitation projections simulated with Representative Concentration Pathways 8.5 (RCP 8.5) are available from three GCMs of the Coupled Model Intercomparison Project Phase 5 (CMIP5). The GCMs are:

1) HadGEM2-ES (Global Environmental Model, Version 2 from the United Kingdom Meteorological Office, the Hadley Centre),
2) MPI-ESM-LR (Earth System Model) running on low resolution (LR) grid from the Max Planck Institute for Meteorology, and
3) GFDL-ESM2M (NOAA Geophysical Fluid Dynamic Laboratory – Earth System Model).

These GCMs were reported to perform well for the southwest U.S. in simulating both winter and summer precipitation. Statistical and dynamic downscaled projections were compared for these three GCMs. For the statistical downscaled simulations, we used the Localized Constructed Analogs (LOCA) dataset available from Scripps Institution of Oceanography at the University of California San Diego. The dynamic downscaled precipitation simulations are from the University of Arizona, using the Advanced Research version of the Weather Research and Forecasting (WRF) model (Version 3.1) as the Regional Climate Model.

Comparing the mid-21st century precipitation projections, we found the DD simulations of the MPI and HAD to have larger projected changes than their corresponding SD simulations. These changes demonstrate contradictory trends since the MPI projected a drying trend, and the HAD projected a wetting trend. In addition to showing overall milder projections for precipitation changes, the other statistical downscaled models and raw GCMs all showed a future drying trend.

For both watersheds, we developed a custom weather generator (WG) that simulates ensembles of hourly precipitation realizations, in which a sufficient number of realizations are created to characterize the variability and uncertainty in the observed historical record. The WG was also used to produce six precipitation ensembles that represent the mid-21st century, developed from the raw and dynamically and statistically downscaled projections of the three GCMs. To produce these ensembles, we modified the WG to reflect changes identified by comparing the historic and projected period for each climate simulation.

These precipitation ensembles were used as input into a hydrological model framework developed for each basin. The framework for the USCR Basin is based on a hydrologic model that takes the WG-simulated rainfall as input and simulates streamflow at the Santa Cruz River near the U.S.-Mexico border. The streamflow is then routed along the river and estimates groundwater recharge into the shallow aquifer from transmission losses at the alluvial sections of the river channel.

A groundwater reservoir model of this shallow aquifer that considers recharge in conjunction with prescribed withdrawal management is implemented to estimate the aquifer's water storage and water levels.

For the BWRW, the hydrologic assessment was carried out using a modeling framework based on the operational hydrologic model configuration used by the NWS CBRFC. The WG was constructed to represent the temporal and spatial statistical characteristics of the observed CBRFC mean areal precipitation used as input to the SAC-SMA hydrologic model. The SAC-SMA hydrologic model runs with hourly mean areal precipitation to generate streamflow in ten internal locations and inflow into Alamo Lake. The lake outflow was simulated using USACE dam operational rules and lake specifications.

For both basins, the projected wetting and drying in the mid-21st century is magnified as precipitation is converted to streamflow and accumulated in microbasins (USCR Basin) or above-ground storage (Alamo Lake). For the USCR, these impacts are shown in the range of cumulative unmet demand for the city of Nogales. This study did not clearly identify changes in risk of flooding for Alamo Lake. However, the main findings suggest that it will become increasingly challenging to operate the lake at its target water level.

While the projections in this study did not show clear directional trends, it provides uncertainty bounds that can be useful for future planning of water supply and lake operations. These uncertainty bounds are much wider when considering the dynamically downscaled models of the MPI and HAD.

In summary, two key trends were observed in both analyses. First, DD projections tended to provide larger estimates of change, either wet or dry, than their respective SD projection with the same GCM. This implies that relying solely on statistically downscaled projections may underestimate the degree of change in projected precipitation. Secondly, the effects of changes in a hydrologic system are magnified as precipitation is converted to streamflow and then to a stored water resource. These examples show that a small change in local precipitation patterns can be magnified by terrestrial systems that control runoff, streamflow and storage.

These results provide important guidance to Reclamation planners concerned with estimating future water supply and demand. For further consideration, if a study's goal is to estimate the potential range of changes in precipitation, it would be prudent to include dynamically downscaled projections in the analysis. Secondly, a relatively small projected change in precipitation may be of concern if the hydrologic system of interest is similar to those described in this study.

A detailed investigation of the hydrologic and water resources system should be conducted before concluding that a region is resilient enough to withstand changes in precipitation patterns. The authors are hopeful that the results of this investigation will assist water resources planners at Reclamation and other agencies in their critical work

.This page intentionally left blank.

VIII. References

Anderson, E. A. (1976), A point energy and mass balance model of a snow cover, *NOAA Tech*. Rep. NWS 19, 150 pp., Natl. Oceanic and Atmos. Admin., Silver Spring, Md.

Arritt, R.W., D.C. Goering, C.J. Anderson. 2000. The North American Monsoon System in the Hadley Centre Coupled Ocean-Atmosphere GCM. *Geophysical Research Letters*, 27(4) 565-568.

Bill Williams River Corridor Technical Committee (1994) Proposed water management plan for Alamo Lake and the Bill Williams River.

Bukovsky, M. S., D. J. Gochis, and L. O. Mearns, 2013: Towards assessing NARCCAP regional climate model credibility for the North American monsoon: Current climate simulations. J. Climate, 26, 8802–8826, doi:10.1175/JCLI-D-11-00588.1.

Bukovsky, M.S., C. M. Carrillo, D. J. Gochis, D.M. Hammerling, R.R. McCrary, L. O. Mearns. 2015. Towards Assessing NARCCAP Regional Climate Model Credibility for the North American Monsoon: Future Climate Simulations. *Journal of Climate*, 28:6707: 6728

Burnash, R.J., R. L. Ferral, and R. A. McGuire (1973). A generalized streamflow simulation system conceptual modeling for digital computers. U.S Department of Commerce National Weather Service and State of California Department of Water Resources.

California Department of Water Resources, Perspective and Guidance for Climate Change Analysis, August 2015, Climate Change Technical Advisory Group.

Carpenter, T.M., and K.P. Georgakakos, 2001: Assessment of Folsom Lake response to historical and potential future climate scenarios: 1, Forecasting. *Journal of Hydrology*, 249, 148-175.

Castro, L.C., H-I. Chang, F. Dominguez, C. Carrillo, J-K. Schemm, and H-M. H. Juang. 2012. Can a regional climate model improve the ability to forecast the North American Monsoon? *Journal of Climate*, 25:8212-8236

Castro L.C and many colleagues. (2017). Assessing climate change impacts for DoD Installations in the Southwest United States during the warm season. A Final Report to Strategic Environmental Research and Development Program (SERDP) Project Number RC-2205, 128pp.

Cook, B.I., and R. Seager, 2013. The response of the North American Monsoon to increased greenhouse gas forcing. *Journal of Geophysical Research*. 118, 1690-1699, doi:10.1002/jgrd.50111.

Dee, D. P., Uppala, S. M., Simmons, A. J., Berrisford, P. , Poli, P. , Kobayashi, S. , Andrae, U. , Balmaseda, M. A., Balsamo, G. , Bauer, P. , Bechtold, P. , Beljaars, A. C., van de Berg, L. , Bidlot, J. , Bormann, N. , Delsol, C. , Dragani, R. , Fuentes, M. , Geer, A. J., Haimberger, L. , Healy, S. B., Hersbach, H. , Hólm, E. V., Isaksen, L. , Kållberg, P. , Köhler, M. , Matricardi, M. , McNally, A. P., Monge-Sanz, B. M., Morcrette, J. , Park, B. , Peubey, C. , de Rosnay, P. , Tavolato, C. , Thépaut, J. and Vitart, F. (2011), The ERA-Interim reanalysis: configuration and performance of the data assimilation system. *Q.J.R. Meteorol. Soc.,* 137: 553-597. doi:10.1002/qj.828

Deser C, Phillips A, Bourdette V, and Teng H. 2012. "Uncertainty in climate change projections: the role of internal variability." *Climate Dynamics,* 38(3-4), 527-546.

Eden, S., S.B. Megdal, E. Shamir, K. Chief, and E. Mott Lacroix. Opening the Black Box: Using a Hydrological Model to Link Stakeholder Engagement with Groundwater Management. Water 2016, 8(5), 216; doi:10.3390/w8050216.

Erwin, G., 2007. Groundwater Flow Model of the Santa Cruz Active Management Area Microbasins International Boundary to Nogales International Wastewater Treatment Plant Santa Cruz County. *Arizona Department of Water Resources, Modeling Report* #15.

Fowler, H. J., S. Blenkinsop. C. Tebaldi. (2007) Review: Linking climate change modelling to impacts studies: recent advances in downscaling techniques for hydrological modelling. *International Journal of Climatology,* 27: 1547–1578.

Garfin, G., A. Jardine, R. Merideth, M. Black, S. LeRoy (Eds.), 2013. Assessment of Climate Change in the Southwest United States: A Report Prepared for the National Climate Assessment. *A Report by the Southwest Climate Alliance*, Island Press, Washington, DC

Geil, K. L., Y. L. Serra, and X. Zeng, 2013: Assessment of CMIP5 model simulations of the North American Monsoon system. *J. Climate*, 26, 8787–8801.

Halpenny, L.C., and Halpenny, P.C., 1988 Review of the hydrogeology of the Santa Cruz Basin in the vicinity of the Santa Cruz-Pima County line: Tucson, Arizona. Water Development Corporation, 59 p.

House, P. K., M. L. Wood, P. A. Pearthree. 1999. Hydrologic and Geomorphic characteristics of the Bill Williams River, Arizona. *Arizona Geological Survey Open-File Report* 99-4 February 1999.

Kirby, K. and Burnham M.W. Technical Consideration for Alamo Lake Operation, U.S Army Corps of Engineers, Hydrologic Engineering Center, April 1998.

Kotamarthi, R., L. Mearns, K. Hayhoe, C.L. Castro, and D. Wuebbles, 2016. Use of Climate Information for Decision Making and Impacts Research: State of Our

Understanding. *Strategic Environmental Research and Development Program (SERDP) Project RC-2242, Technical Report.* 54 pp. www.dtic.mil/dtic/tr/fulltext/u2/1029525.pdf

Liang, X. Z., Zhu, J., Kunkel, K. E., Ting, M., & Wang, J. X. (2008). Do CGCMs simulate the North American monsoon precipitation seasonal–interannual *variability? Journal of Climate,* 21(17), 4424-4448.

Lin, J. L., Mapes, B. E., Weickmann, K. M., Kiladis, G. N., Schubert, S. D., Suarez, M. J., ... & Lee, M. I. (2008). North American monsoon and convectively coupled equatorial waves simulated by IPCC AR4 coupled GCMs. *Journal of Climate*, 21(12), 2919-2937. DOI: 10.1175/2007JCLI1815.1

Liu, T. A.Y. Sun, K. Nelson, W.E. Hipke. Cloud computing for integrated stochastic groundwater uncertainty analysis *Int. J. Digit. Earth*, 2012 (2012), pp. 1-25

Livneh B., E.A. Rosenberg, C. Lin, B. Nijssen, V. Mishra, K.M. Andreadis, E.P. Maurer, and D.P. Lettenmaier, 2013: A Long-Term Hydrologically Based Dataset of Land Surface Fluxes and States for the Conterminous United States: Update and Extensions. *Journal of Climate,* 26, 9384–9392.

Maraun, D., F. Wetterhall, A. Ireson, E. Chandler, RJ. Kendon, E. Widmann, M. Brienen, S. Rust, H. Sauter, T.Theme, M. K. C. Venema, V. Chun, K. Goodess, C G. Jones, R. Onof, C.Vrac, M. Thiele-Eich, Insa (2010). Precipitation downscaling under climate change: Recent developments to bridge the gap between dynamical models and the end user. *Reviews of Geophysics - REV GEOPHYS.* 48. 10.1029/2009RG000314.

Nelson, K. M. (2007). Groundwater Flow Model of The Santa Cruz Active Management Area along The Effluent-Dominated Santa Cruz River, Santa Cruz and Pima Counties, Arizona, Modeling Report No. 14, *Arizona Department of Water Resources.* http://www.azwater.gov/AzDWR/Hydrology/Modeling/documents/Modeling_Report_14.pdf

Nelson K. M. (2010). Risk Analysis of Pumping Impacts on Simulated Groundwater Flow in the Santa Cruz Active Management Area. *Modeling Report No. 21* (May, 2010) http://www.azwater.gov/azdwr/Hydrology/Modeling/documents/Modeling_Report_21.pdf

Page, W.R., Menges, C.M., Gray, Floyd, Berry, M.E., Bultman, M.W., Cosca, M.A., VanSistine, D.P., 2016. Geologic map of the rio rico and Nogales 7.5' quadrangles, Santa Cruz county, Arizona. U.S. Geol. Surv. Sci. Investig. Map 3354, 32 pp. pamphlet, 2 sheets, scale 1:24,000. http://dx.doi.org/10.3133/sim3354.

Pascale, S., S. Bordoni, S.B. Kapnick, G.A. Vecchi, L. Jia, T.L. Delworth, S. Underwood, and W. Anderson, 2016: The Impact of Horizontal Resolution on North American Monsoon Gulf of California Moisture Surges in a Suite of Coupled Global Climate Models. *J. Climate*, 29, 7911–7936, doi: 1

Patterson, l.L. Somers, W.P., 1966, Magnitude and frequency of floods in the United States: Part 9. *Colorado River Basin: U.S. Geological Survey Water-Supply Paper* 1683, 476p.

Pierce DW, Cayan DR, Thrasher BL. 2014. "Statistical Downscaling Using Localized Constructed Analogs (LOCA)." *Journal of Hydrometeorology,* 15, 2558-2585.

Restrepo-Posada, P. J., and P. S. Eagleson, 1982. Identification of independent rainstorms. *J. Hydrol*., 55, 303-319.

Schaake, J., A. Henkel, and S. Cong, 2004: Application of PRISM climatologies for hydrologic modeling and forecasting in the western U.S. *Preprints, 18th Conf. on Hydrology,* Seattle, WA, Amer. Meteor. Soc., 5.3.

Shamir, E. 2017a. The value and skill of seasonal forecasts for water resources management in the Upper Santa Cruz River basin, southern Arizona*. Journal of Arid Environments*. 137: 35-45.

Shamir, E., 2017b: Modification and calibration of the rainfall weather generator for the Upper Santa-Cruz River basin, Arizona HRC Technical Note No. 94. *Hydrologic Research Center,* San Diego, CA, 1 August 2017.

Shamir, E. Megdal, S. Carrillo, C. Castro, LC. Chang, H-I. Chief, K. Corkhill, EF. Eden, S. Georgakakos, PK. Nelson, MK. and Prietto, J. 2015. Climate change and water resources management in the Upper Santa Cruz River, Arizona. *Journal of Hydrology*. 521: 18-33. https://doi.org/10.1016/j.jhydrol.2014.11.062

Shamir, E., E. Halper, T Modrick, K P. Georgakakos, Hsin-I Chang, T M. Lahmers, C. Castro. Statistical and dynamical downscaling impact on projected hydrologic assessment in arid environment: A case study from Bill Williams River basin and Alamo Lake Arizona, *Journal of Hydrology X2 (2019) 1000019.* http://www.elsevier.com/locate/hydroa

Shamir, E., 2014. Modification and Calibration of the Hydrologic Modeling Framework for the Santa Cruz River Basin, Arizona. HRC Technical Note No. 71. *Hydrologic Research Center,* San Diego, CA, http://www.hrc-lab.org/projects/projectpdfs/HRCTN71_20140901.pdf

Shamir, E., Wang, J., Georgakakos, K.P., 2007a. Probabilistic streamflow generation model for data sparse arid watersheds, *J. Amer. Wat. Resour.* Assoc. 43(5) 1142-1154.

Shamir, E., Graham, N.E. Meko, D.M. Georgakakos, K.P., 2007b. Hydrologic model for water resources planning in Santa-Cruz River, Southern Arizona, *J. Amer. Wat. Resour.* Assoc. 43(5) 1155-1170.

Shamir E., NE. Graham, J Wang, DM Meko, and KP Georgakakos. Stochastic streamflow scenarios for the Santa-Cruz River at the Nogales gauge, Prepared for the Arizona Department of Water Resources, Santa Cruz, AMA, *Hydrologic Research Center Technical Report No. 4,* December 2005.http://www.hrc-lab.org/projects/dsp_projectSubPage.php?subpage=santacruz

Sheffield, Justin & Barrett, Andrew & Colle, Brian & Fernando, D & Fu, Rong & L. Geil, Kerrie & Hu, Qi & Kinter, Jim & Kumar, Sanjiv & Langenbrunner, Baird & Lombardo, Kelly & N. Long, Lindsey & Maloney, Eric & Mariotti, Annarita & Meyerson, Joyce & Mo, Kingtse & David Neelin, J & Nigam, Sumant & Pan, Zaitao & Yin, Lei. (2013a). North American Climate in CMIP5 Experiments. Part I: Evaluation of Historical Simulations of Continental and Regional Climatology. *Journal of Climate.* 26. 9209-9245. 10.1175/JCLI-D-12-00592.1.

Sheffield, Justin & Camargo, Suzana & Fu, Rong & Hu, Qi & Jiang, Xianan & Johnson, Nathaniel & B. Karnauskas, Kristopher & Kim, Seon & Kinter, Jim & Kumar, Sanjiv & Langenbrunner, Baird & Maloney, Eric & Mariotti, Annarita & Meyerson, Joyce & David Neelin, J & Nigam, Sumant & Pan, Zaitao & Ruiz-Barradas, Alfredo & Seager, Richard & Zhao, Ming. (2013b). North American Climate in CMIP5 Experiments. Part II: Evaluation of Historical Simulations of Intraseasonal to Decadal Variability. *Journal of Climate.* 26. 9247-9290. 10.1175/JCLI-D-12-00593.1.

Shilo, E., B. Ziv, E. Shamir, A. Rimmer, 2015, Evaporation from Lake Kinneret, Israel, during hot summer days, *Journal of Hydrology*, 528: 264–275.

US Army Corps of Engineers, Los Angeles District, Reservoir Regulation Section CESPL-ED-HR Water Control Manual, Alamo Dam and Lake Colorado River Basin, Bill Williams River, Arizona. October 2003.

Wang, J., Shamir, E., and K.P. Georgakakos, 2007. Study of extreme precipitation over the Panama Canal Watershed. *HRC Technical Report No. 6 Hydrologic Research Center*, San Diego, CA. 1 August 2007 (CDO185933MMP), 136pp.

Wilks, S.D. 2006. Statistical methods in the atmospheric sciences, *International Geophysics Series,* Elsevier 467p

IX. Data Access

The data sets for this study include netCDF files for all climate simulations and reference data including dynamically downscaled (WRF), statistically downscaled (LOCA), raw Global Climate Model (GCM) and Livneh (reference data set) files. The data set also includes comma separated variable files for each of the Bill Williams Watershed sub-basins and code specific to the Sacramento Soil Moisture Accounting Model from the Colorado River Basin Forecast Center.

The geographic location of the data and simulations are the two river basins described in the report. The time period covered by the data includes measurements dating from 1915 and climate simulations through 2100.

Keywords: Dynamical Downscaling, Statistical Downscaling, Weather Generator, Global Climate Model, Upper Santa Cruz River Basin, Bill Williams River Basin, Arid, Hydrology, Climate Change

Contact the Phoenix Area Office Information Management and Technology group to arrange for a copy of the study data sets. The data sets combine for 3.3 Terabytes (TB). The requester will need to provide 4TB USB 3.0 external drives for each full copy of the data sets.

Data Set Contact Information:
Russ Bryant, Supervisory IT Specialist, rbryant@usbr.gov, 623-773-6410
Phoenix Area Office General Line: 623-773-6200

X. Appendix: – Statistical and Dynamical Downscaling Impact on Projected Hydrologic Assessment in Arid Environment: A Case Study from Bill Williams River Basin and Alamo Lake, Arizona;

Statistical and dynamical downscaling impact on projected hydrologic assessment in arid environment: A case study from Bill Williams River Basin and Alamo Lake, Arizona

Eylon Shamir, Eve Halper, Theresa Modrick, Konstantine P. Georgakakos, Hsin-I Chang, Timothy, M. Lahmers, Christopher Castro.

Abstract

A study was conducted to assess the projected impact of future climate on Alamo Lake and the Bill Williams River basin.   We analyzed simulations of three-selected Representative Concentration Pathways 8.5 Global Climate Models (GCM) (i.e. HadGEM2-ES, MPI-ESM-LR and GFDL-ESM2M). These GCMs which, were part of the Intergovernmental Panel on Climate Change (IPCC) Fifth Assessment Report, were selected as well performing GCMs that represent the historic climatology and prevailing precipitation bearing synoptic conditions in the southwest US. An analysis of both statistically and dynamically downscaled simulations projected increase in the frequency of dry winters during the mid-21st century (2020-2059) in two out of the three selected GCMs. For summer precipitation, the statistically downscaled simulations are inconclusive whereas, the dynamically downscaled simulations showed significant but contradicting future projections.

In order to assess the impact of the projected climate on the hydrologic cycle at the Bill Williams River basins, we developed a modeling framework that includes the following components: 1) a weather generator that produces realizations of likely hourly precipitation

events over the basin; 2) a hydrologic model that is based on the Colorado Basin River Forecast Center (CBRFC), National Weather Service modeling configuration that predicts flow at ten internal points and inflow into Alamo Lake; and 3) a lake model with the existing operation rules to simulates the lake outflow and levels.

Using the above-described modeling framework, the impact of the projected mid 21-century climate on Alamo Lake was examined with respect to the total outflow from the dam, the frequency of large outflow events, and the frequency of high and low lake levels. The results show that dynamic downscaling provides a larger range of impacts than those provided by statistical downscaling. The results also indicate a wide range of impact scenarios with contradicting trends among the selected climate projections for mid-21st Century. These results imply increasing challenges in operating the Lake at its target level. This modeling framework can potentially be used to examine various future scenarios and to develop recommendations for a sustainable management scheme for the Alamo Lake.

Keywords: Bill Williams River; Alamo Lake; Statistical downscaling, Dynamical downscaling; Hydrologic Impact Assessment; Arid Hydrology

Highlights

- The precipitation projections are different among the climate models and downscaling methodologies.
- The impact of projected mid 21-century climate conditions on Alamo Lake is uncertain and points to wet or dry trend scenarios.
- Dynamic downscaling showed a larger range of impacts than those of statistical downscaling
- The uncertain projections imply that future management should be adaptive and ready for the projected range of changes.

1. Introduction

We conducted a hydrologic impact assessment using projected climate for the mid-21st century at the Bill Williams River (BWR) watershed and Alamo Lake, a tributary of the Colorado River, upstream of Lake Havasu. Several studies have explored the projected impact of future climate on the Colorado River flow (e.g. Christensen and Lettenmaier, 2007; Vano et al. 2014; Gautam and Mascaro, 2018). However, because of the large spatial climate variability within the Colorado River watershed, these basin-wide studies may not be representative of the BWR tributary. In the arid water-scarce BWR watershed, the precipitation high spatiotemporal variability triggers highly variable streamflow events in ephemeral streams. Therefore, even small projected climatic changes may be a cause of concern.

Our objective in this study is to evaluate the differences in the hydrologic assessment that result from the selection of GCMs or the selection of downscaling methodology. For hydrologic impact assessment studies, a downscaling of Global Climate Models (GCMs) future projections is often needed in order to bridge the scale gap between the coarse GCM simulations and the required finer resolution for regional and local watershed studies. Two fundamental downscaling approaches are often used: Statistical Downscaling (SD) and Dynamical Downscaling (DD).

Statistical downscaling (SD) procedures derive empirical relationships between atmospheric forcing data of the GCM and surface variable of interest in finer resolution to apply those relationships to future GCMs' projections. It assumes that the statistical relationship between the predictors (GCM) and predictand (surface variables) do not change over time and are therefore stationary (e.g., Carpenter and Georgakakos, 2001). The SD procedures main advantage is that they do not require special computational resources and therefore can be used to produce high-resolution simulations and can be applied for a large number of GCMs.

Dynamically downscale (DD) models use Regional Climate Models nested within the GCM to simulate local climate features. They respond in physically consistent ways to resolve regional atmospheric processes and simulate mesoscale variables of interest, such as: convective storms, extreme events, and snowfall versus rainfall. They simulate internally consistent multivariate quantities within an atmospheric column. The main limitation associated with DD is the requirement for intensive computational resources, therefore DD simulations are only available for a limited number of GCMs. General discussion of the pros-and-cons of selecting one downscaling approach over the other have been the subject of multiple manuscripts (e.g. Fowler et al. 2007; Maraun et al. 2010; Kotamarthi et al. 2016).

Local hydrologic impact assessment studies for various objectives often face the dilemma of having to choose between SD and DD approaches. SD simulations are easier to obtain and there are several readily available datasets that include simulations for many different GCMs. DD simulations on the other hand, require a high level of expertise to produce and are available for only a few GCMs. This study is geared to evaluate the differences in the hydrologic assessment that result from selecting one downscaling approach over the other. We compared between the state-of-the-art DD and SD datasets that are available for the study area.

To assess the hydrologic impact of the projected climate a hydrologic modeling framework was developed for the Bill Williams River and Alamo Lake, which consists of a 1) precipitation weather generator (WG) that produces ensembles of equally likely to occur hourly precipitation sequences; 2) hydrologic model that simulates flow in internal points in the basin and inflow into Alamo Lake; and 3) lake model that simulates lake levels and outflow.

The objective of the WG is to transform the climate models simulations into precipitation ensembles that can be used as input to the hydrologic model. A WG ensemble with sufficient realizations represents the spatio-temporal variability of the observed record. In addition, the WG was further modified to reflect changes that were identified by comparing the historic and projected climate models simulations, to generate precipitation ensembles that reflect the projected changes. This approach provides a tool to translate a single climate model simulation into an ensemble that can be used as input for the hydrologic model and thus simulate a distribution of model outcomes, rather than a single simulation. This is an attractive approach for water resources planning in arid regions that have large inter- and intra annual climate variability and its hydrologic response is very sensitive to nuances in precipitation patterns.

In the next section (Section 2), we discuss the selected GCMs and their performance for the study area. The study area and its hydrologic characteristics are presented in Section 3. Section 4 is dedicated to the description of the hydrologic modeling framework that is implemented in this study. Following the results presented in Section 5, in Section 6 we provide a summary and conclusions.

2. Selected Climate Models

Three GCMs from the Coupled Model Intercomparison Project Phase 5 (CMIP5) simulated with Representative Concentration Pathways 8.5 (RCP 8.5) were selected for this study. The selected GCMs are: 1) HadGEM2-ES (Global Environmental Model, Version 2 from the United Kingdom Meteorological Office, the Hadley Centre), 2) MPI-ESM-LR (Earth System Model) running on low resolution (LR) grid from the Max Planck Institute for Meteorology, and 3) GFDL-ESM2M (NOAA Geophysical Fluid Dynamic Laboratory – Earth System Model). These GCMs were selected to be dynamically downscaled because of their good performance over North America and because they represent the range of the North America climate sensitivity that is provided by all CMIP 5 GCMs (Sheffield et al. 2013 I and II).

DD precipitation simulations of the three GCMs are available for the historic period (1950-2005) and future projections with RCP 8.5 (2006-2100) at ~25 km horizontal grid resolution from National Center for Atmospheric Research (NCAR) and the University of Arizona, Department of Hydrology and Atmospheric Sciences. The simulations followed the specifications of the North-America Coordinated Regional Climate Downscaling Experiment (CORDEX) program (https://na-cordex.org/), an initiative sponsored by the World Climate Research Program to provide regional climate downscaling data for regional climate change adaptation and impacts assessment. The three GCMs were downscaled for the domain of the NA-CORDEX program using the Advanced Research version of the Weather Research and Forecasting (WRF) model (Version 3.1) as the Regional Climate Model. The configuration of the WRF model is described in Castro et al. (2017). The simulations are available at 3-hour intervals for the WRF-HadGEM2-ES, and 6-hour intervals for the WRF-MPI-ESM-LR and WRF-GFDL-ESM2M.

An equivalent WRF reanalysis 6-hour precipitation dataset (1979-2015) nested within ERA-Interim global reanalysis (Dee et al. 2011) is also available at a similar spatial resolution and model configuration as the DD simulations.

SD daily precipitation for 1950-2005 and 2006 -2099 at 0.0625° (~6km) horizontal grid spacing for the three GCMs is available for the western U.S from the state-of-the-art Localized Constructed Analogs (LOCA) methodology (Pierce et al., 2014). LOCA’s leading downscaling assumption is that the forecast will evolve the same way as the best matching historical event. An observed gridded precipitation with similar spatiotemporal resolution for 1950-2015 is available from Livneh et al. (2013). This dataset which was used as the reference for the derivation of the LOCA dataset, was developed for the conterminous Mexico, and U.S. and regions in Canada south of 53° N.

In the Southwest U.S., a credible GCM to be used for hydrologic impact assessment should be one that represents the precipitation characteristics of both winter and summer. The prevailing winter storms (November-March) originate from large-scale low-pressure frontal systems approaching from the west and southwest. These storms that may last for a few days to drop persistent rain over large areas, often produce snowfall at higher elevations. However, in our study area, the falling snow commonly melts within a few days and is not a major runoff component into Alamo Lake.

The prevailing summer rainfall (June–September), is driven by the North American Monsson (NAM) climate system, which triggers isolated convective cells that often produce intense short-lived rainfall events. While winter rainfall events generate gradual rising streamflow events with low flow that persists following the rain event, summer rainfall events trigger quick and sudden rising flow followed by short-lived low flow.

A comprehensive evaluation analysis of GCMs for winter precipitation is available from the California Department of Water Resources (2015) who used 3-step model screening process to evaluate the historical performance of 31 CMIP 5 GCMs in three sequential spatial scales (i.e. global, Southwestern U.S, and California). Most winter storms to hit Arizona originate in the mid latitude Pacific Ocean and cross over California. In their analysis, the HadGEM2-ES was selected among the 10 top performing GCMs while the MPI-ESM-LR and GFDL-ESM2M were selected among the 15 top performing models.

Dominated by regional (mesoscale) processes, representing the NAM in the relatively coarse GCM is a challenge (e.g. Castro et al. 2012 and 2017; Bukovsky et al. 2013 and; 2015, Geil et al. 2013). Evaluation of large-scale features of the NAM system by GCMs is an active research topic (e.g. Arritt et al. 2000; Liang et al., 2008; Lin et al., 2008; Geil et al. 2013; Pascale et al., 2016). The selected GCMs for this study were reported to well represent the NAM system (Geil et al., 2013).

Given our study objective to evaluate the selection impact of the downscaling methodology on hydrologic impact assessments, a case can be made that three GCMs and one RCM (i.e. WRF) as analyzed in this study may not be sufficient to reach conclusions that can be generalized for all SD and DD simulations. As mentioned above, the selection of the three GCMs is constrained by the limited availability of DD simulations. The selected datasets, as far as we know, are the only high-resolution datasets readily available and any future climate study conducted in this region would have likely contemplated the use of the DD and SD datasets presented herein. Therefore, it is likely that for the southwest U.S. region the selected datasets well represent the consequence of the selection of a downscaling procedure.

3. Study area

The Bill Williams River watershed (hereinafter BWR) (5,393 mile^2; 13,968 km^2) in west-central Arizona, is a tributary of the Colorado River that drains into Lake Havasu just upstream of Parker Dam. Alamo Dam, 36 miles (58 km) upstream of the confluence with the Colorado River, was built in 1968 to form Alamo Lake as a multi-purpose facility with a primary objective to control flooding downstream of the dam on the Lower BWR. Secondary objectives of the lake include water supply and conservation, recreation, and fish and wildlife enhancement. At the site of the dam, the contributing drainage area is about 4770 mile^2 (12,354 km^2) from mainly three ephemeral tributaries, with a few perennial sections, which drain into Alamo Lake: Big Sandy River, Santa Maria River, and Burro Creek. No significant flood control structures exist in the drainage area of these tributaries. A map of the BWR watershed with the eleven sub basins that were used for the model development (further discussed in Section 4) is in Figure 1.

The diverse physiography of the BWR watershed spans from high elevation forested mountains to rugged desert terrain in the lower elevations. Detailed hydrologic and geomorphic description of the watershed is provided in House et al. (1999).

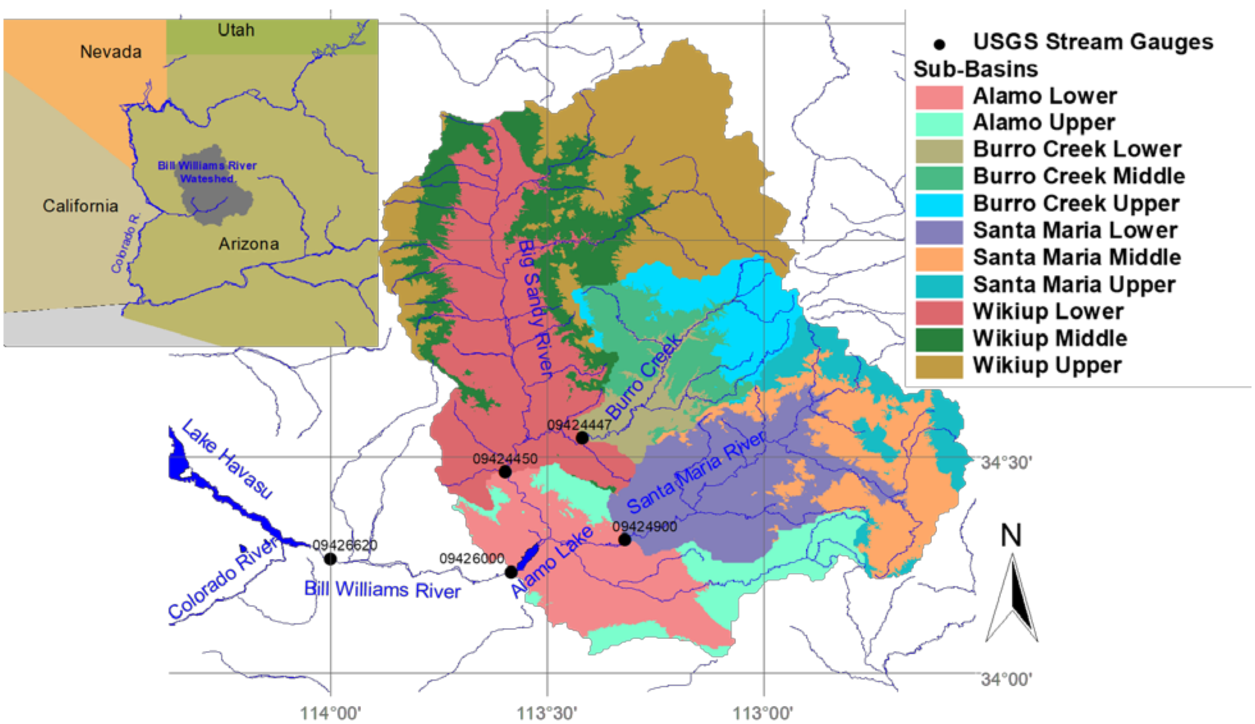

Figure 1: A map of the Bill Williams River Watershed. Description of the eleven sub-basins is in Table 1.

Operated by the U.S Army Corp of Engineers (USACE), releases from Alamo dam have a direct impact on the operation of the Lower Colorado River by the Bureau of Reclamation. Downstream of Alamo Lake, the Lower BWR flows through a series of alternating narrow canyons and wider alluvial valley reaches. The peak discharge in the U.S Geological Survey (USGS) gauge just below Alamo Dam (USGS09426000) during the pre-dam era was estimated at 200,000 cfs (5,660 cms) in February 1891 (Patterson and Somers, 1966), while post-dam maximum discharge, as of October 2017, has not exceeded 7,000 cfs (~200 cms), which is the maximum possible release rate from the dam.

Climate Models Evaluation

A comparison of the average monthly total precipitation among the SD, DD, raw GCM, WRF ERA-Interim reanalysis, and gridded observations for the historical period (1950-2005) is shown in Figure 2 for the Had-GEM2-ES (left), MPI-ESM-LR (center), and GFDL-ESM2M (right). This Figure compares among the spatial averages over the entire BWR watershed and it represents well the results for each of the eleven sub-basins (Figures for the sub-basins are not included). It is seen that the SD simulations closely follow the observed gridded dataset. This is expected because the SD procedure was designed to conform to the observed record. The WRF ERA-Interim reanalysis follows the seasonal patterns fairly well, which is indicative of the skill of WRF for producing monthly climatological averages when it is nested within optimal boundary conditions. The added value of WRF is also seen by comparing the raw GCMs to the DD simulations. Marked differences are seen for the summer, where raw GCMs underestimate the precipitation and DD overestimated by HAD and lagged by about 1-month by the GFDL.

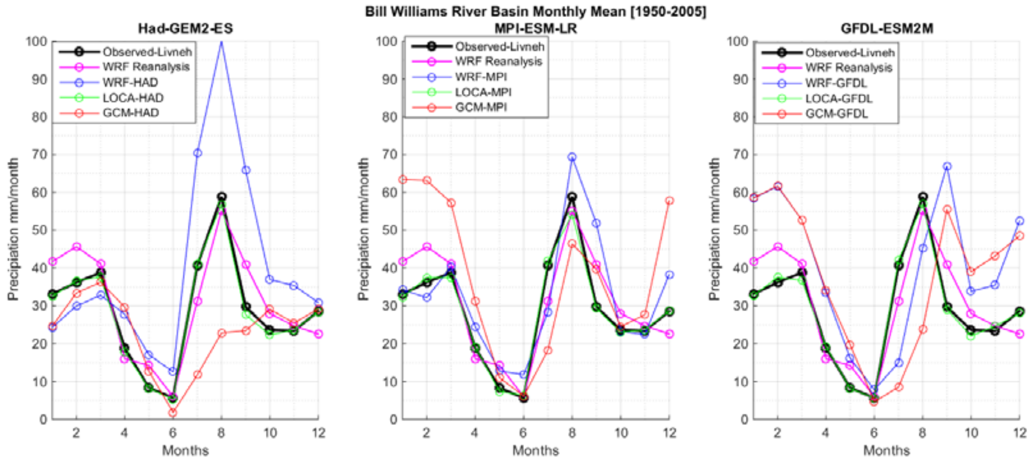

Figure 2: Bill Williams River Watershed mean areal average monthly precipitation totals (1950-2005) from observations, WRF reanalysis, DD, SD, and raw GCMs for the HAD, MPI, and GFDL from left to right, respectively.

Observation Datasets

Hourly Mean Areal Precipitation (MAP) (1 October 1980- 30 September 2010) data from the Colorado Basin River Forecast Center (CBRFC), National Weather Service (NWS) (www.cbrfc.noaa.gov) are available for eleven sub-basins in the BWR watershed (Table 1). These historical MAP time series were derived by CBRFC for the purpose of calibration of their hydrologic models. Using elevation thresholds, each of the three tributaries that drain into Alamo Lake (Figure 1) was divided into three sub-basins (upper, middle, and lower). Two Additional downstream sub-basins (upper and lower) just upstream of the lake were configured by CBRFC. The MAP derivation procedure consists of quality control of the rain gauge records and spatial interpolation with the Mountain Mapper technique used by the NWS River Forecast System (Schaake et al., 2004).

The inflow into Alamo Lake was calculated from a mass balance equation, using lake's water level from the USACE (1980-2010), outflow from the lake as observed at the gauge just below the dam, and estimated monthly lake evaporation from CBRFC. For the analyses of future projections, we used the historic monthly evaporation values. It is likely that future climate may impact the lake evaporation. However, lake evaporation is a complex process and the projection of future evaporation requires analysis of the lake energy balance in addition to the energy and hydrodynamic atmospheric conditions over the lake (e.g. Shilo et al. 2015).

Table 1: CBRFC Sub-basins

	Sub basins		CBRFC Codes	Area (mile^2/km^2)	Elevation (m) centroid and (range)	*Summer / Winter Average MAP (mm/season)
1	Alamo	Upper	alma3luh	287 / 743	992 (758 - 1908)	143 / 194
2		Lower	alma3llh	451 / 1168	588 (363 - 758)	95 / 148
3	Santa	Upper	smba3huh	196 / 508	1654 (1515 - 2092)	213 / 240
4	Maria	Middle	smba3hmh	413 / 1070	1369 (1212 - 1515)	179 /215
5		Lower	smba3hlh	516 / 1336	938 (470 - 1212)	126 / 182
6	Wikiup	Upper	wkpa3luh	823 / 2132	1692 (1515 - 2405)	163 / 202
7		Middle	wkpa3lmh	445 / 1153	1371 (1212 - 1515)	135 / 175
8		Lower	wkpa3llh	850 / 2201	911 (434 - 1212)	93 / 143
9	Burro	Upper	bcba3huh	231 / 598	1654 (1515 - 2092)	220 / 267
10	Creek	Middle	bcba3hmh	224 / 580	1369 (1212 - 1515)	197 / 250
11		Lower	bcba3hlh	151 / 388	938 (620 - 1212)	146 / 202

*Average summer (April-September) and winter (October –March) were calculated for 1980-2010 from CBRFC MAP for the eleven sub-basins.

Hydrologic Analysis

There are two wet seasons (winter and summer) in the BWR watershed. The winter (November-March) peaks in January-February and the summer extends from July to September. The spring (April-June) is relatively dry with mean areal precipitation of 21 mm and less than 1000 acre feet inflow to the lake. The fall (October) is generally very dry with infrequent very wet storms that have synoptic rainfall bearing conditions that are often different than the ones of the winter storms.

The difference between winter and summer MAP is seen in Figure 3 for the average over the entire BWR watershed. Average winter (November-March) and summer (June-September) precipitation, as indicated by the dashed lines, are 180 and 130 mm/season, respectively. Although the winter season is occasionally very wet, with a maximum of 430 mm, it is more often drier than the average, which implies a more skewed distribution (skewness coefficients are 0.95 and 0.52 for winter and summer, respectively). The higher variability of winter precipitation can also be shown by comparing the coefficient of variations (0.6 and 0.4 for winter and summer, respectively).

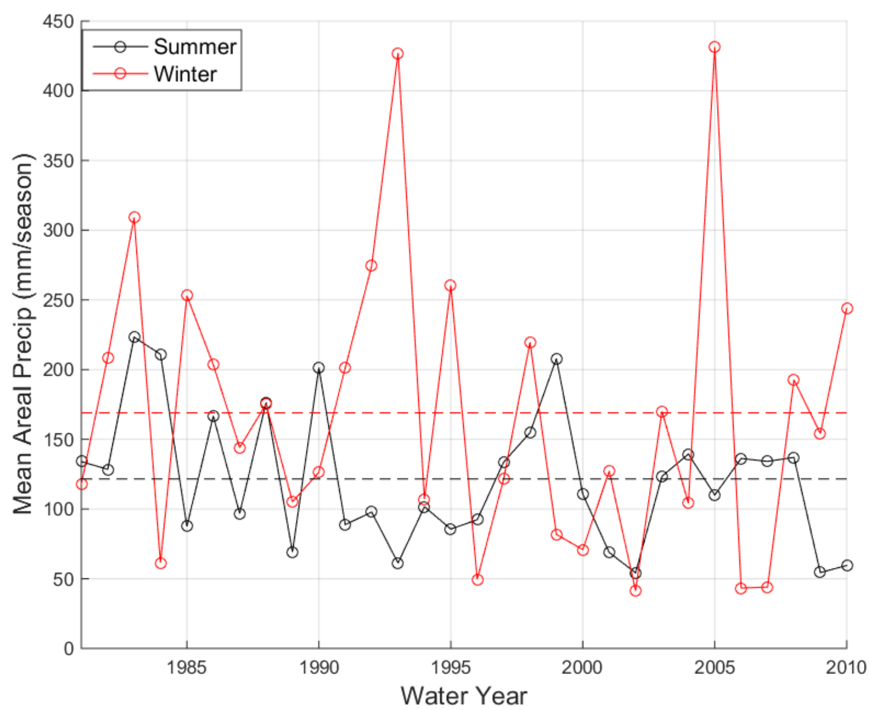

Figure 3: Summer and winter mean areal precipitation (mm/season) over the entire BWR watershed. Dashed horizontal lines are the inter-annual averages.

Compared with summer, winter streamflow events are longer with larger volume, higher daily maximum, and the duration between the streamflow events is shorter. The shorter duration between winter streamflow events may be attributed to the longer events that have long lasting baseflow (Shamir et al. 2017). In Figure 4 total seasonal (winter and summer) inflow into Alamo Lake are compared with total seasonal outflow from the Lake. Notice that although average summer precipitation is ~75% of the average winter precipitation, the average summer inflow into Alamo Lake is only ~10% of the average winter inflow. Even the largest releases recorded for the summer are relatively small compared with winter releases. It is also noted that many of the winters had very low inflows. This large seasonal difference between precipitation and streamflow ratio underscores the necessity to consider the properties of the precipitation events and their interaction with land surface processes that control the generation of streamflow.

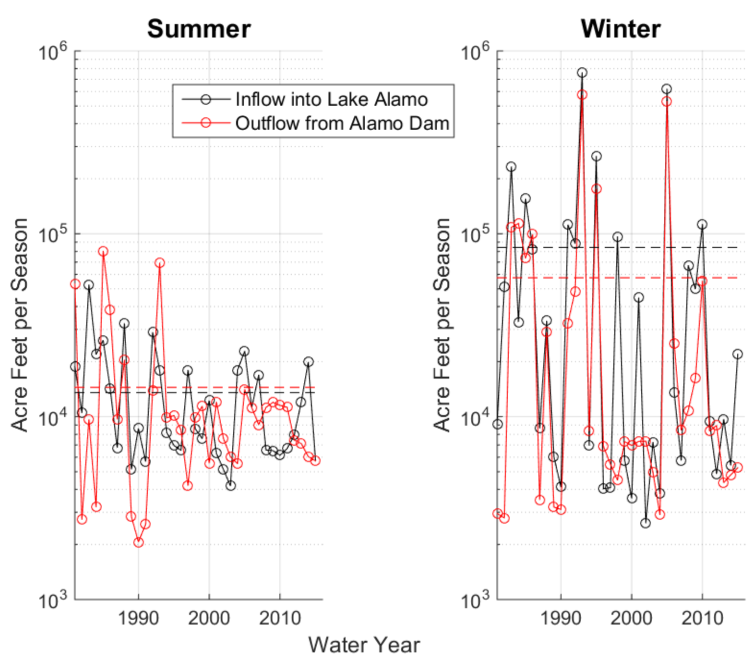

Figure 4: Summer (left) and winter (right), total estimated inflow (black) and outflow (red), into and from Alamo Lake.

4. Hydrologic Modeling Framework

In order to assess the impact of the projected climate on the hydrologic system in the BWR, a hydrologic modeling framework that comprises the following three models was configured: precipitation Weather Generator (WG), hydrologic model, and lake model. Future projections were applied by modifying the WG to generate hourly precipitation ensembles that reflect the projected changes as inferred from comparing between the simulations of the historic and future periods for each of the downscaled climate models. Thus, the only projected future change that is being considered in this study is the projected change in precipitation. The detailed development and evaluation of the hydrologic framework is described in Shamir et al. (2017). In this section, we provide a description of the modeling framework components.

Precipitation Weather Generator

The above analysis of the BWR watershed precipitation and lake inflow points to the importance of representing the temporal and spatial characteristics of the rainfall events. The purpose of the precipitation WG is to produce numerous equally likely (random) realistic scenarios of hourly precipitation sequences. An ensemble that includes a sufficient number of realizations of these scenarios should represent the spatiotemporal statistical characteristics of the observed record, the natural variability of events, and their likelihood to occur.

Based on analysis of the MAP from CBRFC (1980-2010), a WG was developed to simulate likely hourly MAPs for the 11 sub-basins of the BWR watersheds. Since the WG was developed to describe the spatial and temporal characteristics of the MAPs time series that were used as input for the development and calibration of the SAC-SMA hydrologic model, the WG realizations can be used as precipitation input to the hydrologic model.

By modifying the WG to reflect the changes that were identified from comparing between the historic and projected simulations of the climate models, it is also possible to assess the impact of projected future precipitation changes on the lake inflow and lake level. The precipitation WG concept that is presented herein is following on previous work by Shamir et al., (2007a&b, 2015), Shamir (2017), and Wang et al., (2007). A detailed description and evaluation of the WG for the BWR watershed is provided in Shamir et al. (2017) and a brief description is provided below.

The WG is comprised of two successive modules: 1) a point process module to derive hourly MAP that represents the entire BWR watershed (Figure 5, left side) and; 2) a spatial disaggregation module to estimate hourly MAPs in the eleven sub basins (Figure 5, right side).

Point Process Module

The point process model is developed for three wetness categories (wet, medium and dry) for both winter (November-March) and summer (June-September). The spring (April-May) and fall (October) were assumed to be dry. The highly skewed precipitation distribution and the very large inter-annual variability in the arid Southwest U.S. calls for a WG with wetness categories that can be developed independently (Shamir et al. 2007a,b). The wetness categories represent the tercile statistics of the total observed seasonal (summer and winter) precipitation during 1980-2010. The selection of a wetness category in the WG for a given season is sampled from a uniform distribution (i.e. a distribution that has constant probability) and it is independent from the selected wetness category of the previous seasons.

Following the sampling of a wetness category, the duration of winter or summer is determined by sampling the season's precipitation onset and offset. The onsets were identified in the observed record as the duration since 1 June and 1 November for the summer and winter, respectively when the cumulative areal average precipitation over the entire basin exceeded 10mm. The offset of the seasons were selected as the last precipitation event prior to end of September and the end of March for the summer and winter, respectively. The onset and offset of the rainy season are selected from a normal distribution with a mean and standard deviation calculated from the historical record for the winter and summer and for the different wetness categories.

Following the selection of the wetness category and the duration of the rainy period, a precipitation time series is being created for the season (winter or summer) by sequentially sampling from the following distributions: inter arrival time of storms, duration of storms, the chance for an hourly precipitation event to occur, and the magnitude of the hourly event. This sequential sampling repeats until a time series is generated for the duration from the season's onset to its offset, as seen in looping arrow in Figure 5. Each of this distribution was developed independently for the three wetness categories (i.e. wet, medium, and dry).

The point process module is based on the assumption that precipitation storm events tend to arrive in clusters as a response to a transient synoptic scale atmospheric disturbance. Each synoptic event may produce multiple hourly precipitation pulses with possible multiple dry hours in between. The definition of a storm is a key component that is required for the derivation of a sample of observed storms to be used for the development of the WG parameters. Our storm definition procedure is based on the assumption that the distribution of storms inter-arrival time constitutes a Poisson stochastic process and therefore the distribution of storms inter arrival times conforms to an exponential distribution (Restrepo-Posada and Eagleson, 1982).

Thus, it is possible by selecting the minimum inter-arrival time between storms (i.e. the number of dry hours beyond which the occurrence of rainfall marks the beginning of a new event) to develop a statistical sample of storms with inter-arrival distribution that has a coefficient of variation of one, as in an exponential distribution. In this study the minimum inter arrival time were prescribed to 84 and 36 hours for the winter and summer, respectively. A storm event is defined as one that follows the previous storm by a period that is longer than the minimum inter arrival time, starts, and ends with an occurrence of hourly precipitation events.

Precipitation WG Spatial distribution

The BWR basin-wide hourly MAP realizations that were derived by the point process module are further disaggregated into MAP for the 11 sub-basins. The disaggregation consists of two steps. First, for each wet hour, a wetness category in each sub-basin is independently assigned. The wetness categories, which can also include an assignment of no-rain event, were sampled for winter and summer from a uniform random distribution with chances coefficients as calculated from the observed sub-basins MAP records. The chance coefficients indicate the chance of a precipitation event in a sub-basin to be in a particular tercile, independently of the other sub-basins, as a function of the wetness category of the average master time series.

Second, the magnitude of the hourly precipitation in the sub-basins, if in the upper tercile, is assigned from a Generalized Pareto distribution with its threshold parameter being the observed

67th percentile in each of the sub-basins. Otherwise, the precipitation magnitude is selected from a log normal distribution. The parameters of these distributions were derived independently for each sub basin from the observed non-zero hourly events.

In order to better simulate large extreme events, we added a chance of one day per winter to sample an upper tercile precipitation event from Generalized Pareto distributions that were parameterized to represent the annual maxima series of the observed records for each sub-basin. The threshold parameters of the Generalized Pareto distributions are assigned as the lowest value of the annual maxima series in the sub-basins.

Figure 5 outlines the different WG components. The left column describes the sequential sampling process that is used to derive the entire basin areal average hourly time series and the right column describes the sequential sampling process that is used to disaggregate the areal average to areal averages in the sub-basins. Following the selection of a wetness category for a given season (winter or summer) the duration of the rainy season is selected as the time between the seasonal onset and offset. The looping arrow indicates a repetitive sampling sequence that continues until the precipitation simulation is completed for the identified rainy season duration

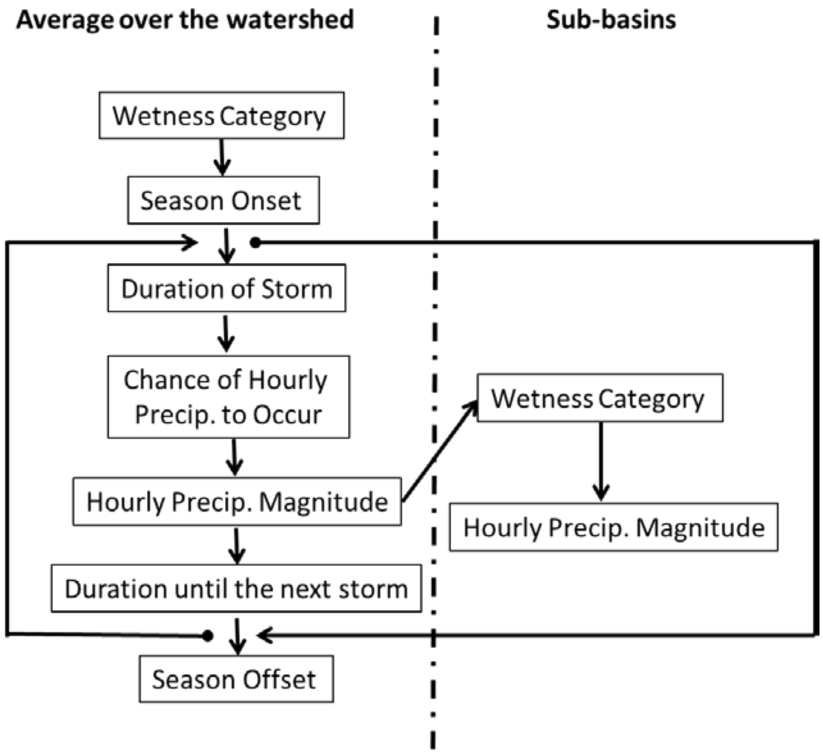

Figure 5: A schematic outline of the WG components in the winter and/or summer. The left column describes the point process sequential sampling to derive basin average hourly time series. The right column is the sequential sampling to disaggregate the synthetic time series to the sub-basins. The looping arrow indicates a repetitive sampling sequence that continues until the precipitation simulation is completed for the duration between the onset and offset of the winter or summer.

In Shamir et al., (2017), in addition to detailed description of the WG development, the performance of the WG was comprehensively assessed for the winter and summer with respect to the distribution of hourly precipitation, frequency of occurrence of hourly events, distribution of seasonal totals and occurrence of extreme hourly events. These are perceived as precipitation features that control runoff generation in ephemeral streams. In Figure 6 and 7, we provide an example for the WG performance in simulating the distribution of the winter hourly precipitation and frequency of occurrence of hourly precipitation, respectively. In these Figures, the cumulative distributions of 100 WG realizations, each 30 years of hourly MAP for the 11 sub-basins (similar to the dimension that available for the observed record) are shown as gray lines. The WG realizations are compared with the cumulative distribution of the observed MAPs from CBRFC, which are shown in red. While the cumulative distributions in Figure 6 are derived for all non-zero precipitation events during the 30-years period, in Figure 7, the distributions are of a seasonal index and therefore the ensemble comprised of 100 realizations, each includes 30 values. The WG simulations of the hourly precipitation show tight spread and overall match very well the distribution shape of the observed records in the sub-basins (Figure 6). Since the WG was designed to represent the inter- and intra-annual variability, tight spread of the realization and a good match of the shape of the observed distributions are considered favorable traits when comparing multi year time series. The lower right panel, which compares the distributions of the areal weighted averages over the entire Bill Williams watershed, offers an evaluation measure for the spatial module performance of the WG.

The inter-annual variability of the ensemble is presented by the spread between the realizations of the count of non-zero precipitation occurrence distributions (Figure 7). The distributions of the ensemble's realizations encompass well the observed distributions in the sub-basins and slightly underestimate the frequency over the entire watershed (lower right panel).

To the authors' knowledge, there is no formal methodology for evaluating the performance of a WG ensemble. The spread of the ensemble realizations should represent the uncertainty that is associated with the observed record. The width of the ensemble spread should neither be too wide or too narrow. A narrow spread does not describe the uncertainty and variability in the data while a spread that is too wide may fail to capture the unique characteristics of the data.

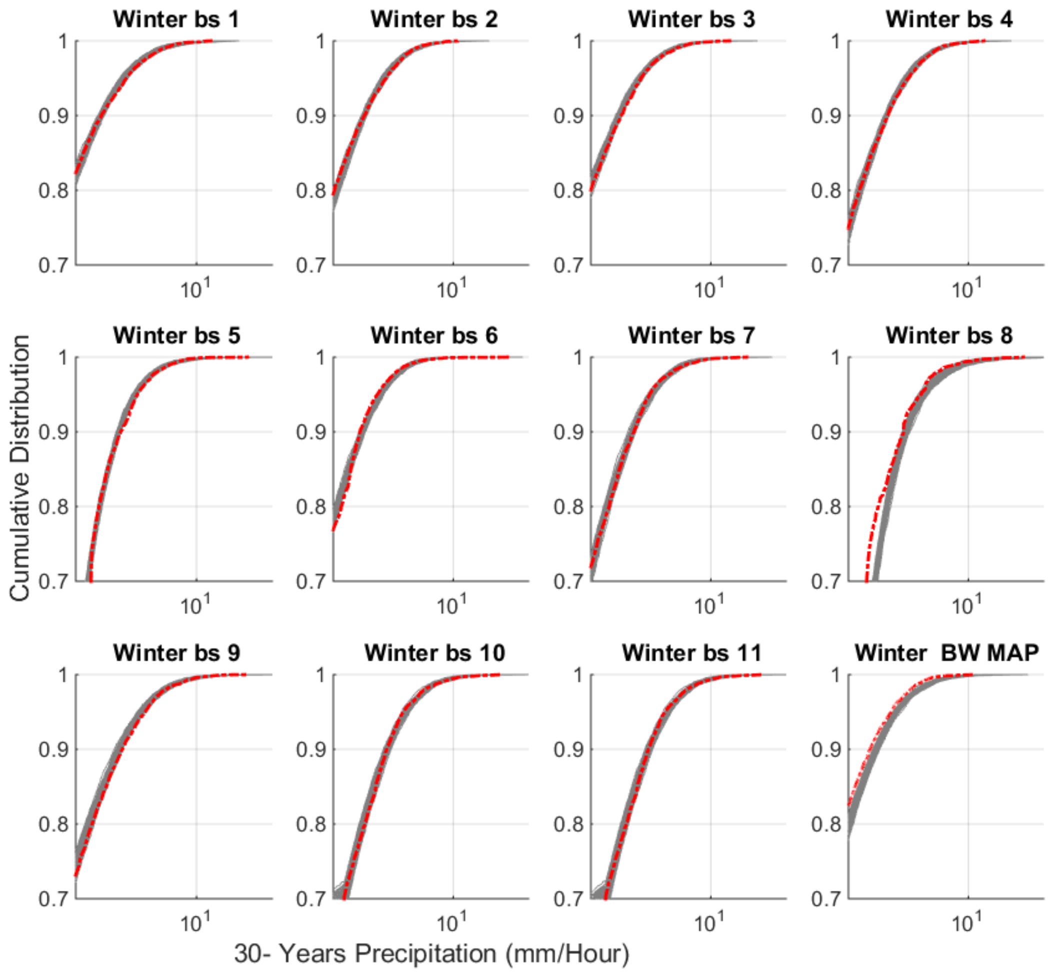

Figure 6: The cumulative distributions of 30-years non-zero hourly winter precipitation (mm/hour) in the sub-basins and the entire Bill Williams watershed. The WG simulated ensemble of 100 realizations are in gray and the observed (1980-2010) MAPs from CBRFC are in red.

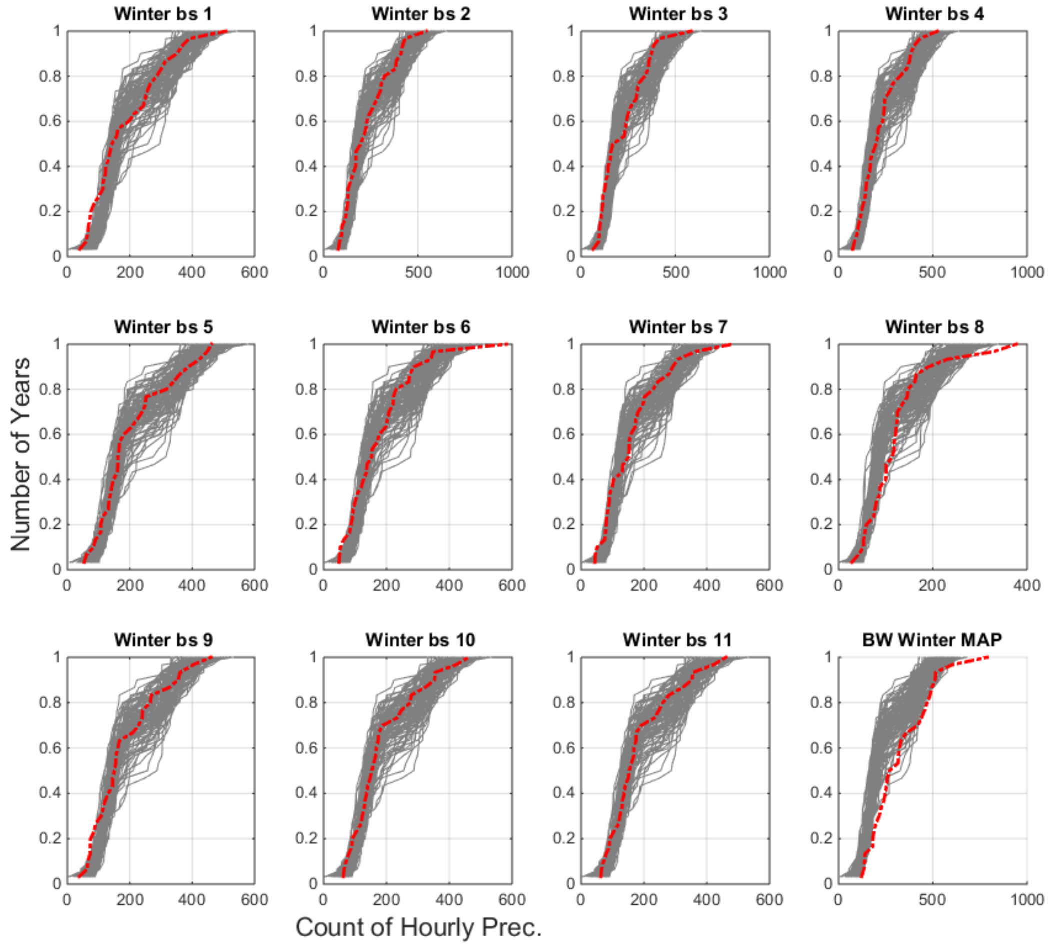

Figure 7: The cumulative inter annual distributions of the number of non-zero hourly precipitation events in the sub-basins and the entire Bill Williams watershed during the winter. The 100 realizations of the WG simulated ensemble are in gray and the observed (1980-2010) sub-basins MAPs from CBRFC are in red.

Hydrologic Model Sacramento Soil Moisture Accounting

In this hydrologic framework, we implemented the CBRFC hydrologic model configuration and parameters for the BWR watershed. The CBRFC uses the NWS River Forecast System, which includes the following components: 1) the Sacramento Soil Moisture Accounting model (SAC-

SMA) as hydrologic model that continuously updates the soil moisture conditions and simulates runoff and streamflow in the channels (Burnash et al., 1973); the Snow17 model which keeps track of snow accumulation and ablation in the basins (Anderson, 1976) and; a unit hydrograph to route the channels' streamflow into the sub basins outlets. The CBRFC operational model is mainly used to simulate high flow events, and in order to accommodate water resources studies, the SAC-SMA parameters were further tuned.

The tuning of the parameters was conducted by comparing the daily streamflow simulations to the observed daily flows at the Big Sandy (USGS 09424450), Burro Creek (USGS 09424447) and Santa Maria (USGS 09424900) (Figure 1). We used the MAP time series as input for the SAC-SMA model in order to simulate the daily streamflow that were used for the tuning of the parameters.

The simulated winter and summer cumulative distributions of the daily inflow into the lake are compared to the calculated inflow in Figure 8. For the winter, the calculated and simulated cumulative distributions matched very well. On the other hand, for the summer the simulation overestimated the calculated record. The weak model performance during the summer period was also visually noticeable in the hydrographs. Calibrating to match well the summer events requires to compromise the winter model performance. The lack of performance during the summer is thought to be attributed to the inability to capture the characteristics of the short and local intense rainfall characteristics of the summer rainfall. The use of MAP over relatively large basins likely has a smoothing effect that misrepresents the convective characteristics of the summer rainfall events. Thus, a good simulation of summer events requires higher resolution model configuration with input data to represents the convective summer storm characteristics.

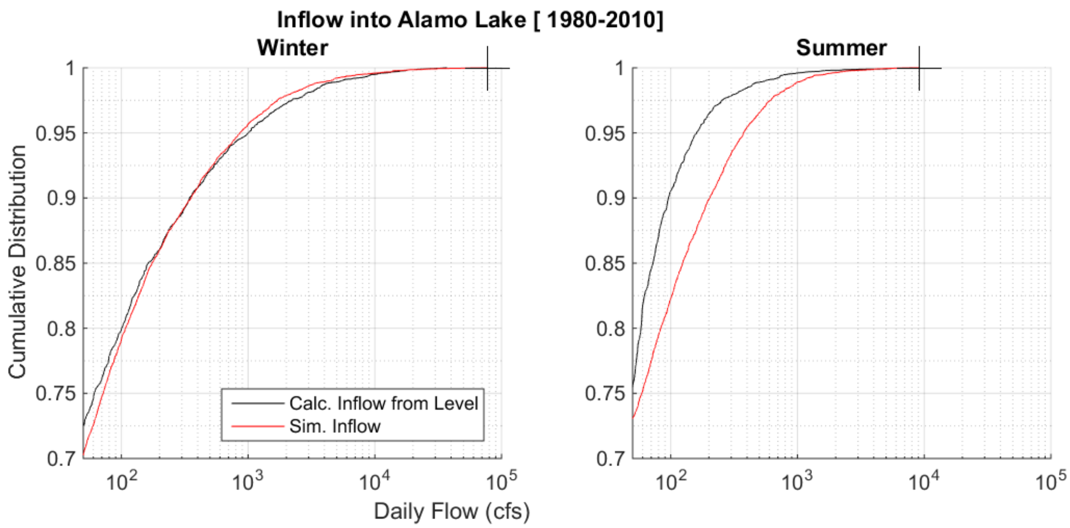

Figure 8: Winter and summer Cumulative distributions of the simulated inflow into the lake compared to the calculated inflow from lake level and observed outflow

Alamo Lake Model

An hourly mass balance model that simulates lake level, storage, and releases from the dam as a function of inflow into the lake is described below. The lake operation rules are based on 'rain on the ground' strategy, which implies that the operation rules are reactive to observed inflow into the lake. The physical dimensions of the lake and the relationships between water level, storage and surface area are from Kirby and Burnham (1998) and the U.S. Army Corps of Engineers (USACE) website (http://resreg.spl.usace.army.mil/pages/alamo.php). The operational rules that specify dam releases as a function of lake level and season, the specification of the dam's dimensions, and the monthly lake evaporation values are from the USACE Operational Manual (2003).

The operation of the lake is intended to maintain the lake water level at, or near, 1125 feet (342.9 m), for as long as possible. This level is considered optimal to satisfy all the objectives of the authorizing legislation and optimize downstream benefits. The actual operation of the dam often deviates from the recommended rules. During storm events that impact large areas of the Colorado River basin, releases from Alamo dam are coordinated in order to control the flow on the Colorado River. Other cases of deviation from the operational rules may be subjective operational considerations such as dam maintenance and specific downstream demands.

The simulations and observations of the lake's water level and outflow are shown in Figure 9. It is seen that although the lake's actual operation had occasionally deviated from the rules, the simulated water level and outflow overall do well at representing the observed record.

It is important to note that the flood control storage compartment of the lake holds about 600,000 acre-feet (740 10^6 m^3), and at this water level the maximum release rate is 7,000 cfs (~200 cms). This is a relatively large storage volume that has been utilized to store water during flood events in the Colorado River basin. However, at the maximum release rate it takes more than 40 days to drain the entire volume of the flood control storage, which may be too slow in emergency situations.

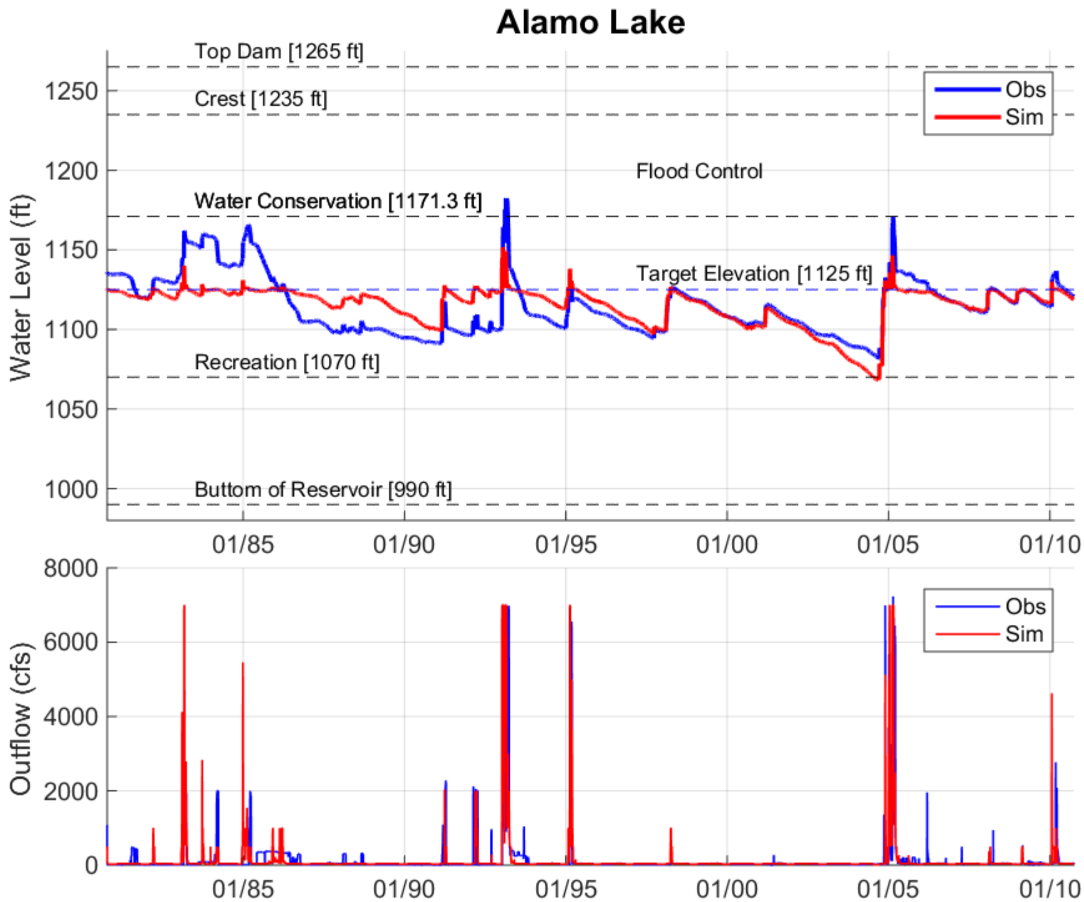

Figure 9: Observed and simulated lake water level and outflow in the upper and lower panels, respectively for 1980 -2010.

5. Results

DD vs. SD historical period

Cumulative distributions of the historical inter-annual daily precipitation characteristics (mean, standard deviation, and number of rainy days from top-to-bottom, respectively) for the DD, SD, reanalysis and observed MAP are compared in Figure 10. The WRF reanalysis simulation matches well the observed MAP distribution, which implies that at least at the scale analyzed herein, the reanalysis simulation captures precipitation features that are important for hydrologic assessment. The SD simulations of the three models are, as expected, very similar to each other, since they were created to conform to the Livneh dataset. However, compared with the observed MAP, the SD simulations and therefore also the Livneh dataset, underestimate the mean and standard deviation and overestimate the number of daily events. This underestimation suggests that although the LOCA well represent the Livneh dataset, it does not do well representing the CBRFC MAP for the study area.

The DD simulations exhibit larger differences among the GCMs. The three DD simulations overestimate the mean and standard deviation, and the frequency of the daily precipitation is underestimated by the MPI and overestimated by both HAD and GFDL.

These differences seen in Figure 10 between the downscaled simulations (DD and SD) and the observed MAP imply that the downscaled simulations are not adequate as rainfall input to the hydrologic model that was developed with the observed MAP time series. In order to use the downscaled simulations as rainfall input to the hydrologic model, it is necessary to modify the simulations to have similar characteristics to the input that was used for the configuration of the hydrologic model. Bias correcting of the SD and DD simulations, a practice commonly used, may show a good fit in the upper panel of Figure 10 but will likely not resolve the differences that are seen in the middle and lower panels, which are important precipitation features in arid environment.

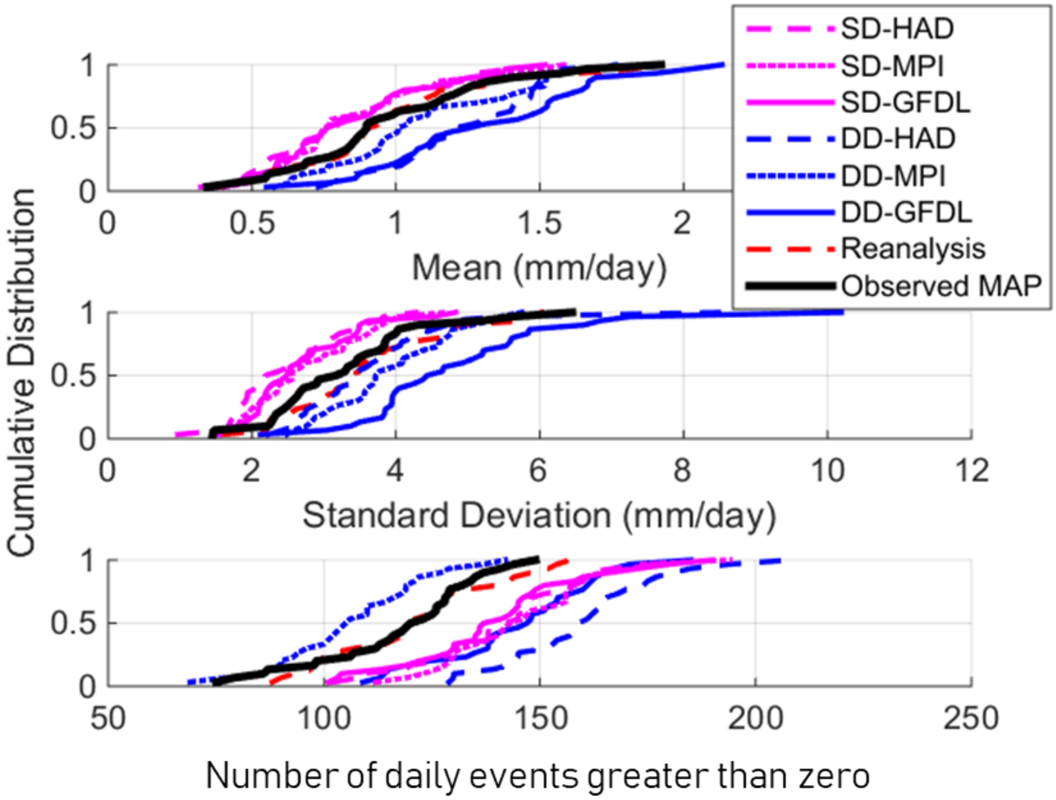

Figure 10. Cumulative distributions of the inter-annual daily mean (upper panel), daily standard deviation (middle panel), and number of daily precipitation events (lower panel) for the three GCMs, historic SD and DD simulations, reanalysis, and the observed MAP for the historic period.

SD vs. DD Future Change

Tercile Analysis

The projected mid-21st century (2020-2059) precipitation changes analysis, looking at rainfall characteristics that were used for the development of the WG, is presented in this section. The distributions of the downscaled simulations of the different WG features, such as the duration of the storms, the time between storms, and the hourly magnitudes were compared between the historic and projected periods for the three wetness categories. This comparison showed no statistically significant differences between the historic and projected periods for these features, which implies that the historic wetness categories represent well the projected rainfall characteristics of the matching wetness category. The most notable difference between the historic and projected periods is the frequency in which the wetness categories are projected to occur in the future.

The projected frequencies of the seasonal wetness categories in mid-21st century as defined by the terciles of the historic period are listed in Table 2. In this table, chances that are significantly different than the historical period are indicated.

The significance test was determined from a Monte Carlo experiment. In this experiment, we randomly sampled from a continuous uniform distribution that is taking values from 0 to 1. We sampled an ensemble of 100,000 members, each member with a sample size of 40 to represent the 40-year the future projection duration of interest. The statistical distribution of the tercile values of the ensemble members can be used to estimate the chance of a randomly selected value to be in a given tercile.

In this Monte Carlo experiment we found that 5% [1%] of the terciles were below 0.22 [0.18] and above 0.46 [0.51]. Thus, it can deduced, for example, that a given projected wetness category with frequency that is either below 0.18 or above 0.51 has chance of less than 1% to be selected from a uniform distribution, and therefore we assume that it is significantly different than 33%.

For winter season, the MPI DD and SD simulations projected a significantly higher frequency of dry winters. The DD-MPI indicates decreased frequency in wet winters and the SD-MPI indicates decreased in normal winters. The DD-GFDL, similarly to the DD-MPI, shows increase and decrease frequency of dry and normal winters, respectively. No significant changes in winter projections are seen for the HAD GCM. The projection for higher frequency of dry winters is congruent with the Assessment of Climate Change in the Southwest U.S report (Garfin et al., 2013) that projected a decrease trend in winter precipitation.

For the summer season, the DD-HAD projected a lower frequency of dry and normal summers and a higher frequency of wet summers in mid-21st century. The only other significant result is shown for the DD-GFDL that projected decrease frequency of dry summers. An analysis of the GCMs that participated in the IPCC Fifth Assessment Report, indicated a delay in the onset of the monsoon season and increase rainfall in the late summer (Cook and Seager, 2013).

Table 2. Projected 2020-2059 chances for the wetness categories to occur

WINTER (November-March)						
	Dynamically Downscaled (DD)			**Statistically Downscaled (SD)**		
	Dry	Normal	Wet	Dry	Normal	Wet
HAD	0.35	0.3	0.35	0.3	0.4	0.3
MPI	0.55**	0.2*	0.25	0.55**	0.15**	0.3
GFDL	0.53**	0.2*	0.28	0.38	0.33	0.3
SUMMER (April – September)						
	Dynamically Downscaled (DD)			**Statistically Downscaled (SD)**		
	Dry	Normal	Wet	Dry	Normal	Wet
HAD	0.18**	0.18**	0.65**	0.33	0.35	0.33

MPI	0.43	0.28	0.3	0.43	0.28	0.3
GFDL	0.2*	0.45	0.35	0.28	0.43	0.3

* less than 5% chance if sampled from a random distribution

** less than 1% chance if sampled from a random distribution

Hydrologic impact results

In order to assess the projected hydrologic impact, we modified the WG by applying the frequencies of winter and summer wetness categories as indicated in Table 2 to generate six additional ensembles (SD and DD for three GCMs) of MAPs for the eleven sub-basins that represent the mid-21st century projections. Each ensemble consists of 100 realizations of hourly precipitation, and each realization is 30-year long. These ensembles were used as input to the hydrologic model and the lake model to generate ensembles of lake inflow, outflow and water level.

In Figure 11, the cumulative distributions from the 100 realizations of the 30-year mean annual precipitation over the entire BWR watershed are shown. The right panel of this figure shows the ratio between the quantiles of the cumulative distributions of the historic and projected simulations. The average changes of all the ratios of the quantiles are indicated in the upper right. While the DD-MPI has a clear signal of drying, the DD-HAD and SD-HAD are showing a wetting trend. The smallest changes are found for the GFDL. For both the MPI and HAD the largest changes are seen for the DD simulations. This behavior is likely the result of the changes in the forcing of the regional climate model as manifested in Table 2.

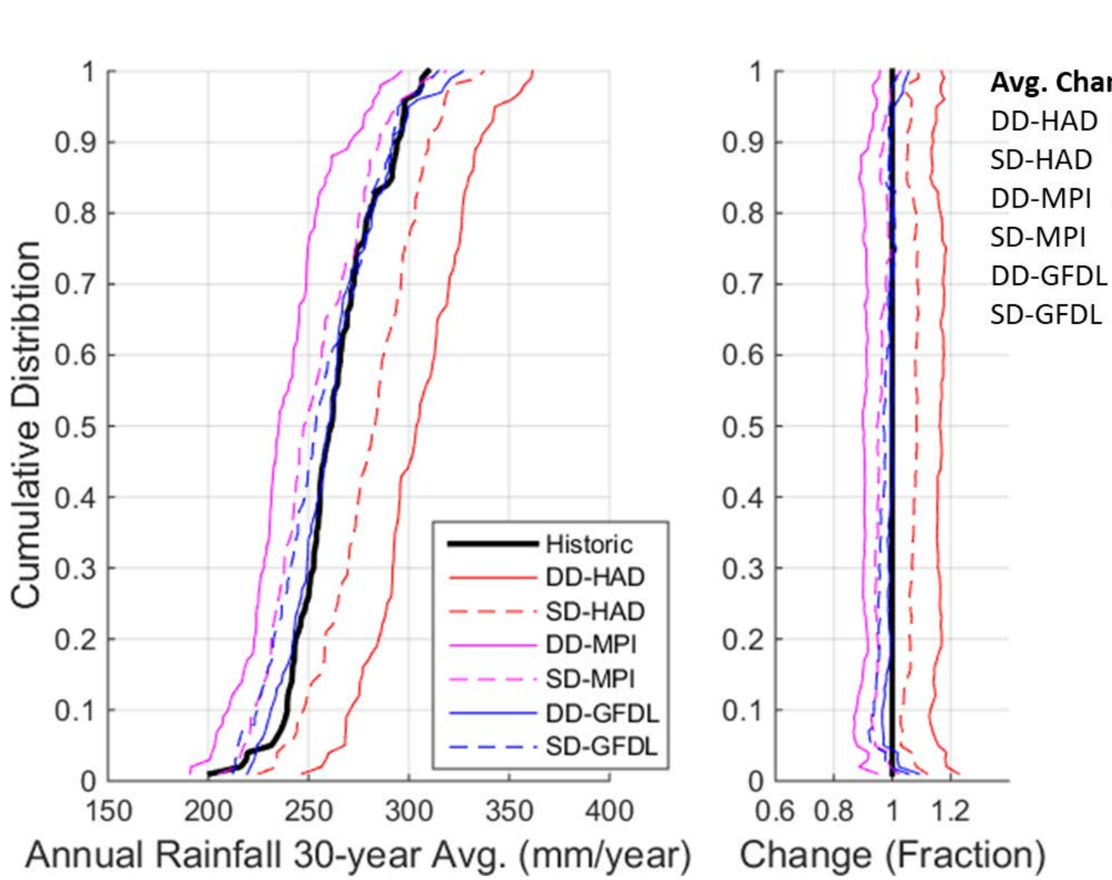

Figure 11. Cumulative distribution of 30-year mean annual precipitation over the entire BWR watershed from the 100 realizations of the 7 ensembles. The right panel shows the quantiles ratio between the historical and projected ensembles. The average changes are indicated in the upper right.

As in Figure 11, in Figure 12 we plot the 30-year mean annual inflow into the lake. As expected the direction of the trends for the different projections are similar to the ones shown in Figure 11 for the precipitation. However, the magnitude of the projected change is much larger for the lake inflow. The two extreme examples are the DD-HAD with average projection to increase the precipitation by 16% and lake inflow by 42%, and the DD-MPI with average projection to decrease the precipitation by 9% and lake inflow by 23%. This underscores the high sensitivity of the BWR watershed to small changes in precipitation, which is attributed to the complex hydrologic response in ephemeral streams.

The results for the projected changes in the outflow from the lake (not shown) are very similar to the changes projected for the inflow (projected average changes are within 2% of the changes indicated in Figure 12).

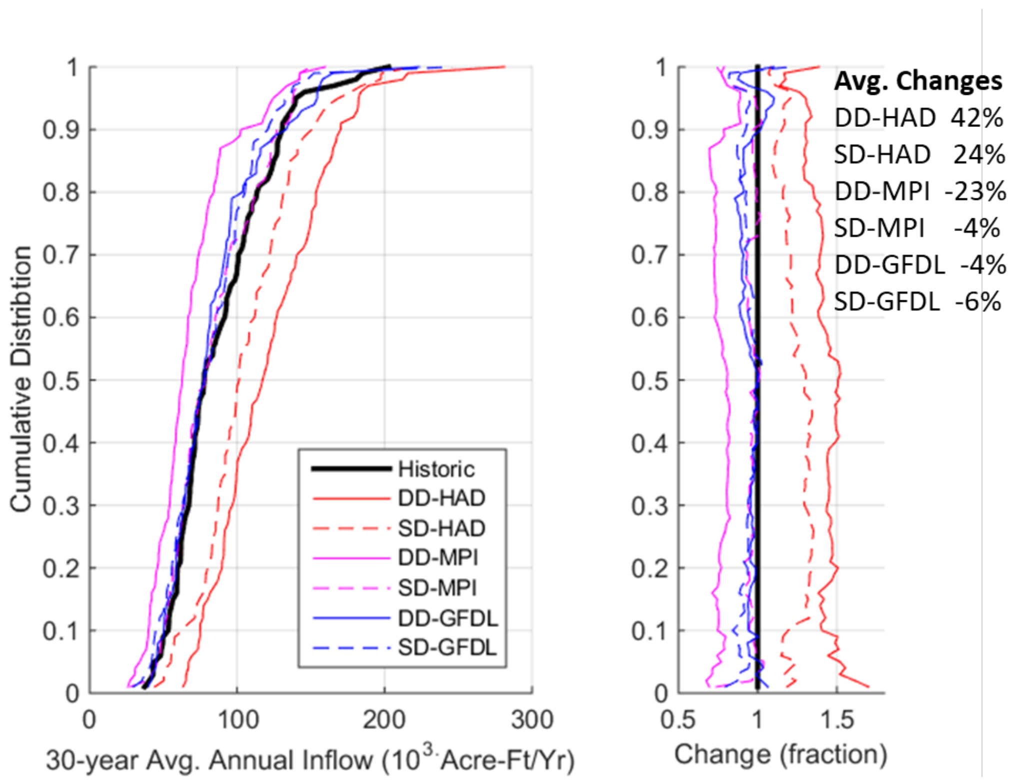

Figure 12. Cumulative distribution of 30-year mean annual inflow into Alamo Lake from the 100 realizations of the 7 ensembles. The right panel shows the quantiles ratio between the historical and projected ensembles. The average changes are indicated in the upper right.

The projected climatic impact on the lake is shown in Figure 13. In this Figure, the cumulative distribution of the percent of the time in the 30-year duration that the water level is projected to drop below 1070 feet, which is the optimal lake level for operations (see Figure 8), is shown. While the HAD showed less events with lake level below this marker, the MPI showed a substantial increase in frequency of the lake levels dropping below this marker. It is seen that the MPI and HAD DD simulations produce the extreme wet and dry events, respectively.

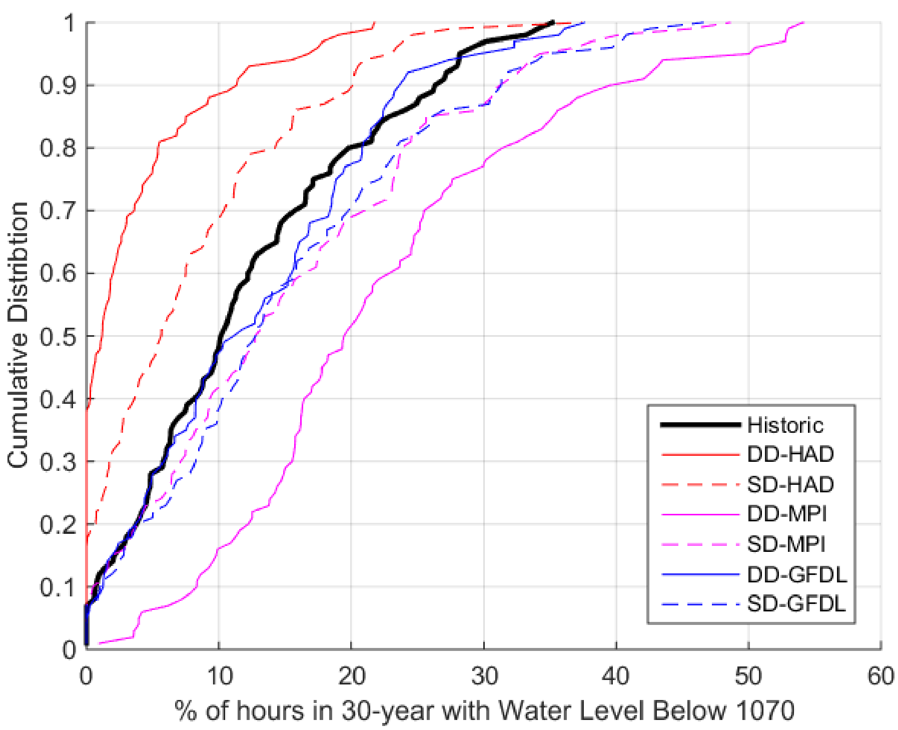

Figure 13: Cumulative distribution of the percent total hours in 30-year duration that the lake level is below the 1070 feet, which is the recreation threshold.

The projected extreme high levels of the lake are explored in Figure 14 for 1171.3 and 1235 feet water levels, which are the flood control threshold and the dam's crest (Figure 9), respectively.

We note that the projected encroachment into the flood control reservoir is not substantially different from the historic period, and the probabilities for this exceedance are fairly small. Moreover, with the current lake operational rules the chance to reach the crest level is less than 0.1 % in frequency of 95%. This is because of the large flood control storage that provides a buffer and requires multiple days of very large flow.

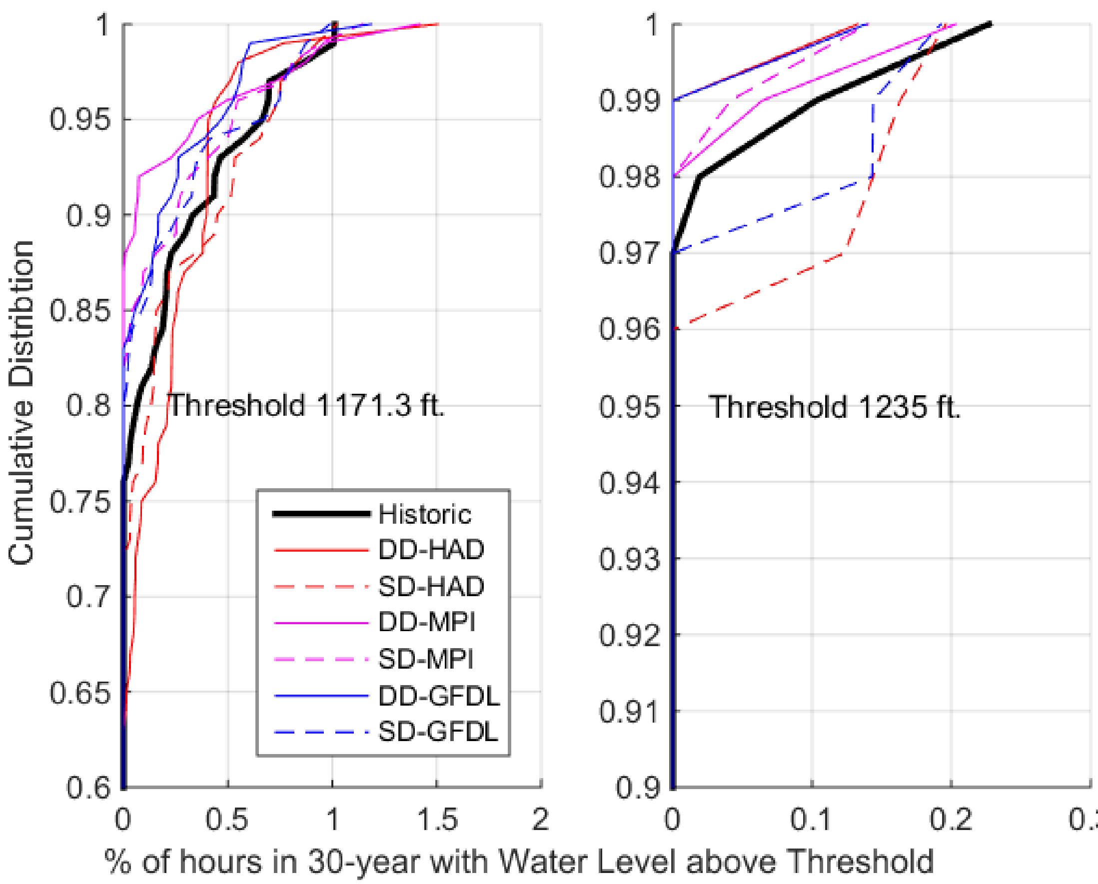

Figure 14: Cumulative distribution of the percent total hours in 30-year duration that exceed the flood control threshold at 1171 ft (left) and the dam crest at 1235 ft (right).

6. Summary and conclusions

The objective of this study is to assess the impact the downscaling methodology (statistical versus dynamical) of the projected mid-21st century on hydrologic assessment in an arid environment. Our study area, the Bill Williams River Watershed that drains into Alamo Lake, is comprised of three ephemeral rivers that are highly sensitive to temporal and spatial precipitation characteristics. Precipitation projections are available from three CMIP5 RCP8.5 GCMs that were found to well perform for Southwest U.S (i.e. HadGEM2-ES, MPI-ESM-LR, and GFDL-ESM2M). For these three GCMs, dynamical downscaled projections using WRF were compared to statistical downscaled projections available from the LOCA dataset. Hydrologic assessment was carried out using a modeling framework that is based on the operational hydrologic model configuration used by the NWS CBRFC. This hydrologic model consists of the SAC-SMA hydrologic model that runs with hourly mean areal precipitation to generate streamflow in ten internal locations and inflow into Alamo Lake. The Lake outflow was simulated using USACE dam operational rules and lake specifications.

A precipitation weather generator that represents the temporal and spatial statistical characteristics of the CBRFC MAP that forces the hydrologic model was developed. This WG is developed to produce ensembles of likely to occur hourly precipitation that are congruent with the hydrologic model input. The WG was further modified to generate ensembles that reflect the projected mid-21st century as found by the SD and DD simulations of the three selected GCMs. These ensembles were created by modifying the WG to reflect the projected precipitation changes that were analyzed by comparing the historic and future periods of the climate projections.

The main findings of this study are that the DD simulations of the MPI and the HAD showed larger range of projected changes than their corresponding SD simulations. These changes however are contradicting in their mid-21st century projection trends, as while the MPI projected a drying trend, the HAD projected a wetting trend. The projected changes in the frequency of occurrence of dry or wet season imply projected increase in climate variability. On the other hand, the contradicting trends between the DD-MPI and DD-HAD points to the increase uncertainty in the projected future precipitation.

These changes in wetting and drying are magnified during the progression from precipitation, to streamflow, to lake inflow, and changes to lake level. Changes in risk of lake flooding were not clearly identified in this study. However, the main finding points to an increasing challenge to operate the lake in its target water level.

We note that although the study did not yield a clear trend of drying or wetting, it provides uncertainty bounds that can be useful for future planning of the lake operations. These uncertainty bounds are much wider when considering the dynamically downscaled models of the MPI and HAD. Relying solely on statistically downscaled projections may underestimate the degree of change in projected precipitation. This information should guide an adaptive lake operation that can adjust and respond to these uncertain lake water level changes.

Finally, we stress that our study used a limited number of downscaled model simulations, which may not represent all other statistically and dynamically downscaling procedures. Moreover, the study was conducted in the Bill Williams River watershed, located in the arid Southwest US.

Thus, the generalization of our conclusions to other downscaled datasets and other regions may not be appropriate.

Acknowledgements

Funding for this project was provided by the Bureau of Reclamation, Science and Technology Grant Program under a cooperative agreement between the Hydrologic Research Center and the Bureau of Reclamation Lower Colorado Region (Agreement # R16AC00024). The authors wish to thank Paul Miller and Craig Peterson from the Colorado River Forecast Center (CBRFC), National Weather Service for their assistance in providing the CBRFC data and SAC-SMA hydrologic model setup. Alamo Lake historic water level data was received from Jason Lee and Jon Sweeten the USACE, Los Angeles District. Thanks are also extended to Santos Noe from Reclamation's Boulder Canyon Operations Office, Boulder Nevada for his advice and technical support. We also would like to thank the two anonymous reviewers for their constructive input. The opinions expressed in this report are those of the authors and do not reflect those of the funding agency or the acknowledged individuals

References

Arritt, R.W., D.C. Goering, C.J. Anderson. 2000. The North American Monsoon System in the Hadley Centre Coupled Ocean-Atmosphere GCM. Geophysical Research Letters, 27(4) 565-568.

Bill Williams River Corridor Technical Committee (1994) Proposed water management plan for Alamo Lake and the Bill Williams River

Bukovsky, M. S., D. J. Gochis, and L. O. Mearns, 2013: Towards assessing NARCCAP regional climate model credibility for the North American monsoon: Current climate simulations. J. Climate, 26, 8802–8826, doi:10.1175/JCLI-D-11-00588.1.

Bukovsky, M.S., C. M. Carrillo, D. J. Gochis, D.M. Hammerling, R.R. McCrary, L. O. Mearns. 2015. Towards Assessing NARCCAP Regional Climate Model Credibility for the North American Monsoon: Future Climate Simulations. Journal of Climate, 28:6707: 6728

Burnash, R.J., R. L. Ferral, and R. A. McGuire (1973). A generalized streamflow simulation system conceptual modeling for digital computers. U.S Department of Commerce National Weather Service and State of California Department of Water Resources.

California Department of Water Resources, Perspective and Guidance for Climate Change Analysis, August 2015, Climate Change Technical Advisory Group.

Carpenter, T.M., and K.P. Georgakakos, 2001: Assessment of Folsom Lake response to historical and potential future climate scenarios: 1, Forecasting. J. Hydrol., 249, 148-175.

Castro, C. L., H. Chang, F. Dominguez, C. Carrillo, J. K. Schemm, and H. M. H. Juang, 2012: Can a regional climate model improve the ability to forecast the North American monsoon? J. Climate, 25, 8212–8236, doi:10.1175/JCLI-D-11-00441.1.

Castro L.C et al. (2017). Assessing climate change impacts for DoD Installations in the Southwest United States during the warm season. A Final Report to Strategic Environmental Research and Development Program (SERDP) Project Number RC-2205, 128pp.

Christensen, N. S., and D. P. Lettenmaier, 2007: A multimodel ensemble approach to assessment of climate change impacts on the hydrology and water resources of the Colorado River basin. Hydrol. Earth Syst. Sci., 3, 1–44.

Cook, B.I., and R. Seager, 2013. The response of the North American Monsoon to increased greenhouse gas forcing. J. Geophys. Res., 118, 1690-1699, doi:10.1002/jgrd.50111.

Garfin, G., A. Jardine, R. Merideth, M. Black, S. LeRoy (Eds.), 2013. Assessment of Climate Change in the Southwest United States: A Report Prepared for the National Climate Assessment. A Report by the Southwest Climate Alliance, Island Press, Washington, DC

Gautam J, Mascaro G. Evaluation of Coupled Model Intercomparison Project Phase 5 historical simulations in the Colorado River basin. Int J Climatol. 2018;1-17. https://doi. org/10.1002/joc.5540.

Geil, K. L., Y. L. Serra, and X. Zeng, 2013: Assessment of CMIP5 model simulations of the North American Monsoon system. J. Climate, 26, 8787–8801.

House, P. K., M. L. Wood, P. A. Pearthree. 1999. Hydrologic and Geomorphic characteristics of the Bill Williams River, Arizona. Arizona Geological Survey Open-File Report 99-4 February, 1999.

Dee, D. P., Uppala, S. M., Simmons, A. J., Berrisford, P. , Poli, P. , Kobayashi, S. , Andrae, U. , Balmaseda, M. A., Balsamo, G. , Bauer, P. , Bechtold, P. , Beljaars, A. C., van de Berg, L. , Bidlot, J. , Bormann, N. , Delsol, C. , Dragani, R. , Fuentes, M. , Geer, A. J., Haimberger, L. , Healy, S. B., Hersbach, H. , Hólm, E. V., Isaksen, L. , Kållberg, P. , Köhler, M. , Matricardi, M. , McNally, A. P., Monge-Sanz, B. M., Morcrette, J. , Park, B. , Peubey, C. , de Rosnay, P. , Tavolato, C. , Thépaut, J. and Vitart, F. (2011), The ERA-Interim reanalysis: configuration and performance of the data assimilation system. Q.J.R. Meteorol. Soc., 137: 553-597. doi:10.1002/qj.828

Fowler, H. J., S. Blenkinsop. C. Tebaldi. (2007) Review: Linking climate change modelling to impacts studies: recent advances in downscaling techniques for hydrological modelling. International Journal of Climatology, 27: 1547–1578.

Kirby, K. and Burnham M.W. Technical Consideration for Alamo Lake Operation, U.S Army Corps of Engineers, Hydrologic Engineering Center, April 1998.

Kotamarthi, R., L. Mearns, K. Hayhoe, C.L. Castro, and D. Wuebbles, 2016. Use of Climate Information for Decision Making and Impacts Research: State of Our Understanding. Strategic Environmental Research and Development Program (SERDP) Project RC-2242, Technical Report. 54 pp. www.dtic.mil/dtic/tr/fulltext/u2/1029525.pdf

Liang, X. Z., Zhu, J., Kunkel, K. E., Ting, M., & Wang, J. X. (2008). Do CGCMs simulate the North American monsoon precipitation seasonal–interannual variability?. Journal of Climate, 21(17), 4424-4448.

Lin, J. L., Mapes, B. E., Weickmann, K. M., Kiladis, G. N., Schubert, S. D., Suarez, M. J., ... & Lee, M. I. (2008). North American monsoon and convectively coupled equatorial waves simulated by IPCC AR4 coupled GCMs. Journal of Climate, 21(12), 2919-2937. DOI: 10.1175/2007JCLI1815.1

Livneh B., E.A. Rosenberg, C. Lin, B. Nijssen, V. Mishra, K.M. Andreadis, E.P. Maurer, and D.P. Lettenmaier, 2013: A Long-Term Hydrologically Based Dataset of Land Surface Fluxes and States for the Conterminous United States: Update and Extensions, Journal of Climate, 26, 9384–9392.

Maraun, D., F. Wetterhall, A. Ireson, E. Chandler, RJ. Kendon, E. Widmann, M. Brienen, S. Rust, H. Sauter, T.Theme, M. K. C. Venema, V. Chun, K. Goodess, C G. Jones, R. Onof, C.Vrac, M. Thiele-Eich, Insa (2010). Precipitation downscaling under climate change: Recent developments to bridge the gap between dynamical models and the end user. Reviews of Geophysics - REV GEOPHYS. 48. 10.1029/2009RG000314.

Pascale, S., S. Bordoni, S.B. Kapnick, G.A. Vecchi, L. Jia, T.L. Delworth, S. Underwood, and W. Anderson, 2016: The Impact of Horizontal Resolution on North American Monsoon Gulf of California Moisture Surges in a Suite of Coupled Global Climate Models. J. Climate, 29, 7911–7936, doi: 1

Patterson, l.L. Somers, W.P., 1966, Magnitude and frequency of floods in the United States: Part 9. Colorado River Basin: U.S. Geological Survey Water-Supply Paper 1683, 476p

Pierce DW, Cayan DR, Thrasher BL. 2014. “Statistical Downscaling Using Localized Constructed Analogs (LOCA).” Journal of Hydrometeorology, 15, 2558-2585.

Restrepo-Posada, P. J., and P. S. Eagleson, 1982. Identification of independent rainstorms. J. Hydrol., 55, 303-319.

Schaake, J., A. Henkel, and S. Cong, 2004: Application of PRISM climatologies for hydrologic modeling and forecasting in the western U.S. Preprints, 18th Conf. on Hydrology, Seattle, WA, Amer. Meteor. Soc., 5.3.

Shamir, E. 2017. The value and skill of seasonal forecasts for water resources management in the Upper Santa Cruz River basin, southern Arizona. Journal of Arid Environments. 137: 35-45.

Shamir, E., T. Modrick-Hansen and KP. Georgakakos 2017. Development of hydrologic Modeling Framework for the Bill Williams River Watershed. HRC Technical Note No. 97. Hydrologic Research Center, San Diego, CA, 1 December 2017. https://www.hrcwater.org/wp-content/uploads/2018/12/HRC_TN97.pdf

Shamir, E. Megdal, S. Carrillo, C. Castro, LC. Chang, H-I. Chief, K. Corkhill, EF. Eden, S. Georgakakos, PK. Nelson, MK. and Prietto, J. 2015. Climate change and water resources management in the Upper Santa Cruz River, Arizona. Journal of Hydrology. 521: 18-33. https://doi.org/10.1016/j.jhydrol.2014.11.062

Shamir, E., Wang, J., Georgakakos, K.P., 2007a. Probabilistic streamflow generation model for data sparse arid watersheds, J. Amer. Wat. Resour. Assoc. 43(5) 1142-1154.

Shamir, E., Graham, N.E. Meko, D.M. Georgakakos, K.P., 2007b. Hydrologic model for water resources planning in Santa-Cruz River, Southern Arizona, J. Amer. Wat. Resour. Assoc. 43(5) 1155-1170.

Sheffield, Justin & Barrett, Andrew & Colle, Brian & Fernando, D & Fu, Rong & L. Geil, Kerrie & Hu, Qi & Kinter, Jim & Kumar, Sanjiv & Langenbrunner, Baird & Lombardo, Kelly & N. Long, Lindsey & Maloney, Eric & Mariotti, Annarita & Meyerson, Joyce & Mo, Kingtse & David Neelin, J & Nigam, Sumant & Pan, Zaitao & Yin, Lei. (2013). North American Climate in CMIP5 Experiments. Part I: Evaluation of Historical Simulations of Continental and Regional Climatology. Journal of Climate. 26. 9209-9245. 10.1175/JCLI-D-12-00592.1.

Sheffield, Justin & Camargo, Suzana & Fu, Rong & Hu, Qi & Jiang, Xianan & Johnson, Nathaniel & B. Karnauskas, Kristopher & Kim, Seon & Kinter, Jim & Kumar, Sanjiv & Langenbrunner, Baird & Maloney, Eric & Mariotti, Annarita & Meyerson, Joyce & David Neelin, J & Nigam, Sumant & Pan, Zaitao & Ruiz-Barradas, Alfredo & Seager, Richard & Zhao, Ming. (2013). North American Climate in CMIP5 Experiments. Part II: Evaluation of Historical Simulations of Intraseasonal to Decadal Variability. Journal of Climate. 26. 9247-9290. 10.1175/JCLI-D-12-00593.1.

Shilo, E., B. Ziv, E. Shamir c, A. Rimmer, 2015, Evaporation from Lake Kinneret, Israel, during hot summer days, Journal of Hydrology, 528: 264–275.

Vano, J.A., B. Udall, D.R. Cayan, J.T. Overpeck, L.D. Brekke, T. Das, H.C. Hartmann, H.G. Hidalgo, M. Hoerling, G.J. McCabe, K. Morino, R.S. Webb, K. Werner, and D.P.

Lettenmaier (2014). Understanding uncertainties in future Colorado River streamflow. Bulletin of the American Meteorological Society, 95(1), 59-97.

US Army Corps of Engineers, Los Angeles District, Reservoir Regulation Section CESPL-ED-HR Water Control Manual, Alamo Dam and Lake Colorado River Basin, Bill Williams River, Arizona. October 2003

Wang, J., Shamir, E., and K.P. Georgakakos, 2007. Study of extreme precipitation over the Panama Canal Watershed. HRC Technical Report No. 6 Hydrologic Research Center, San Diego, CA. 1 August 2007 (CDO185933MMP), 136pp.